NOTICE

The quality of this microform is heavily dependent upon the quality of the original thesis submitted for microfilming. Every effort has been made to ensure the highest quality of reproduction possible.

If pages are missing, contact the university which granted the degree.

Some pages may have indistinct print especially if the original pages were typed with a poor typewriter ribbon or if the university sent us an inferior photocopy.

Reproduction in full or in part of this microform is governed by the Canadian Copyright Act, R.S.C. 1970, c. C-30, and subsequent amendments.

AVIS

La qualité de cette microforme dépend grandement de la qualité de la thèse soumise au microfilmage. Nous avons tout fait pour assurer une qualité supérieure de reproduction.

S'il manque des pages, veuillez communiquer avec l'université qui a conféré le grade.

La qualité d'impression de certaines pages peut laisser à désirer, surtout si les pages originales ont été dactylographiées à l'aide d'un ruban usé ou si l'université nous a fait parvenir une photocopie de qualité inférieure.

La reproduction, même partielle, de cette microforme est soumise à la Loi canadienne sur le droit d'auteur, SRC 1970, c. C-30, et ses amendements subséquents.

ISBN 0-315-59178-1

Simulation of Hot Gas Defrosting of Evaporators

Li Yan

A Thesis

in

The Department

of

Mechanical Engineering

Presented in Partial Fulfilment of the Requirements

for the Degree of Master of Engineering at

Concordia University

Montreal, Quebec, Canada

July 1990

ABSTRACT

Simulation of Hot Gas Defrosting of Evaporators

Yan Li

Defrosting of evaporators is necessary for the operation of air source heat pumps and refrigeration systems operating at air temperature below the water freezing point. Optimization of defrosting process is required for improving the performance of evaporators and systems. In this work, a hot gas defrosting model of evaporators was developed. The defrosting process was idealized for analysis and simulation, which included heat transfer, mass transfer and pressure change. This model divided the defrosting process into four stages, preheating, melting frost, wet surface, and dry surface, based on evaporator outside surface conditions. This model treated a transient dynamic defrosting process as a two dimensional process involving time and space. An assumption of a quasi-static process was made for time simulation. A finite element method was used for space simulation. Continuous change of refrigerant properties inside the evaporator was considered. The analysis concentrated on the required energy and time for defrosting.

Air side heat and mass transfer empirical correlations and coefficients were developed based on the experiments with a glycol cooled coil and a refrigerant cooled coil. Hot gas defrosting experiments with different initial and environmental conditions were also done to verify the model and simulation method proposed in this work.

A computer program written using FORTRAN was developed to perform the simulation of defrosting process of evaporators. The analysis and comparison of simulation results with experimental data showed that the prediction of defrosting process characteristics was acceptable.

ACKNOWLEDGEMENTS

The author is sincerely grateful to his supervisors Professor K. I. Krakow and Dr. S. Lin for their guidance and encouragement throughout the effort which has resulted in this thesis. Without their suggestions, ideas, and insight into the problem, the work could not have been concluded such successfully. This research was sponsored by NSERCC grant Nos. STR0032432 and OGP0001656. The author would like to thank the sponsors.

The author would like to thank Mr. Nguyen T. Le who well performed the experimental work and cordially provided a great deal of encouragement, suggestion and support.

Finally, the author wishes to thank his wife, Dong Pei-fang, family and friends for their understanding, encouragement and support throughout his university years.

TABLE OF CONTENTS

LIST OF FIGURES

LIST OF TABLES

NOMENCLATURE

A	inside cross-section area of coil tube
A	constant
A_c	section area of the fin
A_e	effective surface area of the coil
A_f	total surface area of the fin in an element
A_i	tube inside surface area
A_s	effective wetted surface area of the coil
A_t	outside surface area of the tube in an element
B	constant
C	heat capacity of coil and frost or water film
C_c	heat capacity of an element of the coil
C_g	heat capacity of glycol cooled coil and contents
C_o	constant of integration
C_w	conductance of the water/air layer
$C_{w,ref}$	reference conductance of the water/air layer
C_1	constant
C_2	constant
C_3	constant
C_4	constant
c_f	specific heat of frost (ice)
c_{fin}	specific heat of coil fin
c_l	specific heat of water

c_t	specific heat of coil tube
c_{pl}	specific heat of refrigerant liquid at constant pressure
c_{pr}	specific heat of refrigerant at constant pressure
C_{se}	surface evaporation coefficient
D	bend diameter
D_i	tube inside diameter
D_o	tube outside diameter
D_1	fin height
D_2	fin depth
d	tube diameter
dm_f	mass of frost melted during the time interval
dm_w	mass of water vaporized during the time interval
dP_f	pressure drop due to friction
$dP_{f,l}$	frictional pressure drop of the liquid portion of two-phase flow flowing along in the tube
$dP_{f,tp}$	frictional pressure drop of two-phase flow
dP_v	pressure change due to velocity change
dx	length of an element
E	energy
E_c	energy transferred by convection in an element of the coil
E_f	energy required for melting frost in an element of the coil
E_r	total energy supplied by refrigerant for defrosting
E_s	energy stored in coil, frost and water in an element

	of the coil
E_{tot}	total energy required for defrosting process
E_v	energy required for vaporizing water in an element of the coil
E_{zc}	energy required for a whole coil in a time interval
E_{ze}	energy required for defrosting in an element of the coil in a time interval
E_{2mx}	energy required for melting all frost in an element of the coil
E_{3mx}	energy required for vaporizing all surface water in an element of the coil
F	correction factor for two-phase pressure drop
FXT	function as defined by Equation 4.16
F2	function as defined by Equations 4.20 - 4.22
f	friction factor
f_b	resistance factor for the return bends
f_f	resistance factor for the friction
f_t	resistance factor for the turning of the flow
G	mass flux of refrigerant
h_a	air side convective heat transfer coefficient
h_r	convective heat transfer coefficient on the refrigerant side
$h_{r,tp}$	convective heat transfer coefficient for two-phase refrigerant
h_{fg}	enthalpy of vaporization
h_i	enthalpy at the inlet of an element

h_{if}	enthalpy of melting ice
h_j	enthalpy at the outlet of an element
i	index of time interval
i	index of coil surface condition
j	index of stage
k	index of time spent in each state based on wall temperature
k_f	heat conductivity of the fin
k_l	heat conductivity of refrigerant liquid
k_r	heat conductivity of refrigerant
L	length of the fin
M_{mf}	mass rate of melting frost
m_c	mass of condensate
$m_{c,i}$	mass of collected water
m_f	mass of frost on an element
m_{fin}	mass of an element of coil fin
$m_{f,i}$	mass of frost
$m_{f,o}$	initial mass of frost
$m_{f,ref}$	reference mass of frost on an element
$m_{f,ti}$	mass of frost at time ti, the beginning of the time interval
$m_{f,tj}$	mass of frost at time tj, the end of the time interval
m_h	mass of water vaporized by the humidifier
m_{mf}	mass of melted frost
$m_{mf,ref}$	reference mass of melted frost

m_r	mass flow rate of refrigerant
$m_{w,i}$	mass of water held on coil surface
m_t	mass of an element of coil tube
m_v	mass flow rate of water vapour
$m_{v,i}$	mass of vaporized water
m_w	mass of water remaining on the coil surface
$m_{w,o}$	initial mass of water from melted frost
$m_{w,r}$	mass of water remaining on the coil before experiments
$m_{w,ti}$	mass of water at time ti, the beginning of time interval
$m_{w,tj}$	mass of water at time tj, the end of time interval
n	surface evaporation exponent
n_f	number of fins
n_t	number of time intervals
$n_{t,mx}$	maximum number of time intervals
n_{tub}	number of tubes of the coil
n_z	number of space element
Nu	Nusselt number
p	perimeter of the fin
P	pressure
P_i	inlet pressure of an element
P_j	outlet pressure of an element
Pr	Prandtl number
Pr_l	Prandtl number to refrigerant liquid
Q	heat transfer rate

Q_c	convective heat transfer rate from an element of the coil
Q_e	heat transfer rate of electrical heater
Q_f	heat transfer rate to melting frost on an element of the coil
Q_l	rate of heat leaving from an element of the coil
Q_r	heat transfer rate from the refrigerant
Q_s	rate of heat stored in an element of the coil
Q_v	heat transfer rate to vaporizing water on an element of the coil
Re	Reynold number
Re_l	Reynold number to refrigerant liquid
$Re_{,tpl}$	Reynold number for two-phase liquid portion
RH	relative humidity
r_{sv}	ratio of coil surface vaporization
St	Stanton number
T	average temperature of coil and frost or water film
T_i	inlet refrigerant temperature
T_a	ambient temperature
T_f	temperature of frost
T_o	initial temperature of frost
T_r	refrigerant temperature
T_w	coil wall temperature
T_{wi}	wall temperature at time ti
T_{wo}	initial wall temperature
$T_{w\infty}$	coil wall temperature corresponding to the time

	intending to infinity
t	fin thickness
t	time
t_d	total defrosting time
ti	beginning of time interval
tj	end of time interval
t_{ref}	reference time
u	refrigerant velocity
u_i	refrigerant velocity at the inlet of an element
u_j	refrigerant velocity at the outlet of an element
v	specific volume of refrigerant
v_f	specific volume of refrigerant liquid
v_g	specific volume of refrigerant vapour
v_i	specific volume of refrigerant at the inlet of an element
v_j	specific volume of refrigerant at the outlet of an element
x	quality of refrigerant
x_i	initial refrigerant quality
XTT	function as defined by Equation 4.17
δt_i	time interval
δt_j	time spent in each stage
$\delta t_{j,k}$	time spent in each state based on wall temperature
$\delta t_{j,1}$	time spent in state with $T_w < T_s$
$\delta t_{j,2}$	time spent in state with $T_w = T_s$
δt_1	time spent in stage 1

δt_2	time spent in stage 2
δt_3	time spent in stage 3
δt_4	time spent in stage 4
η_d	defrosting efficiency
η_f	fin efficiency
θ	temperature difference
θ_{ref}	reference temperature difference
μ_f	dynamic viscosity of refrigerant liquid
μ_v	dynamic viscosity of refrigerant vapour
μ_r	dynamic viscosity of refrigerant
ρ	refrigerant density
ρ_{fin}	density of fin material
ρ_t	density of tube material
ρ_{va}	water vapour density corresponding to air temperature
ρ_{vs}	saturated water vapour density corresponding to wall temperature

CHAPTER 1

INTRODUCTION

When an evaporator uses air as source, moisture will deposit on the surface if its surface temperature is below the dew-point temperature of the air, and frost will form on the surface if its surface temperature is below 32 degree Fahrenheit (0°C). The deposition of frost on the evaporator's surface is detrimental to the performance of the evaporator and system. The frost layer reduces the air flow area and increases the air flow resistance. As a result, the quantity of air passing through the coil is decreased. Reduced air flow rate results in a decrease of the heat transfer capacity of the evaporator and the capacity of the system containing the evaporator. Therefore, the frost layer that grows on the cooled surface of the evaporator cannot be permitted to grow without limits but must be removed. Defrosting is required for the operation of air source heat pumps and refrigerating systems with frost formation in order to maintain the capacity of the evaporator and systems.

Defrosting can be done in a number of ways, such as hot gas refrigerant reversed cycle defrosting, hot gas refrigerant bypass defrosting and electrical heating element defrosting.

The most common method of defrosting is hot gas refrigerant defrosting. High temperature superheated

refrigerant is used as the source of energy to melt the frost. Superheated refrigerant from the compressor is directed to the frosted evaporator. Heat from the hot refrigerant transfers to the cooled coil, then to frost layer, warming up frost, melting frost, and evaporating remaining water from melted frost on the coil. During the process of hot gas defrosting, the evaporator acts as a "condenser". Heat transfer progresses with refrigerant condensation. Superheated refrigerant vapour enters the coil and leaves as subcooled liquid or two-phase mixture, undergoing a change of phase. The surface condition of the evaporator is also changed with the defrosting process progressing. A frosted surface becomes a melting frost surface, a wet surface, then a dry surface. Melting frost and evaporating water from melted frost undergo a change of phase, from solid to liquid, from liquid to vapour. At a given time, the entire surface of the evaporator might not be under the same condition. The surface near the inlet of the evaporator may be dry and that near the exit frosted while wet and melting frost surface regions exist in between the inlet area and exit area, since the heat transfer between refrigerant and frost is not uniform, and decreases along the coil. The surface condition of the evaporator from the inlet to the exit progresses from dry, wet, melting frost to frosted. Therefore, the defrosting process is a both time dependent and spacial process with phase change on both refrigerant and air sides.

In this thesis, a numerical model of a defrosting

evaporator is developed for inclusion in system analysis programmes. The model is based on theoretical heat transfer analysis and experimental investigation. The model is also based on the initial conditions, such as refrigerant state and air side surface conditions. For simulation, process data, such as defrosting time, heat transfer rate, refrigerant entering and leaving conditions, air side surface conditions, pressure change, amount of frost, melted frost, surface water and evaporated water, etc., are desired. These data could be obtained by computation, and parameters required for calculation are from theoretical analysis and experiments. The heat transfer coefficient on the refrigerant side is calculated by using suitable equations from literature. Air side heat transfer coefficients are determined by experiments with a glycol cooled, electrically defrosted coil. The entire surface of the glycol cooled, electrically defrosted coil is at the same condition (frosted, wet, or dry) at a given time enabling heat transfer coefficients to be determined. Hot gas defrosting experiments were done to verify the theory and model proposed in this thesis.

In this thesis, the defrosting process is considered as a two dimensional process involving time and space. In order to simulate the time dimension, the evaporator defrosting process is treated as a quasi-static process. The continuous process is divided into a number of small time intervals. For each time interval, computation of heat and mass transfer,

refrigerant state and other parameters is done. Calculated results at one time interval are used for the next time interval. In order to simulate the spacial dimension, the evaporator is subdivided into a large number of elements along the coil tube. A finite element method is used for computation. Parameters, such as heat transfer coefficients, heat transfer rate, refrigerant state and air side surface conditions, will vary from one element to the next element. The calculated output data from one element are the input data for the next element. Combining all results from time and space, a transient dynamic defrosting process might be simulated. Process data, such as required defrosting time, heat transfer and mass transfer, could be obtained.

This research concentrates on the defrosting model, defrosting process and characteristics under different conditions. The model and process simulation such as described are not found in the recent literature.

CHAPTER 2

LITERATURE SURVEY

2.1 Introduction

A large amount of literature exists, indicating the progress over the years, in this field. In this chapter, the works of various investigators are discussed. Among them, however, only Sanders (1974) did an analytical investigation of the defrosting process, which was directly related to this research. The experimental investigations by Stoecker (1983), Niederer (1976), Miller (1982, 1984, 1987), and Bouma (1979) were mainly concerning the performance and characteristics of defrosting. Literature by Hiller (1976), Ellison (1981), and Anand (1982) showed theories and suitable formulas accurately predicting the behaviour of a condenser, which were partly used for the simulation of the refrigerant side of a coil being defrosted since an evaporator would act as a condenser when in defrosting.

2.2 Sanders' Defrosting Model

The most extensive work into the defrosting process is the Ph.D. dissertation by Sanders (1974). He notes that defrosting is essentially a non-stationary process. The melting of the frost layer takes place on the side where the heat is supplied. The resulting water from melting will

initially be absorbed in the frost layer. Free water occurs when the frost layer has become saturated with water from melting. The thickness of the frost layer changes continuously by melting.

Sanders recognizes that it is very difficult to approach the real defrosting process theoretically because it is not known whether the frost layer sticks to the wall or whether air gaps occur between the melting frost layer and the wall. Therefore simplified models for a one-dimensional case are developed for two types of defrosting, constant medium (source) temperature and constant heat flux. Hot gas defrosting is considered to be an approximate constant defrosting medium temperature model and electrical element defrosting an approximate constant heat flux model.

The defrosting process of Sanders' model is divided into two stages. The first stage is the period to raise the temperature of the system to 32°F (0°C). The second stage involves the melting of the frost layer.

The first stage of the defrosting process is common for all models. A heat balance is carried out on the wall. Heat is supplied from the refrigerant side, stored in the heat exchanger wall, and convected to the surroundings if the surface temperature of the frost layer is higher than the ambient temperature. The heat capacity of the frost layer and heat resistance of the wall are neglected.

The second stage is subdivided into two cases. The first

case considers that a frost layer sticks to the heat exchanger wall. In other words, there is no air gap between the wall and frost layer, which corresponds to the ideal situation for defrosting, minimum defrosting time and maximum defrosting efficiency. The second case considers that there is an air gap between the wall and frost layer, which corresponds to the worst situation of defrosting, maximum defrosting time and minimum defrosting efficiency.

In the first case, at the moment that the wall temperature reaches the melting point, frost starts to melt and melting water is immediately absorbed by the frost layer. During frost melting the frost layer is assumed to stick to the wall and the surface temperature of the frost layer is assumed to remain at the melting point. With constant heat flux the frost layer is melted. During the process, heat losses to the surroundings are considered, and the heat resistance of the frost layer with absorbed melting water is neglected.

In the second case, when melting starts, the frost layer loosens from the wall creating an air gap between the wall and the frost. At the beginning of the melting period, the frost layer will be saturated with melting water at the melting point. Freezing will occur on the outside surface of the frost layer, which is saturated with water (melted frost), to form a small ice layer on the frost air interfacing surface because the surrounding air temperature is lower than freezing point.

Heat transfer takes place from the exposed surface to the surroundings by free convection. Heat transfers through the air gap to the frost layer by conduction and radiation, melting frost gradually. The ice layer grows on the side of the layer exposed to coil wall with the water in the frost subsequently freezing to ice. It is assumed that no heat transfer takes place through the frost layer in the duration of melting process. All energy is absorbed by melting process.

Sanders notes that only very approximate conclusions may be drawn from his defrosting models. The defrosting models for the second stage are very hypothetical. In fact, defrosting of coil is not homogeneous. The phenomenon of loosening of the frost layer does not occur at all places, but only locally. The defrosting of frost layer where air gaps do occur determines the defrosting time of the coil. For thick frost layers the possibility of air gaps occurring is greater, however, thick frost layers may yield higher defrosting efficiencies than thin frost layers. For thin frost layers, frost mostly sticks to the coil wall. Shorter defrosting times can be expected, but lower defrosting efficiencies might occur.

Sanders derives equations with assumptions and initial conditions to estimate the defrosting time. From the analysis of the calculation results Sanders notes that the difference between maximum and minimum possible defrosting time for defrosting with constant heat flux (electric defrosting) is

not as great as that for defrosting with constant defrosting medium temperature (hot gas defrosting), which sometimes differs by a factor 100. The defrosting time for defrosting with constant heat flux is generally much longer than that for defrosting with constant defrosting medium temperature.

The defrosting efficiency, heat required for defrosting and economic analysis of different defrosting systems are also discussed in Sanders' paper.

2.3 Performance and Characteristics of Defrosting

Stoecker (1983) does investigations to identify some features that could reduce the energy requirements associated with hot gas defrosting and make the defrosting process more efficient. The experimental results show that the pressure differences across the coil lower than that typically employed will achieve a satisfactory defrost. However, when the hot gas pressure is low, it is reasonable to expect the rate of defrost to be slower. There may be other reasons to artificially maintain a high condensing pressure, but as far as the defrosting process is concerned, a hot gas pressure 15 psi (100 kPa) above the setting of the outlet pressure regulator is probably adequate in an ammonia or R-22 system. Stoecker notes that the efficiency of the hot gas defrosting, defined as the ratio of energy actually needed to perform the defrost to that transferred from the hot gas during the entire defrosting cycle, is low. Stoecker cites from Niederer (1976)

that the efficiency is between 15% and 25%. And Stoecker's experimental results prove that Niederer's figure appears to be valid. Stoecker notes that the necessary energy to perform the defrost is attributed to raising the temperature of the frost, melting it, and warming the melting water to the leaving temperature. In addition, a necessary operation is to bring the coil metal from its refrigerating temperature up to its final temperature at the end of the defrosting cycle. The energy losses during the defrosting are the heat transferred from the warm coil to the refrigerated space and the compressor power required to restore the refrigerant to the hot gas pressure.

The defrosting effects on coil heat transfer are studied by Niederer (1976). Tests indicate that only 15% to 25% of the heat required to defrost actually is carried out by the condensate. The rest is heat losses to the environment surrounding the unit and to heat the metal of the coil and cabinet of the air cooler.

Miller (1982) studies the base-case performance of a high-efficiency, air-to-air split-system residential heat pump of nominal 3-ton capacity and the characteristics of some of its components under both steady-state and frosting-defrosting conditions. The concept that demand defrosting control could feasibly reduce both frosting and defrosting energy losses is developed from experimental data. Experimental results also reveal that the loss in performance due to defrosting is small

for the ambient temperature of 40°F (4.4°C) or less and the relative humidity less than 70%.

Miller (1984) further notes that frosting and defrosting losses are insignificant for all laboratory tests conducted with outdoor relative humidity of 60% or less. However, the use of auxiliary heat during defrosting periods causes significant cumulative reductions in the performance of a heat pump.

It is noted by Miller (1987) that the degradation in performance due to coil frosting is small, only 1% to 5% degradation in capacity for the tube-and-plate-fin outdoor coil of the tested heat pump. The seasonal analysis clearly shows that frequent defrosting causes the frosting-defrosting degradation which is primarily due to the defrosting of the outdoor coil. Therefore, in order to lower seasonal losses due to frosting-defrosting, defrosting time intervals could possibly be extended at the expense of greater frosting losses, provided the system reliability would not be compromised. The results from the investigation through seasonal analysis also show that the demand-defrost control yields better seasonal efficiency than that the normal time-temperature defrost control does.

The need for defrosting clearly depends on the rate of frosting and thus on the air conditions. Bouma (1979) notes that, taking into account the usual temperature difference between air and refrigerant, frost formation occurs at the air

temperature below about 42.8°F (6°C) and at the air humidity above about 73%. On account of the high absolute humidity, the air temperature range between 19.4°F (-7°C) and 35.6°F (2°C) is very important for the frosting and defrosting of outdoor coils, because severe frosting happens at this temperature range. Bouma notes that at the temperature above 35.6°F (2°C) most of frost will melt during the off-periods of the heat pump. Defrosting of outdoor coil seems to be not required. At the temperature below 19.4°F (-7°C) frost formation could be negligible because of the low absolute humidity of the air, therefore, defrosting of outdoor coil is not or seldom necessary. The behaviour of the outdoor coil of a heat pump during frosting and hot gas defrosting is investigated by Bouma in laboratory. It appears that no real defrosting problems occur at none of the test air conditions, and it takes the longest time to defrost in the case of the lowest air temperature.

2.4 Condenser Models

In hot gas defrosting, the evaporator is working as a condenser. The refrigerant side behaviour of an evaporator can be simulated using some condenser model theories.

A general model of condensers is proposed by Hiller (1976), which is used to determine heat transfer performance of cross-flow type condensers. Three heat transfer regions, superheating (single phase vapour), condensing (two-phase),

and subcooling (single phase liquid) could be divided in a normal condenser. Hiller notes that the most important factor governing the condenser performance is the location of the two-phase region in the air flow, since the amount of two-phase heat transfer is much greater than that of single-phase heat transfer. Hiller suggests that the heat transfer coefficients of single phase vapour and liquid may be determined using a fully developed flow correlation such as by McAdams (1954). However, he notes that the actual average heat transfer coefficient may be slightly higher than that found using the above mentioned relation because of entrance effects. For the two-phase region Hiller suggests to use condensation heat transfer relations developed by Traviss (1973), which have been developed for forced convection condensation inside tubes, in laminar, transition, and turbulent flow regimes. Heat transfer correlations for the air side must be determined for each design studied because it varies with the condenser design.

A model of an air-cooled, cross-flow, finned tube condenser with staggered round tubes is further developed by Hiller, which considers the condenser geometry and real flow conditions. The modified expressions for heat transfer coefficients and pressure drop are obtained. The performance predictions of the model are compared to published performance data of a real product. Accuracy is within 5% over the entire heat pump operating range.

A computer model for air-cooled refrigerant condensers with specified refrigerant circuiting is presented by Ellison (1981), based on a tube-by-tube computation approach. The thermal and fluid-flow performance of each tube (the length of tube between two return bends in the conventional geometry) is computed individually, based on the local temperature and heat transfer coefficient.

Ellison notes that for the two-phase region (vapour quality range $0.1 < x < 0.95$) the correlations developed by Traviss are used to calculate the condensing heat transfer coefficient. For the liquid and superheated vapour regions conventional single-phase heat transfer relationships for the turbulent flow in circular tubes are used. Between these regions ($0 \leq x \leq 0.1$ or $0.95 \leq x \leq 1.0$) the heat transfer coefficient is computed by linear interpolation. Ellison notes that in the superheated vapour region, the tube wall temperature may sometimes fall to or below the refrigerant saturation temperature while the bulk temperature of the refrigerant remains above the saturation temperature. In this case, the heat transfer coefficient is computed as though the refrigerant were in two-phase flow with a vapour quality of 0.99.

Friction pressure drop in the straight sections of the tubes is calculated by the method of Lockhart and Martinelli (1949), and pressure drop in the return bends by the method of Pierre (1964).

Two condensers are calculated and analyzed by this model. Calculated quantities agree quite well with condenser performance parameters measured in the laboratory. Therefore, Ellison recommends the model for detailed design analyses or the performance simulation of existing condensers which have complex refrigerant circuiting or unusual air-side geometries.

Anand (1982) proposes a steady state simulation scheme for an externally finned single-tube condenser. In comparison with other computer models, this simulation scheme not only considers variation of fluid properties, friction factor, and heat transfer coefficient due to change of phase, but also considers thermodynamic and flow properties of the refrigerant and the temperature of the air flowing over the condenser to be a function of distance using a finite difference method.

A small control volume, in which the middle sections of the two adjacent fins are assumed vertical boundaries, is used as an element for calculation. A partially implicit method with a weighing factor of 0.5 is chosen. A group of six nonlinear governing equations, including continuity equation for the refrigerant, momentum equation for the refrigerant, energy equations for the refrigerant, tube and air, and state equations for the refrigerant enthalpy and density, is solved using the "Secant" method. Heat transfer coefficients for single-phase refrigerant and air are computed using correlations given by Hiller, and that for two-phase refrigerant by Traviss.

A general equation derived from momentum theorem is used to computed single phase friction pressure drop. The friction factor is from Moody's diagram. The equation for two-phase friction pressure drop is similar to that used in the single-phase flow. The two-phase friction factor is also obtained from Moody's diagram based on the smoothness of the tube and two-phase flow Reynolds number.

Anand notes that the predictions of the simulation program are found to be consistent with the physics of the system although experimental results are not available for the comparison.

CHAPTER 3

HEAT AND MASS TRANSFER THEORY

3.1 Overview

A defrosting process is an unsteady process. It varies not only with time but also with space. It is very difficult to approach a real process. First of all, frost is a porous substance. Its properties, such as density, are variables of its environmental conditions. Secondly, the initial distribution of frost on the evaporator may not be uniform. Thirdly, when frost melts, mass transfer occurs. Part of water from melted frost drains due to gravity. The remaining water on the coil surface forms a water film. The water film may not be uniform. Therefore, the real defrosting process is not homogeneous. It is too complex for detailed theoretical analysis, and an idealized defrosting process model must be considered.

In order to simplify and approach the real process, an idealized evaporator coil is considered as a combination of a large number of elements taken in the direction of the refrigerant flow. Parameters are assumed constant for each element but vary from element to element. For each element, heat transfers from refrigerant to coil wall, from coil wall to frost layer or water (melted frost), and to the surroundings. During the process, some of heat from

refrigerant is stored in the coil and frost layer or water film, resulting in the rise of their temperature.

In hot gas defrosting, superheated refrigerant vapour enters a coil. As it flows through the coil, refrigerant becomes two-phase mixture since it releases heat with condensation. Finally, refrigerant leaves the coil in subcooled liquid state. Therefore, inside an element, refrigerant may exist in one of three conditions: superheated, two-phase or subcooled. Under superheated condition, refrigerant is in vapour state and sensible heat transfer occurs. Under two-phase conditions, vapour and liquid refrigerant coexist in physical equilibrium, and latent heat transfer occurs with condensation. Under subcooled condition, refrigerant is in liquid state and sensible heat transfer occurs.

On the outside of an element, the surface may exist in one of four conditions: subcooled frost, melting frost, wet, or dry. The model of the defrosting process on an outside surface is based on observations of experiments with a glycol cooled, electrically defrosted coil. The experimental results reveal that defrosting process may be separated into four stages based on surface conditions. The curve of surface temperature versus time obtained experimentally from a glycol cooled, electrically defrosted coil, shown in Fig.3.1, indicates the defrosting characteristics. The surface temperature shown in Fig.3.1 is an average of temperatures

obtained from four measuring points. The experimental curve is idealized for discussion as shown in Fig.3.2. The defrosting process from point 1 to point 2 is considered as the preheating stage. Supplied energy is to preheat the subcooled frost and coil to the temperature of melting point. The process from 2 to 3 is considered as the melting frost stage. Supplied energy is to melt frost. The process from 3 to 5 is considered as the wet surface stage. Supplied energy is for warming up and vaporizing water remaining on the coil surface. There appears to be essentially no vaporization during the process from 3 to 4 because of low surface temperature, and increasing vaporization during the process from 4 to 5. The dry surface stage is from 5 to 6. Energy is stored in coil and increases the coil wall temperature. It is obvious, from Fig.3.1 and Fig.3.2, that the surface temperature increases continuously during the whole defrosting process. It means that some of energy must be stored in the coil at any stage.

In general, the total heat supplied for defrosting can be divided into two parts. One part is the heat stored in the coil and water, and another part is the heat leaving from the coil.

In the glycol cooled, electrically defrosted coil experiment, the total heat supplied for defrosting is converted from electrical energy, and is kept to be constant during the process. The more the heat stored in the coil, the less the heat leaving the coil. The stored heat is

proportional to the rate of change of surface temperature with time, which is the slope of the surface temperature versus time curve. The greater the rate of slope, the greater the stored heat. Therefore, the heat leaving from the coil is inversely proportional to the rate of change of surface temperature with time. If the rate is high, the amount of leaving heat will be small, and if the rate is low, the amount of leaving heat will be large. It is found that the curve of process 2-3 is approximately linear and has the lower slope rate in comparison with other stages, which means that highest heat transfer rate to the frost and lowest thermal storage rate take place at this stage. It is also found that the curves of the process 1-2, 3-4, and 5-6 have approximately the same slopes. A conclusion might be made that the heat transfer rate for melting frost (process 2-3) has the highest value, comparing with other stages. The heat transfer coefficients for subcooled frost surface (process 1-2), wet surface without vaporization (process 3-4) and dry surface (process 5-6) have similar values.

3.2 Heat and Mass Transfer in Hot Gas Defrosting

The general equation of heat balance for a refrigerant defrosted coil is

$$Q_r = Q_s + Q_l \tag{3.1}$$

where

Q_r = heat transfer rate from the refrigerant

Q_s = rate of heat stored in an element of the coil

Q_l = rate of heat leaving from an element of the coil

The heat leaving from the coil may be in following ways: heat for convection, heat for melting frost, and heat for vaporizing water, that is

$$Q_l = Q_c + Q_f + Q_v \tag{3.2}$$

where

Q_c = convective heat transfer rate from an element of the coil

Q_f = heat transfer rate to melting frost on an element of the coil

Q_v = heat transfer rate to vaporizing water on an element of the coil

Substituting Equation 3.2 into Equation 3.1, the general equation for heat transfer during hot gas defrosting process becomes

$$Q_r = Q_s + Q_c + Q_f + Q_v \tag{3.3}$$

The heat transfer rates of different stages of process are treated as follows:

Stage 1, preheating stage (process 1-2), shown in Fig.3.3,

$$Q_r = Q_s + Q_c \tag{3.4}$$

For this stage, heat for melting frost is equal to zero, and heat for vaporizing water is assumed to be equal to zero, that is

$$Q_f = 0 \tag{3.5}$$

$$Q_v = 0 \tag{3.6}$$

Stage 2, melting frost stage (process 2-3), shown in Fig.3.4,

$$Q_r = Q_s + Q_f \tag{3.7}$$

For this stage, convective heat transfer and vaporizing heat transfer are assumed negligible, that is

$$Q_c = 0 \tag{3.8}$$

$$Q_v = 0 \tag{3.9}$$

Stage 3, wet surface stage (process 3-5), shown in Fig.3.5,

$$Q_r = Q_s + Q_c + Q_v \tag{3.10}$$

For this stage, heat for melting frost is equal to zero, that is

$$Q_f = 0 \tag{3.11}$$

Stage 4, dry surface stage (process 5-6), shown in Fig.3.6,

$$Q_r = Q_s + Q_c \tag{3.12}$$

For this stage, heat for melting frost and heat for vaporizing water are equal to zero, that is

$$Q_f = 0 \tag{3.13}$$

$$Q_v = 0 \tag{3.14}$$

3.2.1 Refrigerant side heat transfer

In hot gas defrosting, the total heat supplied for defrosting can be calculated as follows:

$$Q_r = h_r \cdot A_i \cdot (T_r - T_w) \tag{3.15}$$

where

h_r = convective heat transfer coefficient on the refrigerant side

A_i = tube inside surface area

T_r = refrigerant temperature

T_w = coil wall temperature

Refrigerant may be in one of three states: superheated, two-phase, or subcooled. Correspondingly, the heat transfer coefficient of refrigerant has different value for different state, and is obtained from different equations.

3.2.2 Thermal storage

The thermal storage is defined as

$$Q_s = C \cdot (dT/dt) \tag{3.16}$$

where

C = heat capacity of coil and frost or water film

T = average temperature of coil and frost or water film

t = time

The average temperature of coil and frost or water film is assumed to be equal to the coil wall temperature, that is

$$T = T_w \tag{3.17}$$

The evaporator surface during defrosting may have one of four conditions: subcooled frost, melting frost, wet and dry. Therefore, the heat capacity may change according to the surface condition which separates the process into corresponding stages. The heat capacity of frost during the preheat stage (process 1-2) could be considered as constant. However, the heat capacity of water from melted frost is a variable and a function of time. When frost starts to melt (melting frost stage, process 2-3), water from melted frost is

absorbed by frost layer. When the frost layer is saturated, free water exists. Part of free water drains by gravity. Part of it remains on the coil surface and forms a wet surface. The thermal storage of water from melted frost may be negligible in this stage. In wet surface stage (process 3-5), the amount of remaining water on the coil surface after all frost of an element is melted is a required input datum for the computation. It may be estimated experimentally. During the process 4-5, vaporization of surface water takes place. The amount of water remaining on the coil surface is decreasing with vaporizing. Therefore, the heat capacity of water from melted frost decreases with defrosting process progressing. In dry surface stage (process 5-6), there is no water at all on the coil surface. The heat capacity of an evaporator coil is only considered. The heat capacity for each stage is as follows:

Stage 1, preheating stage (process 1-2),

$$C = C_c + c_f \cdot m_f \tag{3.18}$$

where

C_c = heat capacity of an element of the coil

c_f = specific heat of frost (ice)

m_f = mass of frost on an element

Stage 2, melting frost stage (process 2-3),

$$C = C_c + c_l \cdot m_{w,o} \tag{3.19}$$

where

c_l = specific heat of water

$m_{w,o}$ = initial mass of water from melted frost

During this stage, the temperature of frost is assumed to be constant, melting point temperature, and no more heat will be stored in frost. Since the actual amount of water from melted frost varies and is indeterminable due to drainage, the initial value of mass of water from melted frost is assumed. The value is a required input datum and is based on the experimental result.

Stage 3, wet surface stage (process 3-5),

$$C = C_c + c_1 \cdot m_w \tag{3.20}$$

where

m_w = mass of water remaining on the coil surface

The mass of water remaining on the coil surface is time dependent, which will be discussed in Section 5.3.

Stage 4, dry surface stage (process 5-6),

$$C = C_c \tag{3.21}$$

The heat capacity of an element of the coil is constant for a given coil, that is

$$C_c = c_t \cdot m_t + c_{fin} \cdot m_{fin} \tag{3.22}$$

where

c_t = specific heat of coil tube

m_t = mass of an element of coil tube

c_{fin} = specific heat of coil fin

m_{fin} = mass of an element of coil fin

3.2.3 Convective heat transfer

The convective heat transfer can be expressed as follows:

$$Q_c = h_a \cdot A_e \cdot (T_w - T_a) \tag{3.23}$$

where

h_a = air side convective heat transfer coefficient

A_e = effective surface area of the coil

T_a = ambient temperature

As mentioned before, air side convective heat transfer coefficients for the process 1-2, 3-5, and 5-6 are approximately equal. The fin efficiency should be considered in the calculation of effective surface area of a coil with fins, that is

$$A_e = A_t + \eta_f \cdot A_f \tag{3.24}$$

where

A_t = outside surface area of the tube in an element

A_f = total surface area of the fin in an element

η_f = fin efficiency

The fin efficiency is the function of fin geometry, fin thermal conductivity and air side convective heat transfer coefficient. It may be evaluated for rectangular plate fin using the method for plate fin with adiabatic tip introduced by McQuiston (1975), that is

$$\eta_f = \tanh(mL) / (mL) \tag{3.25}$$

$$m = [(h_a \cdot p)/(k_f \cdot A_c)]^{1/2} \tag{3.26}$$

where

h_a = air side convective heat transfer coefficient

p = perimeter of the fin

k_f = heat conductivity of the fin

A_c = section area of the fin

L = length of the fin

3.2.4 Conductive heat transfer

During the melting frost stage (process 2-3), the temperature of the coil wall increases, and the temperature of frost layer is constant, keeping at the melting point. With the increase of the coil wall temperature, frost near the wall begins to melt. A layer of water and entrained air is assumed existing between the wall and frost layer. Conductive heat transfer occurs within this layer. It may be calculated as follows:

$$Q_f = C_w \cdot A_e \cdot (T_w - T_f) \tag{3.27}$$

where

C_w = conductance of the water/air layer

T_f = temperature of frost, 32°F (0°C)

This correlation is empirical and the conductance C_w may be determined experimentally. It is found that the conductance of the water/air layer is a variable since the water/air layer is changing with defrosting process progressing. It is observed from experiments that the coil wall temperature varies linearly with defrosting time. Considering these facts, an empirical equation is yielded with a linear variation of the

wall temperature with defrosting time as follows:

$$C_w = C_{w,ref}/(1 - m_f/m_{f,ref}) \quad (3.28)$$

where

$C_{w,ref}$ = reference conductance of water/air layer

$m_{f,ref}$ = reference mass of frost on an element

3.2.5 Vaporizing heat transfer

The heat transfer due to vaporization is

$$Q_v = m_v \cdot h_{fg} \quad (3.29)$$

where

h_{fg} = enthalpy of vaporization

m_v = mass flow rate of water vapour

The mass flow rate of water vapour leaving the coil surface is assumed to be proportional to the vapour concentration gradient and is estimated as follows:

$$m_v = C_{se} \cdot A_s \cdot (\rho_{vs} - \rho_{va}) \quad (3.30)$$

where

C_{se} = surface evaporation coefficient

ρ_{vs} = saturated water vapour density corresponding to wall temperature

ρ_{va} = water vapour density corresponding to air temperature

A_s = effective wetted surface area of the coil

As an approximation, effective wetted surface area of the coil is considered as follows:

$$A_s = A_e \cdot (m_w/m_{w,o})^n \quad (3.31)$$

where

n = surface evaporation exponent

This correlation is empirical and the surface evaporation coefficient, initial mass of water on the coil surface, and surface evaporation exponent, may be determined experimentally.

3.3 Heat Transfer Governing Differential Equations

Combining equations related to the heat transfer based on given conditions and assumptions yields heat transfer differential equations for each stage:

For stage 1, preheating stage, combining Equations 3.4, 3.15, 3.16, 3.17, and 3.23 yields

$$h_r \cdot A_i \cdot (T_r - T_w) = C \cdot (dT_w/dt) + h_a \cdot A_a \cdot (T_w - T_a) \quad (3.32)$$

For stage 2, melting frost stage, combining Equations 3.7, 3.15, 3.16, 3.17, and 3.27 yields

$$h_r \cdot A_i \cdot (T_r - T_w) = C \cdot (dT_w/dt) + C_w \cdot A_a \cdot (T_w - T_r) \quad (3.33)$$

For stage 3, wet surface stage, combining Equations 3.10, 3.15, 3.16, 3.17, and 3.23 yields

$$h_r \cdot A_i \cdot (T_r - T_w) = C \cdot (dT_w/dt) + h_a \cdot A_a \cdot (T_w - T_a) + Q_v \quad (3.34)$$

For stage 4, dry surface stage, combining Equations 3.12, 3.15, 3.16, 3.17, and 3.23 yields

$$h_r \cdot A_i \cdot (T_r - T_w) = C \cdot (dT_w/dt) + h_a \cdot A_a \cdot (T_w - T_a) \quad (3.35)$$

The above differential Equations, 3.32 to 3.35, can be generalized as follows:

$$dT_w/dt + A \cdot T_w = B \quad (3.36)$$

where

A = constant, dimension of (1/time)

B = constant, dimension of (temperature/time)

which are determined by heat transfer coefficients, areas for both sides, air temperature or frost temperature, and heat capacities. The heat capacities are dependent on the stage.

The general solution of differential Equation 3.36 is

$$T_w = B/A + C_o \cdot e^{-A \cdot t} \tag{3.37}$$

where

C_o = constant of integration

The boundary conditions for differential Equation 3.36 are as follows:

At $t = 0$,

$$T_w = T_{wo} \tag{3.38}$$

$$e^{-A \cdot t} = 1$$

where

T_{wo} = initial wall temperature

Substituting initial conditions into Equation 3.37 yields

$$C_o = T_{wo} - B/A \tag{3.39}$$

As time intends to infinity, that is

$$t \dashrightarrow \infty \tag{3.40}$$

Equation 3.37 yields

$$T_w = B/A = T_{w\infty} \tag{3.41}$$

where

$T_{w\infty}$ = coil wall temperature corresponding to the time intending to infinity

Substituting Equation 3.39 and 3.41 into 3.37 yields the general equation for the coil wall temperature, that is

$$T_w = T_{w\infty} \cdot (1 - e^{-A \cdot t}) + T_{wo} \cdot e^{-A \cdot t} \tag{3.42}$$

For stage 1,

$$A = (h_r \cdot A_i + h_a \cdot A_a) \; / \; (C_c + c_f \cdot m_f) \tag{3.43}$$

$$B = (h_r \cdot A_i \cdot T_r + h_a \cdot A_a \cdot T_a) \; / \; (C_c + c_f \cdot m_f) \tag{3.44}$$

$$T_{w\infty} = (h_r \cdot A_i \cdot T_r + h_a \cdot A_a \cdot T_a) \; / \; (h_r \cdot A_i + h_a \cdot A_a) \tag{3.45}$$

For stage 2,

$$A = (h_r \cdot A_i + C_w \cdot A_a) \; / \; (C_c + c_l \cdot m_{w,o}) \tag{3.46}$$

$$B = (h_r \cdot A_i \cdot T_r + C_w \cdot A_a \cdot T_f) \; / \; (C_c + c_l \cdot m_{w,o}) \tag{3.47}$$

$$T_{w\infty} = (h_r \cdot A_i \cdot T_r + C_w \cdot A_a \cdot T_f) \; / \; (h_r \cdot A_i + C_w \cdot A_a) \tag{3.48}$$

For stage 3,

$$A = (h_r \cdot A_i + h_a \cdot A_a) \; / \; (C_c + c_l \cdot m_w) \tag{3.49}$$

$$B = (h_r \cdot A_i \cdot T_r + h_a \cdot A_a \cdot T_a - Q_v) \; / \; (C_c + c_l \cdot m_w) \tag{3.50}$$

$$T_{w\infty} = (h_r \cdot A_i \cdot T_r + h_a \cdot A_a \cdot T_a - Q_v) \; / \; (h_r \cdot A_i + h_a \cdot A_a) \tag{3.51}$$

For stage 4,

$$A = (h_r \cdot A_i + h_a \cdot A_a) \; / \; C_c \tag{3.52}$$

$$B = (h_r \cdot A_i \cdot T_r + h_a \cdot A_a \cdot T_a) \; / \; C_c \tag{3.53}$$

$$T_{w\infty} = (h_r \cdot A_i \cdot T_r + h_a \cdot A_a \cdot T_a) \; / \; (h_r \cdot A_i + h_a \cdot A_a) \tag{3.54}$$

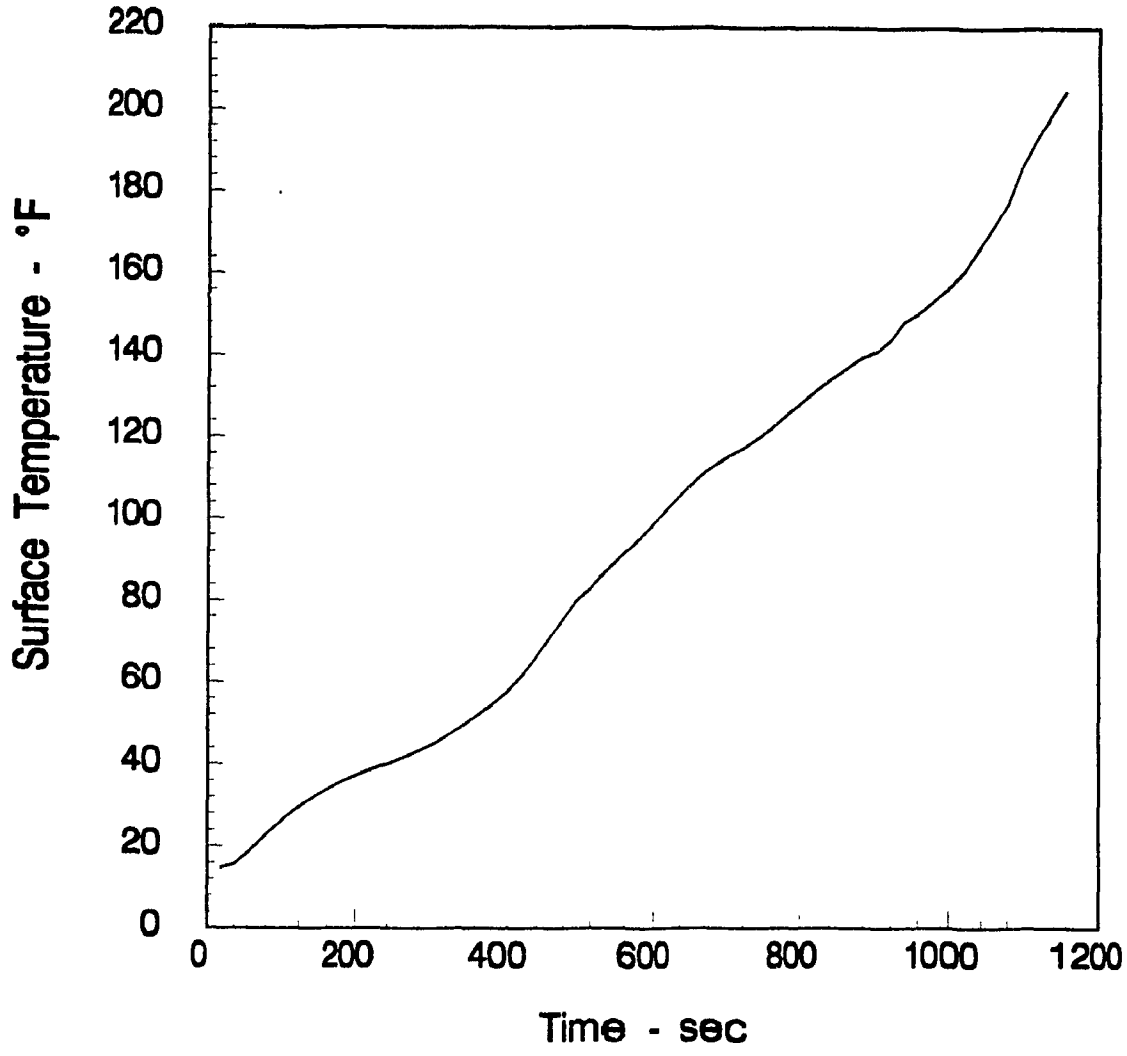

Figure 3.1 Experimental Curve of Temperature versus Time

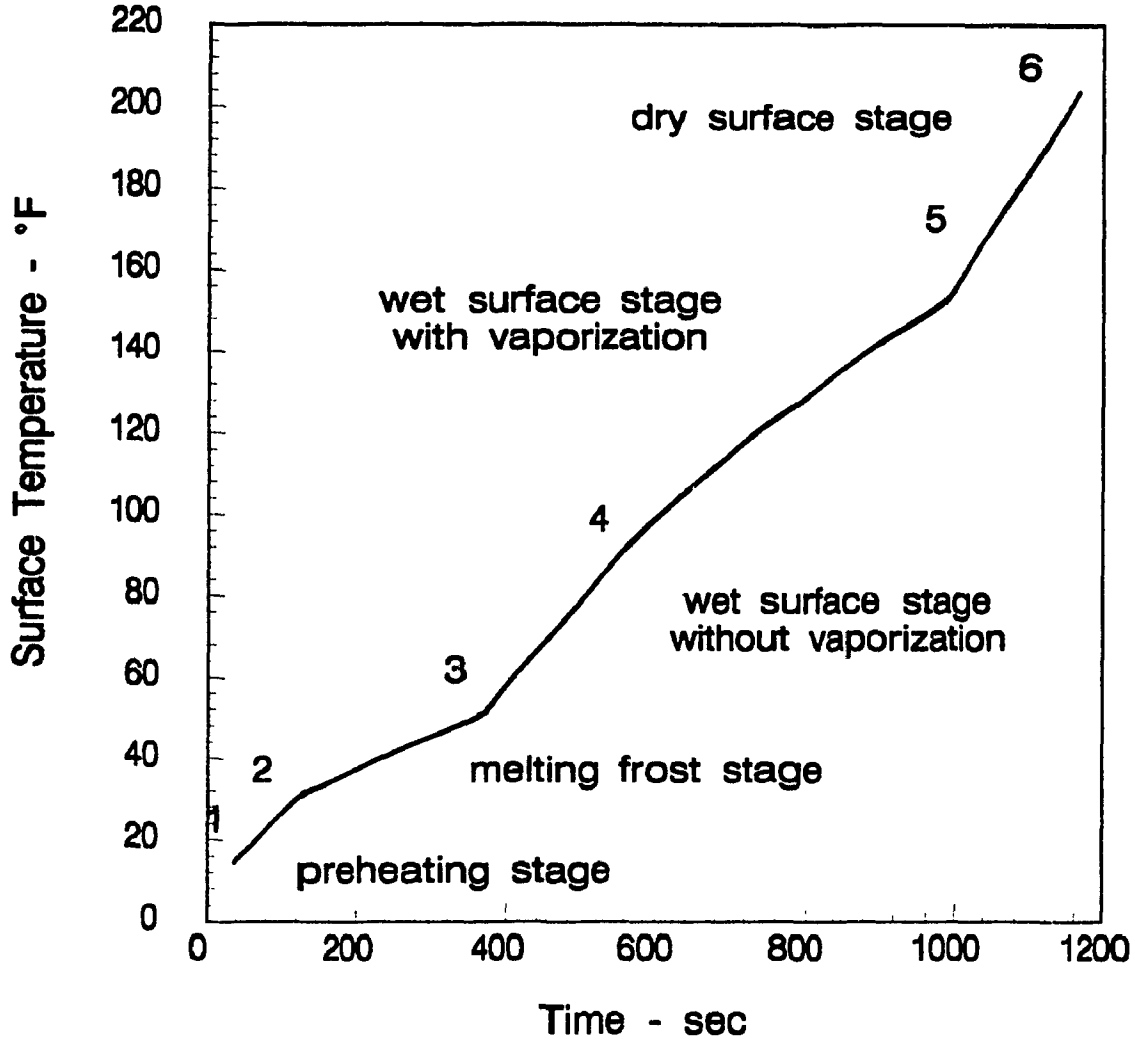

Figure 3.2 Idealized Curve of Temperature versus Time

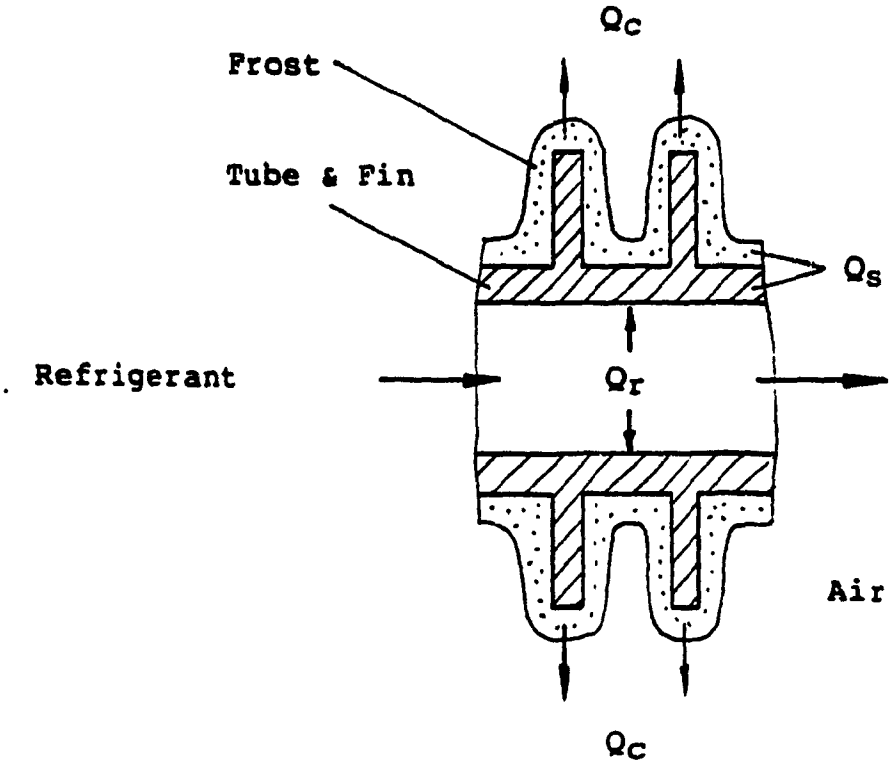

Fig.3.3 Preheating Stage

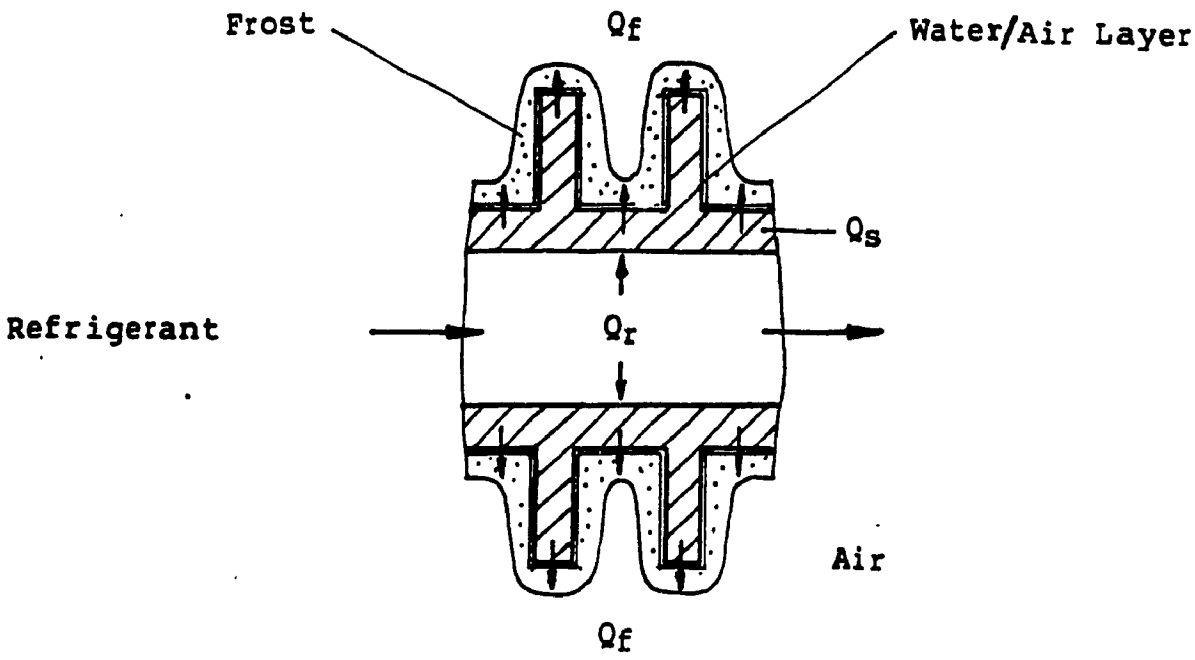

Fig.3.4 Melting Frost Stage

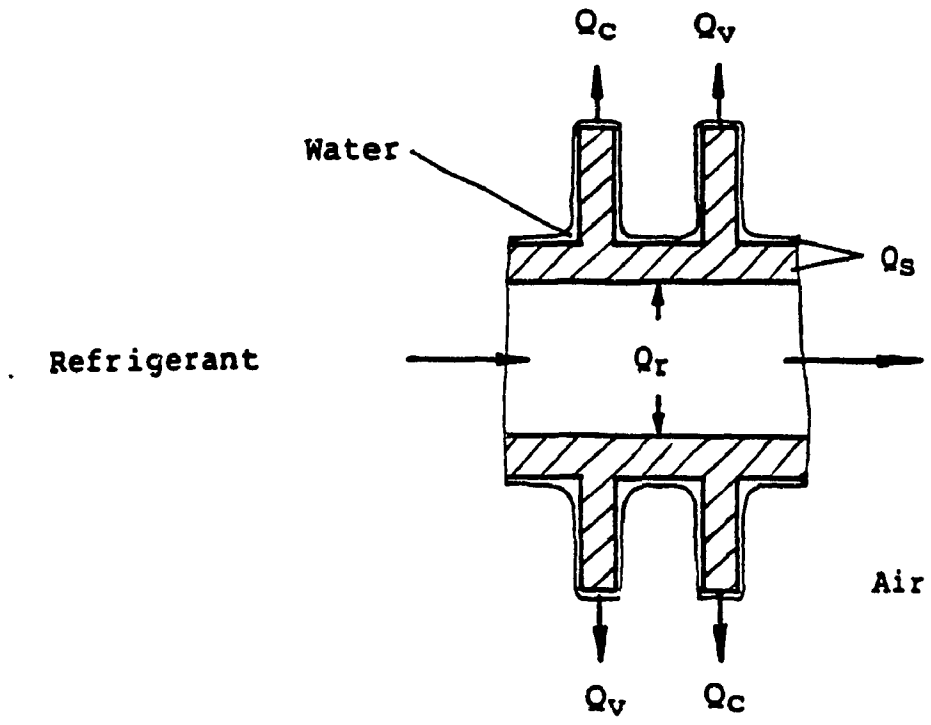

Fig.3.5 Wet Surface Stage

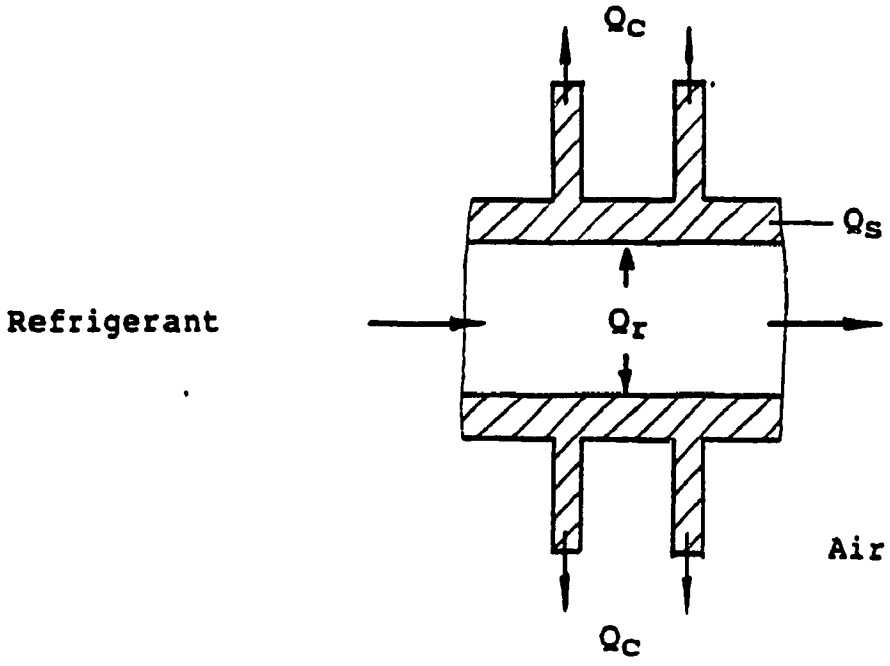

Fig.3.6 Dry Surface Stage

CHAPTER 4

REFRIGERANT SIDE ANALYSIS

4.1 Overview

In hot gas defrosting, refrigerant may pass through three regions, superheated, two-phase and subcooled, as it flows through the evaporator. In the superheated region (inlet of the evaporator) refrigerant enters as vapour and sensible heat of refrigerant transfers to the frost. In the two-phase region condensation occurs on the tube inside wall when the temperature of the tube wall is lower than saturated temperature of refrigerant. Vapour and liquid refrigerant coexist in physical equilibrium. As refrigerant flows through the two-phase region, the quality of the mixture decreases and latent heat of refrigerant transfers to the frost. In this region average refrigerant temperature drops slightly because of fluid pressure drop. When the refrigerant is completely condensed, two-phase region ends and subcooled region begins. In the subcooled region refrigerant is in liquid state and sensible heat of refrigerant transfers to the frost. The heat transfer in the subcooled region is low in comparison with those in the superheated or two-phase regions.

The pressure of refrigerant is changing with refrigerant flowing through the evaporator. It is due to the friction between the refrigerant and coil wall, and due to the velocity

change of the refrigerant because of its specific volume change. The greater the roughness of the coil inside surface, the greater the friction loss. As refrigerant condenses, its specific volume decreases, thus, its velocity decreases since the mass flow rate of refrigerant is constant. The influence of friction is to result in pressure drop, and that of decreasing velocity is to increase the pressure. During the process, the phase of refrigerant, single phase or two-phase, is also an important influence factor which is considered in correlations for pressure change. The transient pressure for each element at any time can be obtained based on the consideration of these main factors. For computation and simulation, the state of refrigerant at the inlet of an element is known. The state of refrigerant at the exit of the element is required. The exit state is determined by the exit enthalpy and pressure. The exit enthalpy is determined from the conservation of energy. The exit pressure is determined from the conservation of impulse momentum.

4.2 Refrigerant Side Heat Transfer

The refrigerant side heat transfer rate to an element of a coil can be calculated as follows:

$$Q_r = h_r \cdot A_i \cdot (T_r - T_w) \tag{3.15}$$

From the viewpoint of energy conservation, refrigerant side heat transfer rate to an element can be expressed by enthalpy, that is

$$Q_r = m_r \cdot (h_i - h_j) \quad (4.1)$$

where

m_r = mass flow rate of refrigerant

h_i = enthalpy at the inlet of an element

h_j = enthalpy at the outlet of an element

The enthalpy at the outlet of an element can be obtained by combining Equations 3.15 with 4.1, that is

$$h_j = h_i - h_r \cdot A_i \cdot (T_r - T_w)/m_r \quad (4.2)$$

The heat transfer coefficient can be obtained by using equations from literature.

4.3 Refrigerant Side Heat Transfer Coefficients

The equations used for calculating heat transfer coefficient are adopted based on refrigerant state, single phase (superheated or subcooled) or two-phase.

4.3.1 Single phase

The flow of refrigerant in superheated region and subcooled region is in single phase state, vapour and liquid respectively, with forced convection heat transfer. Two sets of equations can be used for calculating: Set 1, correlations given by Hiller (1976); Set 2, correlations given by McAdam (1954).

Set 1:

for Re < 3500

$$St \cdot Pr^{2/3} = 1.1064 \cdot Re^{-0.78992} \quad (4.3)$$

for $3500 \leq Re \leq 6000$

$$St \cdot Pr^{2/3} = 3.5194 \cdot 10^{-7} \cdot Re^{1.03804} \quad (4.4)$$

for $Re > 6000$

$$St \cdot Pr^{2/3} = 0.0108 \cdot Re^{-0.13750} \quad (4.5)$$

Set 2:

for $Re > 10000$

$$Nu = 0.023 \cdot Re^{0.8} \cdot Pr^{0.333} \quad (4.6)$$

where

Nu = Nusselt number

$$Nu = (h_r \cdot D_i)/k_r \quad (4.7)$$

Re = Reynold number

$$Re = (G \cdot D_i)/\mu_r \quad (4.8)$$

Pr = Prandtl number

$$Pr = (\mu_r \cdot c_{pr})/k_r \quad (4.9)$$

St = Stanton number

$$St = h_r/(G \cdot c_{pr}) \quad (4.10)$$

D_i = inside diameter of coil tube

k_r = heat conductivity of refrigerant

G = mass flux of refrigerant

$$G = m_r / A \quad (4.11)$$

A = inside cross-section area of coil tube

μ_r = dynamic viscosity of refrigerant

c_{pr} = specific heat of refrigerant at constant pressure

The heat transfer coefficient corresponding to equation Set 1 is

$$h_r = St \cdot G \cdot c_{pr} \quad (4.12)$$

The heat transfer coefficient corresponding to equation Set 2 is

$$h_r = (\bar{Nu} \cdot k_r)/D_i \quad (4.13)$$

Both Equation Set 1 and Set 2 were used in the beginning stage of this research for the verification and comparison. The results from both equations were quite close. The Equation Set 2 was finally adopted for computation and simulation since it was simpler than Equation Set 1 and refrigerant flow is under the specified condition, Reynold number greater than 10000.

4.3.2 Two-phase

In two-phase region the refrigerant inside the tube is a mixture of vapour and liquid. Heat transfer is forced convection with condensation. The correlation obtained by Traviss, Rohsenow and Baron (1973) is used to calculate condensation heat transfer coefficient.

For $0.1 < FXT < 1$

$$(Nu \cdot F2)/(Pr_l \cdot Re_l^{0.9}) = FXT \quad (4.14)$$

For $1 \leq FXT < 15$

$$(Nu \cdot F2)/(Pr_l \cdot Re_l^{0.9}) = FXT^{1.15} \quad (4.15)$$

where

$$FXT = 0.15 \cdot (1/XTT + 2.85/XTT^{0.476}) \quad (4.16)$$

$$XTT = [(1 - x)/x]^{0.9} (v_f/v_g)^{0.5} (\mu_f/\mu_g)^{0.1} \quad (4.17)$$

Re_l = Reynold number to refrigerant liquid

$$Re_l = G \cdot (1 - x) \cdot D_i/\mu_l \quad (4.18)$$

Pr_l = Prandtl number to refrigerant liquid

$$Pr_l = (\mu_l \cdot c_{pl})/k_l \tag{4.19}$$

x = quality of refrigerant

v_f = specific volume of refrigerant liquid

v_g = specific volume of refrigerant vapour

μ_f = dynamic viscosity of refrigerant liquid

μ_g = dynamic viscosity of refrigerant vapour

k_l = heat conductivity of refrigerant liquid

c_{pl} = specific heat of refrigerant liquid at constant pressure

for Re < 50

$$F2 = 0.707 \cdot Pr_l \cdot Re_l^{0.5} \tag{4.20}$$

for $50 \leq Re_l \leq 1125$

$$F2 = 5Pr_l + 5\ln[1 + Pr_l(0.0963Re_l^{0.585} - 1)] \tag{4.21}$$

for Re > 1125

$$F2 = 5Pr_l + 5\ln(1+5Pr_l) + 2.5\ln(0.00313Re_l^{0.812}) \tag{4.22}$$

where

$$Nu = (h_{r,tp} \cdot D_l)/k_l \tag{4.23}$$

The heat transfer coefficient corresponding to Equation 4.14 is

$$h_{r,tp} = (k_l \cdot FXT \cdot Pr_l \cdot Re_l^{0.9})/(D_l \cdot F2) \tag{4.24}$$

where

$h_{r,tp}$ = convective heat transfer coefficient for two-phase refrigerant

The heat transfer coefficient corresponding to Equation 4.15 is

$$h_{r,tp} = (k_l \cdot FXT^{1.15} \cdot Pr_l \cdot Re_l^{0.9})/(D_i \cdot F2) \quad (4.25)$$

4.3.3 Evaluation of the Heat Transfer Coefficient

In hot gas defrosting, refrigerant may pass through three states. The determination of refrigerant state is based on its quality. Theoretically, when its quality is equal to one, refrigerant is in superheated state. When its quality is equal to zero, it is in subcooled state. When between both, refrigerant is in two-phase state. In fact, there must be transient regions between superheated and two-phase as well as between two-phase and subcooled states. From literature, equations for single phase are valid in the following conditions:

$x = 1$ or $x = 0$

And correlations for two-phase developed by Traviss (1973) are valid in the following condition:

$0.95 > x > 0.1$

Therefore, there are no suitable equations for the regions of refrigerant quality between 1 and 0.95 as well as between 0.1 and 0. These regions may be considered as transient regions. The calculated results from two-phase equations show that heat transfer coefficient increases with the increase of refrigerant quality. In the lower quality transient range ($0.1 > x > 0$), the value of heat transfer coefficient at two-phase is low. Hence, a linear interpolation between values from two-phase and subcooled states is used. It is found that this

interpolation yields a smooth transition. At higher quality transient range ($1 > x > 0.95$), however, if Traviss correlation is extended with the increase of refrigerant quality from 0.95 to 1, the heat transfer coefficient will tend to infinity. Therefore, in order to avoid either unreasonable high heat transfer coefficient or sharply dropping heat transfer coefficient caused by linear interpolation between superheated and two-phase states, a maximum value of refrigerant quality of 0.95 is used for this region ($1 > x > 0.95$).

4.3.4 Influence of wall temperature

The average refrigerant temperature may be above its saturated temperature, but the wall temperature may be below the saturated temperature. Near the wall, refrigerant is assumed to be condensating. Therefore, if wall temperature is lower than refrigerant saturated temperature, the heat transfer coefficient is calculated as though the refrigerant flow were in two-phase state.

4.4 Pressure Change in Tubes

From the conservation of impulse momentum, the general correlation for pressure change of refrigerant in an element can be obtained as follows:

$$P_j = P_i - dP_f - dP_v \tag{4.26}$$

where

P_i = inlet pressure of an element

P_j = outlet pressure of an element

dP_f = pressure drop due to friction

dP_v = pressure change due to velocity change

In general, the correlation of pressure drop due to friction derived from shear stress of an element is as follows:

$$dP_f = f \cdot (\rho \cdot u^2/2) \cdot (\pi \cdot D_i \cdot dx)/A \quad (4.27)$$

where

f = friction factor

ρ = refrigerant density

u = refrigerant velocity

dx = length of an element

The correlation of pressure change due to velocity change obtained from the law of conservation of impulse and momentum is as follows:

$$dP_v = (u_j - u_i) \cdot m_r/A \quad (4.28)$$

where

u_i = refrigerant velocity at the inlet of an element

u_j = refrigerant velocity at the outlet of an element

Equations used for computation, considering different state, are detailed in followings.

4.4.1 Pressure drop by friction (single phase)

For a round tube, the general correlation for pressure drop can be simplified. Since

$$\rho \cdot u^2/2 = G^2 \cdot v/2 \quad (4.29)$$

where

G = mass flux of refrigerant

$$G = \rho \cdot u = u/v \tag{4.30}$$

v = specific volume of refrigerant

$$\pi \cdot D_i \cdot dx/A = 4 \cdot dx/D_i \tag{4.31}$$

Substituting Equations 4.29 and 4.31 into 4.27 yields the equation used for calculating the pressure drop of refrigerant caused by friction in superheated region or subcooled region (single phase) as follows:

$$dP_f = f \cdot (2 \cdot G^2 \cdot v) \cdot dx/D_i \tag{4.32}$$

The friction factor is obtained based on the nature of the flow and smoothness of the tube, using equations from Incropear (1981). Under the condition of smooth surface,

for $Re < 2500$

$$f = 16/Re \tag{4.33}$$

for $2500 \leq Re \leq 20000$

$$f = 0.079 \cdot Re^{-0.25} \tag{4.34}$$

for $Re > 20000$

$$f = 0.046 \cdot Re^{-0.2} \tag{4.35}$$

where

$$Re = (G \cdot D_i)/\mu_r \tag{4.36}$$

4.4.2 Pressure drop by friction (two phase)

The pressure drop of refrigerant caused by friction in two phase region can be calculated using the method proposed by Lockhard and Martinelli (1949). They related pressure drop

of two-phase flow to the pressure drop of the liquid portion of the flow flowing along in the tube by the dimensionless parameter XTT. That is

$$dP_{f,tp} = dP_{f,l} \cdot F \tag{4.37}$$

$$F = f(XTT) \tag{4.38}$$

where

$dP_{f,tp}$ = frictional pressure drop of two-phase flow

$dP_{f,l}$ = frictional pressure drop of the liquid portion of two-phase flow flowing along in the tube

F = correction factor for two-phase pressure drop

The pressure drop of the liquid portion can be calculated as follows:

$$dP_{f,l} = f \cdot (2 \cdot G^2 \cdot v) \cdot dx/D_i \tag{4.39}$$

where

$$f = 0.046 \cdot Re_{,tpl}^{-0.2} \tag{4.40}$$

$Re_{,tpl}$ = Reynolds number for two-phase liquid portion

$$Re_{,tpl} = (1 - x) \cdot G \cdot D_i/\mu_l \tag{4.41}$$

The correction factor for two-phase frictional pressure drop can be calculated using correlation obtained by Domanski (1982), that is

$$\log F = A1 + A2(\log XTT) + A3(\log XTT)^2 + A4(\log XTT)^3 + A5(\log XTT)^4 \tag{4.42}$$

where

A1 = 1.4

A2 = -0.87917

A3 = 0.14062

A4 = 0.0010417

A5 = -0.00078125

XTT is given by Equation 4.17

4.4.3 Pressure change by velocity change

The pressure change due to acceleration of refrigerant flow are calculated based on the mass flux and specific volume of refrigerant. Substituting Equations 4.11 and 4.30 into 4.28 yields the equation used for computation and simulation as follows:

$$dP_v = G^2 \cdot (v_j - v_i) \tag{4.43}$$

where

v_i = specific volume of refrigerant at the inlet of an element

v_j = specific volume of refrigerant at the outlet of an element

4.5 Pressure Drop in Return Bends

The pressure drop in the return bends is calculated by using the method of Pierre (1964), that is

$$dP_b = f_b \cdot G^2 \cdot v/2 \tag{4.44}$$

where

dP_b = pressure drop in the return bends

f_b = resistance factor for the return bends

The pressure drop in the return bends is considered as the combination of pressure drop due to the friction and that due

to the turning of the flow. Corresponding resistance factors are used for calculation, that is

$$f_b = f_f + f_t \tag{4.45}$$

where

f_f = resistance factor for the friction

f_t = resistance factor for the turning of the flow

The correlations and values of resistance factors can be obtained from Pierre's work based on the ratio of the bend diameter to the tube diameter, the amount of oil in the refrigerant, as well as refrigerant quality. Resistance factors of the friction, for R-12, are as follows:

	f_f	f_f
D/d	Oil-free medium	Oil present
3	0.14	0.33
4	0.19	0.44
6	0.28	0.66
8	0.38	0.88
10	0.47	1.10

where

D/d = ratio of bend diameter to tube diameter

The resistance factor for the turning of the flow is considered as a function of refrigerant quality, that is

x	f_t
0.0	0.7
0.2	0.8
0.4	1.0
0.6	1.1
0.8	1.0
1.0	0.6

For simulation, linear interpolation equations are obtained based on above data points.

CHAPTER 5

FROSTED SIDE ANALYSIS

5.1 Overview

As heat from refrigerant is transferred to frosted side, the condition of the frosted side is changed, from a subcooled frost surface, to a melting frost surface, to a wet surface, to dry surface. Heat and mass transfer take place during the process. For heat transfer in each stage, general equations are described in previous chapters. During the process, heat transfer occurs and is associated with mass transfer. Some heat, which is carried by frost or water, leaves as water draining and vaporizing from the coil. Some heat is transferred to surroundings by free air convection. The process and the amount of mass transfer differ from stage to stage. For stage 1, the mass transfer of water is assumed to be equal to zero, since under subcooled frost surface condition, the surface mass transfer by vaporization is considered negligible. For stage 2, when frost is melted to water, the water will be absorbed by remaining frost layer. When the frost layer is saturated, free water exists and starts to drain due to gravity, which means that mass of frost decreases and mass of water from melted frost increases. For stage 3, all frost is melted, which means that the mass of frost is equal to zero and mass transfer of frost is

completed. The mass transfer of stage 3 is considered only for the water remaining on the coil surface and its vaporization, which is not equal to the total mass of frost, since part of water from melted frost drains by gravity, and only part of it remains on the coil surface and vaporizes. At the beginning of stage 3, the vaporization of surface water is assumed to be equal to zero. The sum of mass of water remaining on the coil surface and water draining by gravity is assumed to be equal to the mass of frost. For stage 4, there is no mass transfer of frost or surface water, since frost and surface water are completely gone at the end of stage 3. Therefore, the main mass transfer of defrosting process on the frosted side takes place in stage 2 and 3. The mass transfer under melting frost surface condition (stage 2) is the most complicated part of the defrosting process since it is related with not only the mass change of both frost and water but also the phase change.

Defrosting process is a transient process. The continuous process is divided into a number of small time intervals. For each time interval, the process is considered to be quasi-static, and parameters have fixed values. For the frosted side analysis, the mass of frost and the mass of water on the coil surface are required data at all times, which is based on the initial amount of mass on each increment. The energy required for melting frost or vaporizing water of an element in a time interval is also a required datum and can be calculated by integration. For any time interval, the initial conditions,

the amount of mass of frost and that of water, are known from initially specified data or from previous calculation results. The mass of frost and that of water are desired data for simulation, which are obtained by calculation. The accuracy of the calculation depends on the length of the time interval. The more time intervals the process is divided into, the more accuracy the simulation has.

5.2 Analysis under Melting Frost Surface Condition

The mass transfer under melting frost condition is treated as quasi-static process by using time interval method. For each time interval, the amount of mass of frost and water is assumed to be constant, and the increment of mass of frost or water from melted frost is considered between two continuous time intervals, that is

$$m_{f,tj} = m_{f,ti} - dm_f \tag{5.1}$$

where

$m_{f,ti}$ = mass of frost at time ti, the beginning of time interval

$m_{f,tj}$ = mass of frost at time tj, the end of time interval

dm_f = mass of frost melted during time interval

From the energy conservation, heat transfer rate to melting frost on an element of the coil can be expressed as follows:

$$Q_f = h_{if} \cdot (dm_f/dt) \tag{5.2}$$

where

h_{if} = enthalpy of melting ice

Energy required for melting frost of an element of the coil in a time interval is calculated by integration, that is

$$E_f = \int_{ti}^{tj} Q_f \cdot dt \qquad (5.3)$$

where

E_f = energy required for melting frost on an element of the coil

Combining Equations 5.2 with 5.3 yields the equation for calculating the amount of mass of melted frost as follows:

$$dm_f = E_f / h_{if} \qquad (5.4)$$

For the simulation, at the beginning of this stage (stage 2), the mass of frost on the coil is specified. At the end of time interval, the mass of frost on the coil is determined by using Equation 5.1. Finally, at the end of this stage, all frost is melted. The mass of frost is equal to zero. The total energy required for a stage is the sum of energy supplied in each time interval. Detailed discussion of energy required for melting frost will be in the next chapter.

5.3 Analysis under Wet Surface Condition

At the beginning of this stage (stage 3), the mass of water on the coil surface is initially specified. Its amount will decrease gradually since the mass transfer due to vaporization. The mass transfer under wet surface condition is treated similarly as under melting frost surface condition, that is

$$m_{w,tj} = m_{w,ti} - dm_w \quad (5.5)$$

where

$m_{w,ti}$ = mass of water at time ti, the beginning of time interval

$m_{w,tj}$ = mass of water at time tj, the end of time interval

dm_w = mass of water vaporized during time interval

The heat transfer rate to vaporizing surface water on an element of the coil can be expressed as follows:

$$Q_v = h_{fg} \cdot (dm_w/dt) \quad (5.6)$$

Energy required for vaporizing surface water on an element of the coil in a time interval is calculated by integration, that is

$$E_v = \int_{ti}^{tj} Q_v . dt \quad (5.7)$$

where

E_v = energy required for vaporizing water on an element of the coil

Combining Equations 5.6 with 5.7 yields the equation for calculating the amount of mass of vaporizing water as follows:

$$dm_w = E_v/h_{fg} \quad (5.8)$$

The mass of water on the coil surface initially specified at the beginning of the simulation for this stage is only part of water from melted frost. The estimation of initial value of mass of water is based on experiments (detailed in Chapter 9). At the end of time interval, the mass of water remaining on the coil surface is calculated using Equation 5.5. Finally, at

the end of this stage, all water on the coil surface is completely vaporized. The mass of surface water is equal to zero. The energy for vaporizing water in a time interval and this stage will be discussed in the next chapter.

CHAPTER 6

ENERGY CONSIDERATIONS

6.1 General Energy Equations

In hot gas defrosting, energy from refrigerant is converted into the energy stored in the coil, frost and water, the energy transferred by convection, and the energy consumed for melting frost and vaporizing surface water on the coil. As described in Chapter 3, the heat transfer during hot gas defrosting process is considered as

$$Q_r = Q_s + Q_c + Q_f + Q_v \tag{3.3}$$

Therefore, the general equation of energy balance for the hot gas defrosting process can be obtained as follows:

$$E_r = E_s + E_c + E_f + E_v \tag{6.1}$$

where

E_r = total energy supplied by refrigerant for defrosting

E_s = energy stored in a coil element, and in the frost or water on the element

E_c = energy transferred by convection on an element of the coil

Similarly, for difference surface conditions, through stage 1 to stage 4, the equations of energy balance can be obtained based on heat transfer correlations.

If defrosting process is divided into a series of small time intervals, the amount of energy transferred in a time

interval can be obtained by integration of heat transfer rate with time, that is

$$E = \int_{ti}^{tj} Q \cdot dt \qquad (6.2)$$

where

E = energy

Q = heat transfer rate

ti = the beginning of time interval

tj = the end of time interval

The total amount of energy is the sum of energy calculated in each time interval.

6.2 Specific Energy Equations

Applied energy equations are obtained from substituting specified equations of heat transfer rate into general equation 6.2. Different heat transfer rates yield different energy equations suitable for calculating energy for refrigerant, thermal storage, convection, melting frost and vaporizing water.

6.2.1 Equation for refrigerant

For the refrigerant, the heat transfer rate is

$$Q_r = h_r \cdot A_i \cdot (T_r - T_w) \qquad (3.15)$$

The energy transferred from refrigerant is

$$E_r = \int_{ti}^{tj} Q_r \cdot dt \qquad (6.3)$$

Substituting Equation 3.15 into 6.3 yields

$$E_r = \int_{ti}^{tj} [h_r \cdot A_i \cdot (T_r - T_w)]dt \qquad (6.4)$$

Substituting Equation 3.42 for the coil wall temperature into Equation 6.4 yields

$$E_r = h_r \cdot A_i \cdot \int_{ti}^{tj} [T_r - T_{w\infty} \cdot (1 - e^{-A \cdot t}) - T_{wi} \cdot e^{-A \cdot t}]dt \qquad (6.5)$$

where

T_{wi} = initial wall temperature at time ti

Integrating Equation 6.5 yields

$$E_r = h_r \cdot A_i \cdot [(T_r - T_{w\infty}) \cdot \delta t + (T_{w\infty} - T_{wi}) \cdot (e^{-A \cdot ti} - e^{-A \cdot tj})/A] \qquad (6.6)$$

where

δt = time interval

$$\delta t = tj - ti \qquad (6.7)$$

6.2.2 Equation for thermal storage

For the thermal storage,

$$Q_s = C \cdot (dT/dt) \qquad (3.16)$$

The energy stored in coil, frost and water is

$$E_s = \int_{ti}^{tj} Q_s \cdot dt \qquad (6.8)$$

Substituting Equation 3.16 into 6.8 yields

$$E_s = \int_{ti}^{tj} C \cdot (dT_w/dt) \cdot dt \qquad (6.9)$$

Substituting Equation 3.42 for the coil wall temperature into Equation 6.9 yields

$$E_s = C \int_{ti}^{tj} dT_w \tag{6.10}$$

Integrating Equation 6.10 yields

$$E_s = C \cdot (T_{w\infty} - T_{wi})(e^{-A \cdot ti} - e^{-A \cdot tj}) \tag{6.11}$$

6.2.3 Equation for convection

For the convection, the heat transfer rate is

$$Q_c = h_a \cdot A_e \cdot (T_w - T_a) \tag{3.23}$$

The energy transferred by convection is

$$E_c = \int_{ti}^{tj} Q_c \cdot dt \tag{6.12}$$

Substituting Equation 3.23 into 6.12 yields

$$E_c = \int_{ti}^{tj} h_a \cdot A_e \cdot (T_w - T_a) \cdot dt \tag{6.13}$$

Substituting Equation 3.42 for the coil wall temperature into Equation 6.13 yields

$$E_c = h_a \cdot A_e \cdot \int_{ti}^{tj} [T_{w\infty} \cdot (1 - e^{-A \cdot t}) + T_{wi} \cdot e^{-A \cdot t} - T_a] dt \tag{6.14}$$

Integrating Equation 6.14 yields

$$E_c = h_a \cdot A_e \cdot [(T_{w\infty} - T_a) \cdot \delta t - (T_{w\infty} - T_{wi}) \cdot (e^{-A \cdot ti} - e^{-A \cdot tj})/A] \tag{6.15}$$

6.2.4 Equation for melting frost

For melting frost, the heat transfer rate is

$$Q_f = C_w \cdot A_e \cdot (T_w - T_f) \tag{3.27}$$

The energy consumed for melting frost is

$$E_f = \int_{ti}^{tj} Q_f \cdot dt \tag{6.16}$$

Substituting Equation 3.27 into 6.16 yields

$$E_f = \int_{ti}^{tj} C_w \cdot A_e \cdot (T_w - T_f) \cdot dt \tag{6.17}$$

Substituting Equation 3.42 for the coil wall temperature into Equation 6.17 yields

$$E_f = C_w \cdot A_e \cdot \int_{ti}^{tj} [T_{w\infty} \cdot (1 - e^{-A\,t}) + T_{wi} \cdot e^{-A \cdot t} - T_f] dt \tag{6.18}$$

Integrating Equation 6.18 yields

$$E_f = C_w \cdot A_e \cdot [(T_{w\infty} - T_f) \cdot \delta t - (T_{w\infty} - T_{wi}) \cdot (e^{-A \cdot ti} - e^{-A \cdot tj})/A] \tag{6.19}$$

6.2.5 Equation for vaporizing water

For vaporizing water, the heat transfer rate is

$$Q_v = m_v \cdot h_{fg} \tag{3.29}$$

The energy consumed for vaporizing water is

$$E_v = \int_{ti}^{tj} Q_v \cdot dt \tag{6.20}$$

Substituting Equation 3.29 into 6.20 yields

$$E_v = \int_{ti}^{tj} m_v \cdot h_{fg} \cdot dt \tag{6.21}$$

Integrating Equation 6.21 yields

$$E_v = m_v \cdot h_{fg} \cdot \delta t \tag{6.22}$$

6.3 Total Energy

The consideration of total energy for defrosting is based on the combination of energy consideration from space element and time interval. For a space element in a time interval, the energy required for defrosting is

$$E_{ze} = E_s + E_c + E_f + E_v \tag{6.23}$$

where

E_{ze} = total energy required for defrosting on an element of the coil in a time interval

For the whole coil, the energy required for defrosting in a time interval is

$$E_{zc} = \sum_{i=1}^{n_z} E_{ze,i} \tag{6.24}$$

where

E_{zc} = total energy required for the defrosting of a whole coil in a time interval

n_z = the number of space element

i = index of space element

For the whole defrosting process, the total energy required is

$$E_{tot} = \sum_{j=1}^{n_t} E_{zc,j} \tag{6.25}$$

where

E_{tot} = total energy required for defrosting process

n_t = the number of time intervals

j = index of time interval

Substituting Equation 6.24 into 6.25 yields

$$E_{tot} = \sum_{i=1}^{n_z} \sum_{j=1}^{n_t} E_{ze,i,j} \tag{6.26}$$

Substituting Equation 6.23 into 6.26 yields

$$E_{tot} = \sum_{i=1}^{n_z} \sum_{j=1}^{n_t} (E_a + E_c + E_f + E_v)_{i,j} \tag{6.27}$$

6.4 Defrosting Efficiency

The defrosting efficiency can be defined as the ratio of minimum energy required for defrosting, which includes the energy for preheating frost to the temperature of melting point and the energy for melting frost, to the total supplied energy, that is

$$\eta_d = m_{f,o} \cdot [c_f \cdot (T_f - T_o) + h_{if}] / E_{tot} \tag{6.28}$$

where

η_d = defrosting efficiency

$m_{f,o}$ = initial mass of frost

T_o = initial temperature of frost

CHAPTER 7

TIME CONSIDERATIONS

7.1 Overview

Since a defrosting process is a transient process, a series of time intervals are used to approach the real process. Obviously, the greater the number of time intervals used to simulate the defrosting process, the greater the accuracy obtained for the simulation. If the number of time intervals tends to infinity, which also means that the time interval tends to zero, the simulation result can be considered the same as the real one. However, a very large number of time intervals will take too long a time to complete the calculation. Conversely, if the number of time intervals is small, which also means that the time interval is large, considerable errors may be involved in simulation. Since there are three states (superheated, two-phase and subcooled) for inside refrigerant and four stages (preheating frost, melting frost, wet surface and dry surface) for outside surface conditions, a longer time interval will cover more than one state and/or stage. Therefore, proper time interval should be chosen to satisfy both simulation accuracy and computation time.

For simulation, parameters, such as refrigerant properties, heat transfer coefficient on refrigerant side,

etc. are kept to be constant in each element at each time interval, and based on the values at the beginning of time interval. However, a transition of state of refrigerant as well as stage of outside surface conditions must take place, and it must be in certain time interval. In these cases, the time interval has to be broken into two parts to consider different conditions and different treatment respectively.

7.1.1 Time subdivision

For each element, the total defrosting time is the sum of time intervals, that is

$$t_d = \sum_{i=1}^{n_t} \delta t_i \tag{7.1}$$

where

t_d = total defrosting time

δt_i = time interval

i = index of time interval

Each time interval may be subdivided due to the change of stages based on the outside surface conditions and the change of states of refrigerant during that time interval. For each time interval, the combination of time spent in each stage based on outside surface conditions is considered, that is,

$$\delta t_i = \sum_{j=1}^{4} \delta t_j \tag{7.2}$$

where

δt_j = time spent in each stage

j = index of stage

or

$$\delta t_1 = \delta t_1 + \delta t_2 + \delta t_3 + \delta t_4 \tag{7.3}$$

where

δt_1 = time spend in stage 1

δt_2 = time spend in stage 2

δt_3 = time spend in stage 3

δt_4 = time spend in stage 4

The range of time spent in each stage is

$$0 < \delta t_j < \delta t_1 \tag{7.4}$$

7.1.2 Wall temperature consideration

For the case of condensing refrigerant, the coil wall temperature must not exceed the saturated temperature of refrigerant inside the tube. Otherwise, there will be no condensation of refrigerant inside the tube. Therefore, it is reasonable to consider a limitation of the wall temperature by the refrigerant saturated temperature. Before the wall temperature reaches the refrigerant saturated temperature, that is

$$T_w < T_s \tag{7.5}$$

the wall temperature increases exponentially as shown by Equation 3.42. When it reaches the refrigerant saturation temperature, that is

$$T_w = T_s \tag{7.6}$$

the wall temperature is kept the same as the refrigerant

saturation temperature. Under this consideration, the time spent in each stage may be broken into two parts. One part is corresponding to the wall temperature increasing exponentially, and another part is corresponding to the constant wall temperature as shown in Fig.7.1. In this case, the time spent in each stage is subdivided into two parts based on the wall temperature, that is

$$\delta t_j = \sum_{k=1}^{2} \delta t_{j,k} \tag{7.7}$$

where

$\delta t_{j,k}$ = time spent in each state based on wall temperature

k = index of time spent in each state based on wall temperature

or

$$\delta t_j = \delta t_{j,1} + \delta t_{j,2} \tag{7.8}$$

where

$\delta t_{j,1}$ = time spent in state with $T_w < T_s$

$\delta t_{j,2}$ = time spent in state with $T_w = T_s$

The range of time spent in each state based on the wall temperature is as follows:

$$0 < \delta t_{j,k} < \delta t_j \tag{7.9}$$

The heat transfer rate of refrigerant is based on the difference between the average refrigerant temperature and the wall temperature. In each time interval, the time spent in either stages or states can be equal to zero, which means that these stages and/or states are passed by during that time

interval.

7.2 Defrosting Time for Preheating (stage 1)

When defrosting process starts, the frost temperature is the same as the coil wall temperature in subcooled condition. With heat supplied to defrost, the frost temperature and the wall temperature will rise. They are assumed to be still the same until the temperature reaches melting point of frost, as the contact heat resistance between the wall and frost is so small that any temperature difference can be neglected. Therefore, the wall temperature can be used as a critical condition for defrosting time in stage 1.

If a time interval is considered and substituted into the Equation 3.42, the equation of the wall temperature can be rewritten as follows:

$$T_w = T_{w\infty} \cdot (1 - e^{-\lambda \cdot \delta t}) + T_{wi} \cdot e^{-\lambda \cdot \delta t} \qquad (7.10)$$

where

T_{wi} = initial wall temperature corresponding to $\delta t = 0$

In stage 1, the wall temperature must not exceed the temperature of melting point, that is

$$T_w < T_f = 32^\circ F \ (0^\circ C) \qquad (7.11)$$

If the wall temperature is equal to the melting point temperature, that is

$$T_w = T_f \qquad (7.12)$$

the preheating stage is completed. Substituting the melting point temperature into Equation 7.10 yields

$$T_f = T_{w\infty} \cdot (1 - e^{-A \cdot \delta t_1}) + T_{wi} \cdot e^{-A \cdot \delta t_1} \quad (7.13)$$

The defrosting time for stage 1 can be obtained by solving Equation 7.13, that is

$$\delta t_1 = [\ln(T_{w\infty} - T_{wi}) - \ln(T_{w\infty} - T_f)]/A \quad (7.14)$$

where

δt_1 = defrosting time for stage 1

For computation, a time interval is specified. For each time interval, the final wall temperature is obtained by substituting the time interval into the coil wall temperature Equation 7.10. Comparing calculated wall temperature with the melting point temperature, the defrosting stage can be determined. If the wall temperature is less than the melting point temperature, which means that, during this time interval, frost layer can not be warmed up to the melting point temperature, the defrosting process should be still in stage 1 for the next time interval. It may take several time intervals to complete the process in stage 1. Conversely, if the wall temperature is greater than the melting point temperature, it means that the time required for warming frost up to the melting point temperature is less than the specified defrosting time for stage 1. In this case, this time interval should be broken into two parts for consideration. The first part is the defrosting time spent in stage 1. The second part is considered as the defrosting time spent in stage 2 or further in other stages.

7.3 Defrosting Time for Melting Frost (stage 2)

When the temperature of frost reaches the melting point temperature, defrosting process goes into stage 2. In stage 2, energy from refrigerant is mainly used to melt frost. Therefore, the calculation of defrosting time in stage 2 is based on energy equations of melting frost. The energy required to melt all frost to water is

$$E_{2mx} = m_{f,ti} \cdot h_{if} \tag{7.15}$$

where

E_{2mx} = energy required for melting all frost on an element of the coil

$m_{f,ti}$ = mass of frost at the beginning of the time interval (ti = 0)

The energy transferred for melting frost during a specified time interval is

$$E_f = C_w \cdot A_e \cdot [(T_{w\infty} - T_f) \cdot \delta t - (T_{w\infty} - T_{wi}) \cdot (e^{-A \cdot ti} - e^{-A \cdot tj})/A] \tag{6.19}$$

In stage 2, the transferred energy for melting frost does not exceed the required energy, that is

$$E_f < E_{2mx} \tag{7.16}$$

If the transferred energy is equal to the required energy, that is

$$E_f = E_{2mx} \tag{7.17}$$

the melting frost stage is completed. Based on the energy balance between transferred and required, combining Equations 7.15 with 6.19 yields

$$m_{f,t1} \cdot h_{1f} = C_w \cdot A_e \cdot [(T_{w\infty} - T_f)\delta t_2 - (T_{w\infty} - T_{wi})(1 - e^{-A \cdot \delta t2})/A] \quad (7.18)$$

where

δt_2 = defrosting time for stage 2

δt_2 = tj - ti = tj

Defrosting time for stage 2 is obtained by solving Equation 7.18 numerically, using an interaive algorithm.

For computation, required energy and transferred energy are compared to determine the defrosting stage. If transferred energy is less than required energy, which means that all frost can not be melted completely during the time interval, defrosting process should be still in this stage, stage 2, at next time interval. It may take several time intervals to melt frost. If transferred energy is greater than required energy, it means that time required for melting all frost is less than specified defrosting time for stage 2. In this case, this time interval should be broken into two parts for consideration. The first part is the defrosting time spent in stage 2. The second part is considered as the defrosting time spent in stage 3 or further in stage 4.

7.4 Defrosting Time for Vaporizing Water (stage 3)

When all frost has been melted to water, defrosting process goes into stage 3. Part of water from melted frost drains by gravity. Other part remaining on the coil surface forms a wet surface and begins vaporizing. Since defrosting

process in stage 3 is mainly related with vaporizing surface water, the calculation of defrosting time in stage 3 is based on the energy equations of vaporizing surface water. The energy required for vaporizing all surface water is

$$E_{3mx} = m_{w,ti} \cdot h_{fg} \tag{7.19}$$

where

E_{3mx} = energy required for vaporizing all surface water on an element of the coil

$m_{w,ti}$ = mass of water at the beginning of the time interval (ti = 0)

The energy transferred for vaporizing water during a specified time interval is

$$E_v = m_v \cdot h_{fg} \cdot \delta t \tag{6.22}$$

In stage 3, the transferred energy for vaporizing surface water does not exceed the required energy, that is

$$E_v < E_{3mx} \tag{7.20}$$

If the transferred energy is equal to the required energy, that is

$$E_v = E_{3mx} \tag{7.21}$$

the wet surface stage is completed. Based on the energy balance between transferred and required, combining Equations 7.19 with 6.22 yields

$$m_{w,ti} \cdot h_{fg} = m_v \cdot h_{fg} \cdot \delta t_3 \tag{7.22}$$

where

δt_3 = defrosting time for stage 3

Solving Equation 7.22 yields the defrosting time for stage 3,

that is

$$\delta t_3 = m_{w,ti}/m_v \tag{7.23}$$

For computation, required energy and transferred energy are compared to determine the defrosting stage. If transferred energy is less than required energy, which means that all water can not be vaporized completely during the time interval, defrosting process should be still in this stage, stage 3, at next time interval. It may take several time intervals to vaporize surface water. If transferred energy is greater than required energy, it means that time required for vaporizing water is less than specified defrosting time for stage 3. In this case, this time interval should be broken into two parts for consideration. The first part is the defrosting time spent in stage 3. The second part is the defrosting time spent in stage 4.

7.5 Time for Dry Surface (stage 4)

When all water leaves the coil surface, defrosting process goes into stage 4, dry surface. For a specified defrosting time, the time spent in dry surface stage (stage 4) depends on the time spent on previous stages as described before.

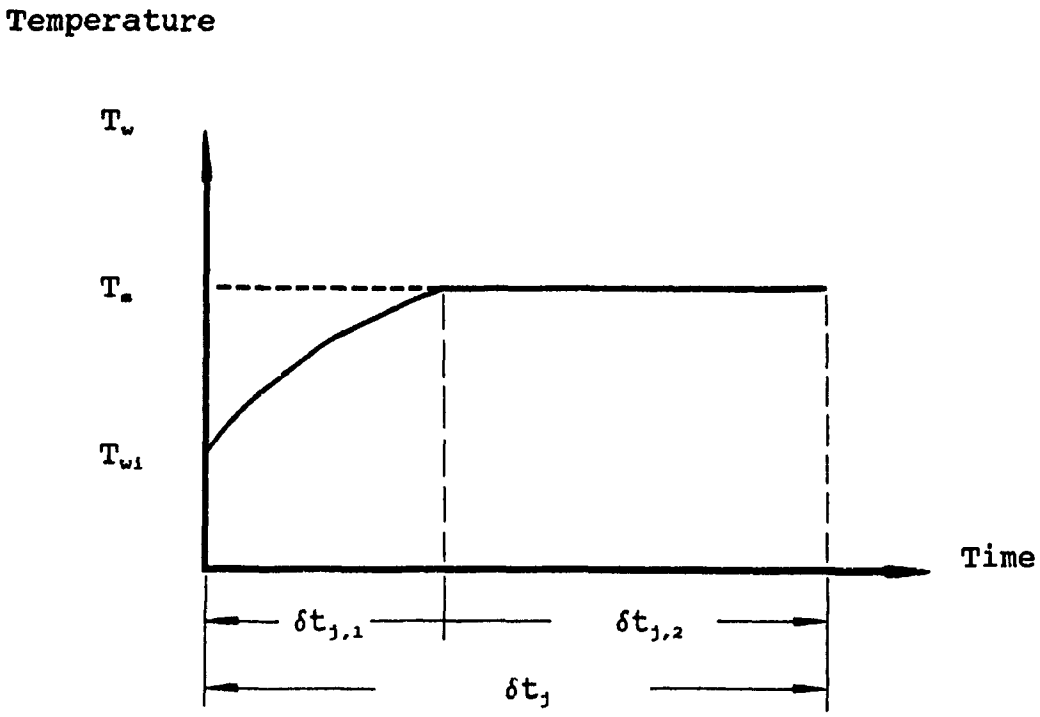

Figure 7.1 Evaporator Wall Temperature

CHAPTER 8

SOLUTION ALGORITHM

8.1 Overview

For computation, a finite element method is used, considering two dimensions, space and time. At first, a time interval is set up. The computation progresses along the space elements from the inlet of evaporator to the exit. Then, the computation develops along the time dimension from the first time interval to the specified last time interval. The computation is essentially for the four defrosting stage model based on surface conditions, that is, from preheating stage, melting frosting stage, wet surface stage to dry surface stage. During each stage, heat transfer, mass transfer, and the wall temperature are calculated. Refrigerant data at leaving state are obtained by computation. Before the simulation goes into defrosting stage, initial and boundary conditions are set up. Evaporator geometry, refrigerant state, environmental conditions, and other coefficients are required as input data. At the end of the simulation, time of defrosting process, refrigerant leaving state, amount of transferred energy, mass of vaporizing water and defrosting efficiency are obtained. Numerical methods are used for the computation.

The following is a brief outline of the solution

algorithm noting the key steps. Program listings appear in Appendix I.

8.2 Input

For computer simulation, specific parameters, such as evaporator geometry, refrigerant state, environmental conditions, coefficients and other specified data, are required as input data. Among them, some are constants, and some are variables.

8.2.1 Constants

Evaporator geometry and other constant properties requiring specification are as follows:

Tube inside diameter, D_i

Tube outside diameter, D_o

Fin height, D_1

Fin depth, D_2

Fin thickness, t

Number of fins, n_f

Number of tubes, n_{tub}

Length of coil, L

Specific heat and density of tube material, c_t & ρ_t

Specific heat and density of fin material, c_{fin} & ρ_{fin}

Refrigerant number

Initial mass of water held on coil surface, $m_{w,o}$

Resistance factor of friction in return bends, f_{bo}

8.2.2 Refrigerant parameters

Refrigerant parameters requiring specification are as follows:

Mass flow rate of refrigerant, m_r

Inlet pressure, P_i

Inlet temperature, T_i

8.2.3 Environmental conditions

Environmental conditions requiring specification are as follows:

Initial mass of frost, $m_{f,o}$

Initial evaporator wall temperature, T_{wo}

Ambient temperature, T_a

Relative humidity, RH

8.2.4 Coefficients

The coefficients requiring specification for the calculation of heat and mass transfer on the air side, which are determined experimentally, are as follows:

Convective heat transfer coefficient on air side, h_a

Reference conductance of water/air layer, $C_{w,ref}$

Reference mass of frost, $m_{f,ref}$

Surface evaporation coefficient, C_{se}

Surface evaporation exponent, n

8.2.5 Specified data for calculation

Specified date for space element and time interval are as follows:

Number of elements, n_z

Length of time interval, δt

Maximum number of time intervals, $n_{t,mx}$

8.3 Output

Leaving conditions for the elements and evaporator in each time interval are obtained by calculating, which is considered as the function of time and in quasi-static state in each step. The final results at leaving condition are as follows:

Time

Refrigerant leaving state: pressure, temperature and quality

Total amount of energy transferred from refrigerant for thermal storage, melting frost, vaporizing water and spreading to surroundings

Total mass of vaporized water

Defrosting efficiency

8.4 Solution Algorithm

The computation steps are as follows:

1. Input specified data and constants as per Section 8.1.
2. Divide an evaporator into elements, calculate element

geometry parameters (volume and area) and heat capacity.

3. Set up initial and boundary conditions, such as initial wall temperature, mass of frost and mass of liquid, for each element.
4. Set the index of time interval to zero.
5. Increase the index of time interval by one.
6. Input refrigerant initial state: mass flow rate, pressure, temperature and quality, and environmental conditions: ambient temperature and relative humidity as per Section 8.1.
7. Set the index of space element to zero.
8. Increase the index of space element by one.
9. Set up defrosting stage based on coil surface conditions:
   - 9.1. If the wall temperature is less than the melting point temperature, go to preheating stage, Step 10.
   - 9.2. If the wall temperature is equal to the melting point temperature, go to melting frost stage, Step 11.
   - 9.3. If all frost is melted, go to wet surface stage, Step 12.
   - 9.4. If all surface water is vaporized, go to dry surface stage, Step 13.
10. Simulate preheating stage (stage 1):
    - 10.1. Calculate fin efficiency, Equation 3.25.
    - 10.2. Calculate air side effective surface area, Equation 3.24.
    - 10.3. Calculate refrigerant heat transfer coefficient as

per Section 4.3.

10.4. Calculate coil wall temperature as per Section 3.3.

10.5. If calculated wall temperature is less than the melting point temperature,

10.5.1. Calculate transferred energy for convection and storage, Equations 6.15 & 6.11.

10.5.2. Go to Step 14.

10.6. If calculated wall temperature is greater than the melting point temperature,

10.6.1. Calculate time period from the beginning of the time interval to the end of preheating stage as per Section 7.2, when the wall temperature reaches the melting point temperature.

10.6.2. Calculate transferred energy for convection and storage, Equations 6.15 & 6.11, based on calculated time period in Step 10.6.1.

10.6.3. Preheating stage is completed and calculate remaining time for this time interval.

11. Simulate melting frost stage (stage 2):

11.1. Calculate conductance of water/air layer, Equation 3.28.

11.2. Calculate fin efficiency, Equation 3.25.

11.3. Calculate air side effective surface area, Equation 3.24.

11.4. Calculate refrigerant heat transfer coefficient as

per Section 4.3.

11.5. Calculate coil wall temperature as per Section 3.3.

11.6. If two-phase refrigerant heat transfer coefficient is used and calculated wall temperature is greater than refrigerant saturation temperature, divide the time interval into two parts as per Section 7.1.2.

11.7. Calculate required and transferred energy for melting frost, Equations 5.3 & 6.19.

11.8. If transferred energy is less than required energy,

11.8.1. Calculate stored energy, Equation 6.11.

11.8.2. Calculate total transferred energy, Equation 6.1.

11.8.3. Calculate mass of melting frost and mass of remaining frost as per Section 5.2.

11.8.4. Go to Step 14.

11.9. If transferred energy is greater than required energy,

11.9.1. Calculate time period from the beginning of the time interval to the end of melting frost stage based on energy balance, Equation 7.18.

11.9.2. Calculate coil wall temperature as per Section 3.3.

11.9.3. Calculate energy for melting frost, Equation 6.19.

11.9.4. Calculate energy for thermal storage,

Equation 6.11.

11.9.5. Calculate total transferred energy, Equation 6.1.

11.9.6. Calculate mass of melting frost and mass of remaining frost as per Section 5.2.

11.9.7. Calculate total energy accumulated for melting frost.

11.9.8. Melting frost stage is completed and calculate remaining time in this time interval.

12. Simulate wet surface stage (stage 3):

12.1. Calculate fin efficiency, Equation 3.25.

12.2. Calculate air side effective surface area, Equation 3.24.

12.3. Calculate refrigerant heat transfer coefficient as per Section 4.3.

12.4. Calculate effective wetted surface area, Equation 3.31.

12.5. Calculate mass flow rate of surface water vapour, Equation 3.30.

12.6. Calculate heat transfer rate of vaporizing water, Equation 3.29.

12.7. Calculate coil wall temperature as per Section 3.3.

12.8. If two-phase refrigerant heat transfer coefficient is used and calculated wall temperature is greater than the refrigerant saturation temperature, divide

the time interval into two parts as per Section 7.1.2.

12.9. Calculate required and transferred energy for vaporizing water, Equations 5.7 & 6.22.

12.10. If transferred energy is less than required energy,

12.10.1. Calculate energy for convection, Equation 6.15.

12.10.2. Calculate energy for thermal storage, Equation 6.11.

12.10.3. Calculate total transferred energy, Equation 6.1.

12.10.4. Calculate mass of vaporizing water and mass of remaining water as per Section 5.3.

12.10.5. Go to Step 14.

12.11. If transferred energy is greater than required energy,

12.11.1. Calculate time period from the beginning of the time interval to the end of wet surface stage based on energy balance, Equation 7.23.

12.11.2. Calculate wall temperature as per Section 3.3.

12.11.3. Calculate energy for convection, Equation 6.15.

12.11.4. Calculate energy for thermal storage,

Equation 6.11.

12.11.5. Calculate energy for vaporizing water, Equation 6.22.

12.11.6. Calculate total transferred energy, Equation 6.1.

12.11.7. Calculate mass of vaporizing water and remaining water as per Section 5.3.

12.11.8. Wet surface stage is completed and calculate remaining time in this time interval.

13. Simulate dry surface stage (stage 4):

13.1. Calculate fin efficiency, Equation 3.25.

13.2. Calculate air side effective surface area, Equation 3.24.

13.3. Calculate refrigerant heat transfer coefficient as per Section 4.3.

13.4. Calculate coil wall temperature as per Section 3.3.

13.5. If two-phase refrigerant heat transfer coefficient is used and calculated wall temperature is greater than the refrigerant saturation temperature, divide the time interval into two parts as per Section 7.1.2.

13.6. Calculate energy for convection, Equation 6.15.

13.7. Calculate energy for thermal storage, Equation 6.11.

13.8. Calculate total transferred energy, Equation 6.1, and dry surface stage is completed.

14. Calculate total energy transferred for the element, Equation 6.23.
15. Calculate refrigerant pressure drop and refrigerant pressure at the exit of the element as per Section 4.4 and 4.5.
16. Calculate enthalpy of refrigerant at the exit of the element.
17. Calculate all refrigerant properties at the exit of the element based on the enthalpy and pressure.
18. Calculate refrigerant pressure change by velocity for next time interval as per Section 4.4.
19. If the index of space element is less than specified maximum number, go back to Step 8 and start the simulation of next element.
20. Calculate total energy transferred in a time interval, Equation 6.24.
21. If the index of time interval is less than specified maximum number, go back to Step 5 and start the simulation of next time interval.
22. Calculate total energy transferred in defrosting process, Equation 6.27.
23. Calculate total time, Equation 7.1, defrosting efficiency, Equation 6.28, and other designed output data.

8.5 Utilities of Refrigerant and Moist Air

Utilities of thermodynamic properties of refrigerants (pressure, temperature, specific volume, and enthalpy) are from computer subroutines based on Kartsonnes and Earth (1971). Utilities of physical properties of refrigerants (conductivity, specific heat, and viscosity), and properties of moist air (vapour density and relative humidity) are from computer subroutines based on ASHRAE Handbook 1981 Fundamentals (1981). Computer utility subroutine listings appear in Appendix II.

CHAPTER 9

EXPERIMENTAL DETERMINATION OF INPUT PARAMETERS

9.1 Overview

For simulating a defrosting process, the following parameters and coefficients are required: initial mass of water held on coil surface, surface evaporation coefficient, surface evaporation exponent, reference mass of frost, reference conductance of water/air layer and convective heat transfer coefficient on the air side. However, they are not available directly from measuring or other current literature, and have to be determined by experiments. Therefore, experiments with a refrigerant cooled coil and a glycol cooled coil were designed to obtain these parameters and coefficients.

9.1.1 Experiment with refrigerant cooled coil

For determining initial mass of water held on the coil and estimating coil surface vaporization, experiments with a refrigerant cooled coil were done in a conventional heat pump system with a normal 1 ton (3½ kw) capacity. A single circuit 2-row 20-tube evaporator, which has the geometry listed in Table 9.2, was installed in an insulated cold test box with an inside volume of 216 ft^3 (6.11 m^3). A humidifier was used to humidify the air inside the test box. The coil was frosted by

a heat pump. The defrosting of the coil was done by a reversed cycle. During the defrosting, water from melting frost drained by gravity and was collected. The environmental condition of the experiment was controlled by a microprocessor controller. All measured data were analyzed by computers.

9.1.2 Experiment with glycol cooled coil

The convective heat transfer coefficient on the air side, reference conductance of water/air layer and reference mass of frost were determined by experiments with a glycol cooled coil. A 2-row 10-tube coil, which has the geometry listed in Table 9.3, was installed in the test box. Each tube had an electrical cartridge heater of 160 watts which was equal in length to the finned surface. A humidifier was used to humidify air in the test box. The frosting of the coil was by cooled glycol. The defrosting of the coil was by the electrical heaters. During the experiment, heat supplied by electrical heaters was kept to be constant. The wall temperature of the coil was measured. The change rate of wall temperature versus time and its curve were obtained.

9.2 Estimation of Initial Mass of Water Held on Coil

The initial mass of water held on coil is estimated based on the experiments with a refrigerant cooled coil. When the coil is frosted, the amount of frost on the coil surface is equal to the amount of water vaporized from a source, since

the amount of vaporized water remaining in moist air is so small that it can be neglected, that is

$$m_f = m_h \tag{9.1}$$

where

m_h = mass of water vaporized by the humidifier

When the coil is defrosted, total frost on the coil surface is melted. Part of water from melted frost drains due to gravity, which is collected and measured. Part of it vaporizes to humidify moist air in the box and condenses on the wall of the box. The other part remains on the coil surface to form a water film, that is

$$m_{f,i} = m_{c,i} + m_{v,i} + m_{s,i} \tag{9.2}$$

where

$m_{f,i}$ = mass of frost

$m_{c,i}$ = mass of collected water

$m_{v,i}$ = mass of vaporized water

$m_{s,i}$ = mass of water held on coil surface

i = index of coil surface initial condition,

i = d means dry surface initial condition,

i = w means wet surface initial condition

The experiment was performed under two different initial conditions: dry surface and wet surface. For the dry surface initial condition, the coil surface was dry when the experiment started. And for the wet surface initial condition, the coil surface was covered with water film, which was formed from previous frosting-defrosting cycle. When experiment

started frosting with dry surface, the mass transfer after defrosting was

$$m_{f,d} = m_{c,d} + m_{v,d} + m_{s,d} \tag{9.3}$$

When experiment started frosting with wet surface, the mass transfer after defrosting was

$$m_{f,w} = m_{c,w} + m_{v,w} + m_{s,w} \tag{9.4}$$

For both experiments, the amount of vaporized water from the source was controlled to be the same, the amount of frost formed in both experiments was

$$m_{f,d} = m_h \tag{9.5}$$

$$m_{f,w} = m_h + m_{w,r} \tag{9.6}$$

where

$m_{w,r}$ = mass of water remaining on the coil before experiments

Since the environmental condition is controlled to be the same for both experiments, the mass of surface vaporization is the same, that is

$$m_{v,d} = m_{v,w} \tag{9.7}$$

and the amount of water held on the coil surface is the same, that is

$$m_{s,d} = m_{s,w} \tag{9.8}$$

Combining Equations 9.3 to 9.8 yields the amount of mass of water remaining on the coil at the end of experiments, that is

$$m_{w,r} = m_{c,w} - m_{c,d} \tag{9.9}$$

It is found from the experiment that approximate 0.7 lbm (0.32 kg) of water remains on the experiment coil surface

after defrosting. This experimental result was from 68 data points. Experimental data of mass of water remaining on the coil surface scattered in the range from 0.3 lbm (0.14 kg) to 1.0 lbm (0.45 kg). The experimental coil had a surface area of 98 ft^2 (9.1 m^2). If the water film is assumed uniformly on the coil surface, the mass of water remaining on the coil, $m_{w,r}$, for an unit area is 0.0071 lbm/ft^2 (0.035 kg/m^2).

At the beginning of defrosting stage of wet surface, that is, at the beginning of coil surface vaporization, the initial mass of water held on the coil is

$$m_{w,o} = m_{w,r} + m_v \tag{9.10}$$

Since the average value of coil surface vaporization obtained from experiments is approximate 0.3 lbm (0.14 kg), which is detailed in the next section, the average value of the initial mass of water held on the coil is approximate 1.0 lbm (0.45 kg). If the water film is assumed uniformly on the coil surface, the initial mass of water held on the coil, $m_{w,o}$, for an unit area is 0.010 lbm/ft^2 (0.050 kg/m^2).

9.3 Estimation of Surface Vaporization

The determination of surface vaporization parameters is based on the experiments with a refrigerant cooled coil. The experiment starts with the frosting of the coil. A certain amount of water is vaporized by a humidifier and becomes frost on the coil surface. Then, the coil is defrosted and the condensate is collected. Based on the experimental data of the

amount of water vaporized by the humidifier and the amount of collected condensate, the amount of mass of coil surface vaporization is obtained.

In the experiment, as the amount of water humidifying air is negligible, almost all amount of water vaporized by the humidifier becomes frost on the coil surface. The total amount of frost on the coil surface is

$$m_f = m_h + m_{w,r} \tag{9.11}$$

After defrosting, frost on the coil surface is converted to surface water film, condensate and water vapour, that is

$$m_f = m_{w,r} + m_c + m_v \tag{9.12}$$

where

m_c = mass of condensate

If the experiment starts frosting the coil at wet surface condition and ends the defrosting process at wet surface condition, the amount of water held on the coil is not changed. Combining Equation 9.11 with 9.12 yields that the mass of water vaporized by the humidifier is equal to the mass of collected condensate and water vaporized from the coil surface, that is

$$m_h = m_c + m_v \tag{9.13}$$

The amount of mass of coil surface vaporization is

$$m_v = m_h - m_c \tag{9.14}$$

If the experiment starts frosting the coil at dry surface condition and ends the defrosting process at wet surface condition, Equation 9.11 becomes

$$m_f = m_h \tag{9.15}$$

Substituting Equation 9.15 into 9.12 yields the amount of mass of coil surface vaporization, that is

$$m_v = m_h - m_c - m_{w,r} \tag{9.16}$$

In the experiment, the amount of water vaporized by the humidifier and the amount of collected condensate are measured. A mass loss between water vaporized by the humidifier and collected condensate is obtained. For the experiment starting at wet surface condition, the mass loss between water vaporized by the humidifier and collected condensate gives the approximate value of mass of surface vaporization. For the experiment starting at dry surface condition, the amount of water remaining on the coil should be considered. 59 data points were obtained from the experiments under wet surface condition. The average amount of water vaporized by the humidifier was 2.0 lbm (0.91 kg). The average amount of lost mass was 0.3 lbm (0.14 kg). Therefore, the mass of coil surface vaporization is approximate 0.3 lbm (0.14 kg). 9 data points were obtained from the experiments under dry surface condition. The average amount of water vaporized by the humidifier was 2.7 lbm (1.23 kg). The average amount of lost mass was 1.0 lbm (0.45 kg). Since the mass of water remaining on the experimental coil is approximate 0.7 lbm (0.32 kg) (refer to Section 9.2), from Equation 9.16, the mass of coil surface vaporization is approximate 0.3 lbm (0.14 kg).

9.4 Surface Evaporation Coefficient and Exponent

The ratio of coil surface vaporization is defined as

$$r_{sv} = m_v/m_r \tag{9.17}$$

where

r_{sv} = ratio of coil surface vaporization

Based on experimental data, the ratio of coil surface vaporization is approximate 11 % for both wet surface initial condition and dry surface initial condition. The experimental data of ratios of coil surface vaporization scattered in the range from 0% to 25%.

In computation, surface evaporation coefficient and surface evaporation exponent were selected to approach the value of ratio of coil surface vaporization obtained from the experiments, 11%, that is, 0.3 lbm (0.14 kg) water for the experimental coil. At the same time, a best approach to the experimental data of refrigerant leaving state is also considered. The approach with a surface evaporation coefficient of 55 ft/h (16.8 m/h) and a surface evaporation exponent of 0.5 gave the overall best results.

9.5 Estimation of Reference Conductance of Water/Air Layer

The reference conductance of water/air layer and reference mass of frost were obtained based on the defrosting experiment with a glycol cooled coil during melting frost stage. The heat transfer during melting frost stage can be expressed as follows:

$$Q_e = Q_s + Q_f \tag{9.18}$$

where

Q_e = heat transfer rate of electrical heater, constant

Q_s = rate of heat stored in glycol cooled coil

$$Q_s = C_g \cdot (dT_w/dt) \tag{9.19}$$

C_g = heat capacity of glycol cooled coil and contents

$$Q_f = C_w \cdot A_e \cdot (T_w - T_f) \tag{3.27}$$

Substituting Equations 9.19 and 3.27 into 9.18 yields

$$C_g \cdot (dT_w/dt) + C_w \cdot A_e \cdot (T_w - T_f) = Q_e \tag{9.20}$$

or $$C_g \cdot (d\theta/dt) + C_w \cdot A_e \cdot \theta = Q_e \tag{9.21}$$

where

θ = temperature difference

$$\theta = T_w - T_f \tag{9.22}$$

The differential Equation 9.21 has an analytical solution. The solution of wall temperature versus time has exponential form unless the heat transfer rate to melting frost is a constant with the time. It was found from the experiment that the change rate of wall temperature versus time was approximately constant, that is

$$C \cdot (d\theta/dt) = C_1 \tag{9.23}$$

where

C_1 = constant

In the experiment, heat flux from electrical heaters was kept to be constant, that is

$$Q_e = C_2 \tag{9.24}$$

where

C_2 = constant

Substituting Equations 9.23 and 9.24 into Equation 9.21 yields a result that the heat transfer rate to melting frost is a constant, that is

$$Q_f = C_w \cdot A_e \cdot \theta = C_3 \tag{9.25}$$

where

C_3 = constant

The required heat transfer rate for melting frost is also given by

$$Q_f = (m_{mf}/t) \cdot h_{if} = C_3 \tag{9.26}$$

where

m_{mf} = mass of melted frost

t = time corresponding to melt frost

Therefore, mass rate of melting frost is a constant, that is

$$m_{mf}/t = M_{mf} = C_4 \tag{9.27}$$

where

M_{mf} = mass rate of melting frost

C_4 = constant

Combining Equations 9.25 with 9.26 yields the conductance of water/air layer, that is

$$C_w = (m_{mf}/t) \cdot h_{if}/(A_e \cdot \theta) \tag{9.28}$$

If a reference point is chosen at the end of melting frost stage, that is

At $t = t_{ref}$

$$m_{mf} = m_{mf,ref} \tag{9.29}$$

$$\theta = \theta_{ref}$$

the reference conductance of water/air layer at the end of melting frost stage is

$$C_{w,ref} = (m_{mf,ref}/t_{ref}) \cdot h_{if}/(A_e \cdot \theta_{ref}) \quad (9.30)$$

where

$C_{w,ref}$ = reference conductance of water/air layer

$m_{mf,ref}$ = reference mass of melted frost

t_{ref} = reference time

θ_{ref} = reference temperature difference

Combining Equations 9.28 with 9.30 yields

$$C_w/C_{w,ref} = (m_{mf}/m_{mf,ref}) \cdot (t_{ref}/t) \cdot (\theta_{ref}/\theta) \quad (9.31)$$

or $$C_w/C_{w,ref} = (m_{mf}/m_{mf,ref}) \cdot (t_{ref}/t)^2 \cdot (\theta_{ref}/t_{ref})/(\theta/t) \quad (9.32)$$

Based on the linear correlation of wall temperature versus time obtained from the experiment

$$\theta/t = \theta_{ref}/t_{ref} \quad (9.33)$$

Substituting Equation 9.33 into Equation 9.32 yields

$$C_w/C_{w,ref} = (m_{mf}/m_{mf,ref}) \cdot (t_{ref}/t)^2 \quad (9.34)$$

From Equation 9.27

$$m_{mf}/t = m_{mf,ref}/t_{ref} = C_4 \quad (9.35)$$

or $$m_{mf}/m_{mf,ref} = t/t_{ref} \quad (9.36)$$

Substituting Equation 9.36 into Equation 9.34 yields

$$C_w/C_{w,ref} = m_{mf,ref}/m_{mf} \quad (9.37)$$

At the reference point, the end of melting frost stage, the mass of melted frost and initial mass of frost have the same value, that is

$$m_{mf,ref} = m_{f,ref} \quad (9.38)$$

Since

$$m_{mf} = m_{f,ref} - m_f \quad (9.39)$$

Substituting Equation 9.38, 9.39 into 9.37 yields the conductance of water/air layer as follows:

$$C_w = C_{w,ref}/(1 - m_f/m_{f,ref}) \quad (3.28)$$

In the experiment, mass of frost, time, wall temperature and ambient temperature at the reference point, the end of melting frost stage, were measured. Substituting these experimental data into Equation 9.30, the total conductance of water/air layer at reference point $C_{w,ref} \cdot A_e$ is obtained. The effective surface area is based on the fin efficiency (detailed in Section 3.2.3), which is a function of conductance of water/air layer in melting frost stage, that is

$$A_e = f(\eta_f) = f(C_w) \quad (9.40)$$

A curve of total conductance versus conductance of water/air layer was made by assuming a series of conductance of water/air layer. From the curve, the reference conductance of water/air layer was obtained based on the total conductance.

When the mass of frost is equal to the reference mass of frost, the conductance of water/air layer obtained from Equation 3.28 will tend to infinity. Therefore, a maximum value of the conductance of wall/air layer is set for limitation. In order to let Equation 3.28 be valid for all cases, a maximum possible value of reference mass of frost should be used, which is corresponding to the situation that whole coil is blocked by frost and the rate of the free air flow across the coil is zero. It was found that the maximum

value of the reference mass of frost for the experimental coil was approximate 1.5 lbm (0.68 kg). 5 sets of data with the maximum value of the reference mass of frost were obtained from the experiments. The reference conductance of water/air layer was approximate 3.7 Btu/(h·ft²·°F) (6.5 w/(m²·K)). The experimental data of the reference conductance of water/air layer scattered in the range from 2.6 Btu/(h·ft²·°F) (4.6 w/(m²·K)) to 5.3 Btu/(h·ft²·°F) (9.3 w/(m²·K)), which were from 5 sets of experimental data with the maximum value of the reference mass of frost. If the frost layer is assumed uniformly on the coil surface, the maximum value of the reference mass of frost on the experimental coil is 0.031 lbm/ft² (0.150 kg/m²). The density of frost on the coil varies with coil geometry and environmental conditions. The experimental coil had a free space of 0.468 ft³ (0.0132 m³). Since the frost layer can be assumed uniformly on the coil surface, the approximate density of frost held on the coil is 3.2 lbm/ft³ (51.4 kg/m³). A detailed discussion of frost density based on the work of Malhammar (1986) was presented by Oskarsson, Krakow and Lin (1990).

9.6 Estimation of Air Side Heat Transfer Coefficient

The air side heat transfer coefficient was determined based on experiments with the glycol cooled coil. The experiment was done by heating and cooling the coil. For heating the coil, constant heat flux was supplied by

electrical heating elements. For cooling the coil, no heat was supplied. A heat coil was cooled by free convection. The heat transfer of the experiment can be expressed as follows:

$$Q_e = Q_s + Q_c \tag{9.41}$$

where

$$Q_c = h_a \cdot A_e \cdot (T_w - T_a) \tag{3.23}$$

Substituting Equations 9.19 and 3.23 into 9.41 yields

$$C_q \cdot (dT_w/dt) + h_a \cdot A_e \cdot (T_w - T_a) = Q_e \tag{9.42}$$

or $$C_q \cdot (d\theta/dt) + h_a \cdot A_e \cdot \theta = Q_e \tag{9.43}$$

where

$$\theta = T_w - T_a \tag{9.44}$$

The general solution of differential equation 9.43 is

$$\theta = Q_e/(h_a \cdot A_e) + C_o \cdot e^{-s \cdot t} \tag{9.45}$$

where

$$s = h_a \cdot A_e/C_q \tag{9.46}$$

9.6.1 Solution for heating the coil

For the heating coil experiment, the initial conditions are as follows:

$$t = 0$$

$$\theta = T_w - T_a = 0$$

$$e^{-s \cdot t} = 1$$

Substituting into Equation 9.45 yields the constant of integration for the heating coil experiment, that is

$$C_o = - Q_e/(h_a \cdot A_e) \tag{9.47}$$

Substituting Equation 9.47 into Equation 9.45 yields the total

heat transfer coefficient, that is

$$h_a \cdot A_s = Q_e \cdot (1 - e^{-s \cdot t})/\theta \qquad (9.48)$$

This equation is an exponential equation with more than one variables and can not be solved directly.

9.6.2 Solution for cooling the coil

For the cooling coil experiment, no heat is supplied, that is

$$Q_e = 0 \qquad (9.49)$$

Substituting Equation 9.49 into general solution, Equation 9.45, yields

$$\theta = C_o \cdot e^{-s \cdot t} \qquad (9.50)$$

The initial conditions for the cooling coil experiment are as follows:

$$t = 0$$

$$\theta = \theta_o$$

$$e^{-s \cdot t} = 1$$

Substituting into Equation 9.50 yields the constant of integration, that is

$$C_o = \theta_o \qquad (9.51)$$

Substituting Equation 9.51 into Equation 9.50 yields

$$\theta = \theta_o \cdot e^{-s \cdot t} \qquad (9.52)$$

or $$\ln \theta = \ln \theta_o - s \cdot t \qquad (9.53)$$

Differentiating Equation 9.53 yields

$$s = - d(\ln \theta)/dt \qquad (9.54)$$

which means that "s" is the negative slope of the curve of

logarithm of temperature difference versus time.

9.6.3 Solution for air side heat transfer coefficient

In the cooling experiment, the coil was cooled by free convection. The wall temperature, ambient temperature and time were measured. A curve of logarithm of temperature difference between the wall and ambient versus time was plotted. The slope of the curve was determined. In the heating experiment, the coil was heated. The wall temperature, ambient temperature, time and power input to the electrical heaters were measured. Substituting the calculated value of the slope from the cooling experiment and values of temperature difference, time, and power input obtained from the heating experiment into Equation 9.48 yielded the total heat transfer coefficient $h_a \cdot A_e$. The effective surface area is based on the fin efficiency, which is a function of air side heat transfer coefficient, that is

$$A_e = f(\eta_f) = f(h_a) \tag{9.55}$$

A curve of total heat transfer coefficient versus air side heat transfer coefficient was made by assuming a series of air side heat transfer coefficient. From the curve, the convective heat transfer coefficient on the air side was obtained.

It is found from the experiment that the convective heat transfer coefficient on the air side is approximate 0.54 Btu/(h·ft²·°F) (0.95 w/(m²·K)). The experiment data of convective heat transfer coefficient on the air side scattered

in the range from 0.28 Btu/(h·ft²·°F) (0.49 w/(m²·K)) to 0.64 Btu/(h·ft²·°F) (1.12 w/(m²·K)). These results were from 5 sets of experimental data.

Table 9.1

Experimentally Determined Parameters

Initial mass of water held on coil surface per unit area, $m_{w,o}$	0.010 lbm/ft² (0.050 kg/m²)
Reference conductance of water/air layer, C_w	3.7 Btu/(h·ft²·°F) (6.5 w/(m²·K))
Reference initial mass of frost per unit area, $m_{f,ref}$	0.031 lbm/ft² (0.150 kg/m²)
Air side convective heat transfer coefficient, h_a	0.54 Btu/(h·ft²·°F) (0.95 w/(m²·K))
Surface evaporation coefficient, C_{ae}	55 ft/h (16.8 m/h)
Surface evaporation exponent, n	0.5

Table 9.2

Geometry of Refrigerant Coil

Tube inside diameter, D_i	0.485 in (1.23 cm)
Tube outside diameter, D_o	0.537 in (1.36 cm)
Fin height, D_1	1.25 in (3.18 cm)
Fin depth, D_2	1.20 in (3.05 cm)
Fin thickness, t	0.006 in (0.015 cm)
Number of fins	8 per in (10 / 3.175 cm)
Height	10 row
Depth	2 row
Number of circuits	1
Finned length per tube	32 in (81.28 cm)
Total outside surface area	98 ft^2 (9.1 m^2)
Free volume	0.935 ft^3 (0.0265 m^3)
Tube material	Copper
Fin material	Aluminum

Table 9.3

Geometry of Glycol Coil

Tube inside diameter, D_i	0.485 in (1.23 cm)
Tube outside diameter, D_o	0.537 in (1.36 cm)
Fin height, D_1	1.25 in (3.18 cm)
Fin depth, D_2	1.20 in (3.05 cm)
Fin thickness, t	0.006 in (0.015 cm)
Number of fins	8 per in (10 / 3.175 cm)
Height	5 row
Depth	2 row
Finned length per tube	32 in (81.28 cm)
Total outside surface area	49 ft^2 (4.55 m^2)
Free volume	0.468 ft^3 (0.0132 m^3)
Tube material	Copper
Fin material	Aluminum

CHAPTER 10

VERIFICATION OF SIMULATION

10.1 Overview

A computer program was written using FORTRAN to simulate the defrosting process of evaporators. The simulation results were compared with data obtained from hot gas defrosting experiments with different initial and environmental conditions. These experiments were done with a normal 1 ton (3½ kw) manually reversed conventional heat pump system with refrigerant R-12. Twelve sets of comparison data of simulation against experiment were used to verify the accuracy of the simulation. Three sets of data were with dry surface initial condition, and other nine sets of data were with wet surface initial condition. The deviation between simulation results and experimental data, errors and reasons are discussed in this chapter.

10.2 Simulation Input Data

For computer simulation, required input data are evaporator geometry, refrigerant parameters, environmental conditions, coefficients, and other specified data: number of elements, length of time interval, etc. The input data of evaporator geometry are specified using the data from the experimental coil, which are listed in Table 9.2. The input

data of refrigerant parameters and environmental conditions are from experiment measuring. At the inlet of the evaporator, refrigerant is in superheated state. Since defrosting processes are transient processes, refrigerant states change as the process progresses. As refrigerant passing through the evaporator, certain amount of heat is transferred from refrigerant to the outside frost layer or surface water of the evaporator. A pressure drop of refrigerant takes place due to friction, velocity change and turning of flow in bends. The leaving state of refrigerant differs from entering state. Therefore, initial refrigerant pressure, temperature, quality and mass flow rate are required as input data for each time interval. These data are used to verify the simulation results from the one time interval, and to set up new refrigerant state for the simulation of the next time interval. At the beginning of the defrosting process, the evaporator is fully frosted. As the process progresses, the environmental conditions of the insulated cold test box changes slightly. Environmental air temperature increases due to free convective heat transfer. Relative humidity increases due to surface water vaporization. Therefore, environmental air temperature and relative humidity are also required input data for the simulation of each time interval. Sample input data of refrigerant state and environmental conditions are presented in Appendix III. The input data of coefficients, initial mass of water held on coil surface, reference conductance of

water/air layer, reference initial mass of frost, air side convective heat transfer coefficient, surface evaporation coefficient and surface evaporation exponent, are from the experimental determination of refrigerant cooled coil and glycol cooled coil, which are listed in table 9.1. The specified data for the layout of spacial elements and time intervals are considered as follows:

Number of elements, $n_s = 100$

Length of time interval, $\delta_t = 24$ seconds

Maximum number of time intervals, $n_{t,mx} = 8$ to 14

In order to compare simulation results with experimental data easily, the values of length of time interval and maximum number of time interval are specified to be the same as those used in corresponding experiments.

10.3 Comparison of Simulation and Experimental Data

Twelve sets of data of simulation against experiment were compared. For each set of comparison data, following characteristic parameters were compared based on the same point in time:

Leaving refrigerant temperature, T_r ($^\circ$F)

Total energy consumed for defrosting, E (Btu)

Refrigerant pressure drop for the evaporator, dP (psi)

Amount of subcooling, $T_r - T_s$ ($^\circ$F)

Leaving refrigerant quality, x

Total mass of vaporized surface water, m_v (lbm)

Curves of leaving refrigerant temperature versus time are plotted as shown in Fig.10.1 to Fig.10.12. Curves of total energy versus time are plotted as shown in Fig.10.13 to Fig.10.24. Other data are tabulated in Tables 10.1 to 10.3. Data Sets 1 to 3 are based on the evaporator with dry surface initial conditions. Data Sets 4 to 12 are based on the evaporator with wet surface initial conditions. It can be seen from the curves of leaving refrigerant temperature versus time shown in Fig.10.1 to 10.12 that the simulation results are quite well close to the experimental data. Whatever the surface initial condition the evaporator has, the curves of T_r versus t have the similar trend, beginning at around 32°F (0°C) and ending at 80°F - 90°F (26.7°C - 32.2°C). The maximum deviation usually occurs in the middle of process and has an approximate average value of 5°F (2.8°C). From the curves of total energy versus time shown in Fig.10.13 to 10.24, it is observed that the simulation curves are approximately parallel with experimental curves. The simulation curve and experimental curve are close, and keep approximate constant amount of deviation. The deviation of total energy at the end of defrosting process is 5 % to 9 %. Larger errors appear in the simulation of refrigerant pressure drop in Table 10.1. Average 1.6 psi (11.0 kPa) deviation is found. The leaving states of refrigerant, amount of subcooling and quality, are compared between the simulation and experimental data in Table 10.2. They are satisfactory. In Table 10.3, the comparison

results of total mass of vaporized surface water are shown. The average deviation is 0.3 lbm (0.136 kg). Comparisons of other parameters, such as total heat transfer rate, leaving refrigerant enthalpy, etc., were also done. The results were satisfactory. The predictions from the simulation are quite close to the experimental data. However, these comparison results are not included in this work since they are of secondary importance in the defrosting process. The computer output file presented in Appendix III gives a sample of total computation results.

10.4 Analysis of Deviation

Factors causing deviation are from either computation or experiments. For the computation, idealization of defrosting process causes errors for simulating a practical process. For the experiments, instrument accuracy is a source of errors.

10.4.1 Simulation errors

To set up a defrosting model and to simulate defrosting process, a practical process is idealized based on the experimental observation. An assumption of the quasi-static process is made. Some less significant terms are neglected. And total defrosting time is divided into limited intervals. These treatments simplify the modelling, however, may cause errors.

In melting frost stage, the temperature difference

between the evaporator surface and surroundings is small. Therefore, convective heat transfer between frost layer surface and surroundings is neglected. Vaporizing heat transfer of surface water is neglected (detailed in Section 3.2). These omissions may result in small errors for the simulation of energy consumption at the beginning of the defrosting process, and result in accumulated errors for the whole defrosting process.

For the evaporator used in the experiments and normal commercial evaporators, tubes are connected by fins. Therefore, conductive heat transfer between tubes, using fins as a path, must take place since the temperature gradient between tubes. Some elements lose energy but some elements obtain energy. However, in the simulation, this heat transfer is neglected. This may result in some errors for heat transfer computation, refrigerant leaving state simulation as well as required energy estimation.

From the comparison of leaving refrigerant temperature, it is clear that larger deviation exists in the middle of defrosting process, which is corresponding to the transient range from the end of melting frost stage to the beginning of wet surface stage. In the theoretical model, mass transfer and heat transfer of surface water due to drain and vaporize occur only if all frost is melted. In fact, when frost starts to melt, mass transfer and heat transfer of surface water form melted frost take place. The difference between ideal process

and practical process may result in errors for the simulation.

For the estimation of pressure drop in the evaporators, involved errors may be due to some equations used for the computation.

For the simulation of total mass of vaporized surface water, this model only considers vaporization in wet surface stage. The surface vaporization in preheating stage and that in melting frost stage are neglected, since small temperature difference between the evaporator surface and surroundings only causes a small amount of heat and mass transfer in these stages. However, this may result in errors for the simulation.

10.4.2 Experiment errors

Hot gas defrosting experiments were done in a convectional heat pump system. At first, the evaporator was frosted by heat pump cycle. Then, the system was manually reversed to reversing cycle to perform the defrosting of the evaporator. When the leaving refrigerant temperature reached 80°F - 90°F (26.7°C - 32.2°C), all frost was melted. The defrosting experiment was considered to be completed. Characteristic parameters, temperature, pressure, mass flow rate, relative humidity, input power, etc., were measured during the whole process. A data acquisition system was used to scan 38 measurement channels once every 24 seconds. The system measurements were analyzed by computers. The data picked up once in a time interval were used as representative

values for the whole time interval.

Since data logging is done in sequence, 0.63 second for each measurement channel, time lag occurs between corresponding temperature and pressure measurements. It is apparent that time lag of measurements causes errors for the results. Errors may also be from that measurement values obtained once per time interval are used for 24 seconds.

As a defrosting process tends to end, less heat is required for the process, which will result in the increase of refrigerant temperature and rapid increase of refrigerant pressure. Therefore, when refrigerant pressure increases rapidly, the defrosting process could be considered as being completed. In the experiments, time intervals are set up to be uniform for the whole process. Measuring data picked up once per channel per time interval are used for the whole time interval. Near the end of defrosting process, rapid change of refrigerant pressure and other properties takes place within the time interval. However, constant values of refrigerant pressure and other properties are still used for the whole time interval, which may result in larger errors at the end of defrosting process. Obviously, the influence of time lag of measurements near the end of defrosting process will be more serious than that during the beginning of the process. Poor data is obtained due to the time lag of measurements.

The defrosting process is started with a frosted evaporator as the initial conditions. In other words, the

defrosting experiment is initialized immediately after the frosting cycle. When the system is manually reversed to the defrosting cycle, hot gas refrigerant with high pressure in the line from the compressor, oil separator, to reversing valve flows into the evaporator which contains low pressure refrigerant initially. A transient process of equalizing refrigerant pressure takes place. It is found from the experiments that the transient period is too short to obtain more measurement data. And the measurements obtained during that period are so fluctuating that it is hard to use these data for analyzing. However, when pressure equalization period is ended, released heat from previous hot gas refrigerant in the line has already preheated the evaporator to the melting point temperature, 32°F (0°C). Therefore, larger fluctuation and errors appear in the measurements at the beginning of defrosting process. In order to obtain reasonable conclusions, the comparison of simulation results with experimental data begins at melting frost stage. Even so, errors involved in preheating stage are accumulated and still affect the simulation of other defrosting stages as well as the whole process.

The experimental determination of mass of vaporized surface water is based on other experimental determined average values and estimation, such as initial mass of water held on the coil. Wide variation range of initial mass of water held on the coil was observed from refrigerant cooled

coil experiments (detailed in Section 9.2). Errors from these experimental determined data influence the accuracy of estimating the mass of vaporized surface water. Besides, the moisture in the air of the test box from vaporized surface water, which is approximate 0.05 lbm (0.023 kg) on the average, is neglected. Condensed water on the test box wall makes it impossible to make an accurate mass balance of the water.

Of course, for experiments, instrument accuracy and personal judgement of process termination are factors causing the deviations.

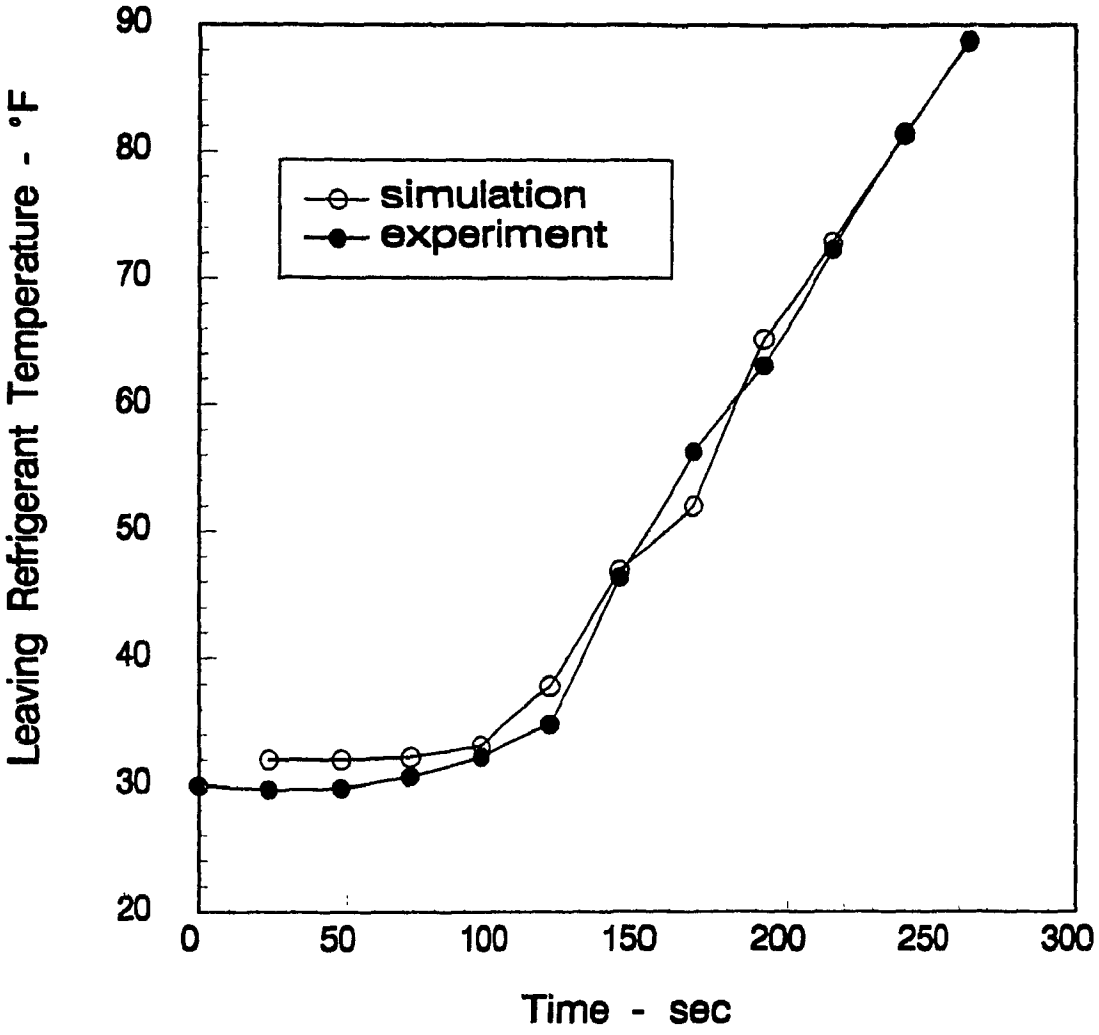

Figure 10.1 Temperature Comparison of Data Set 1

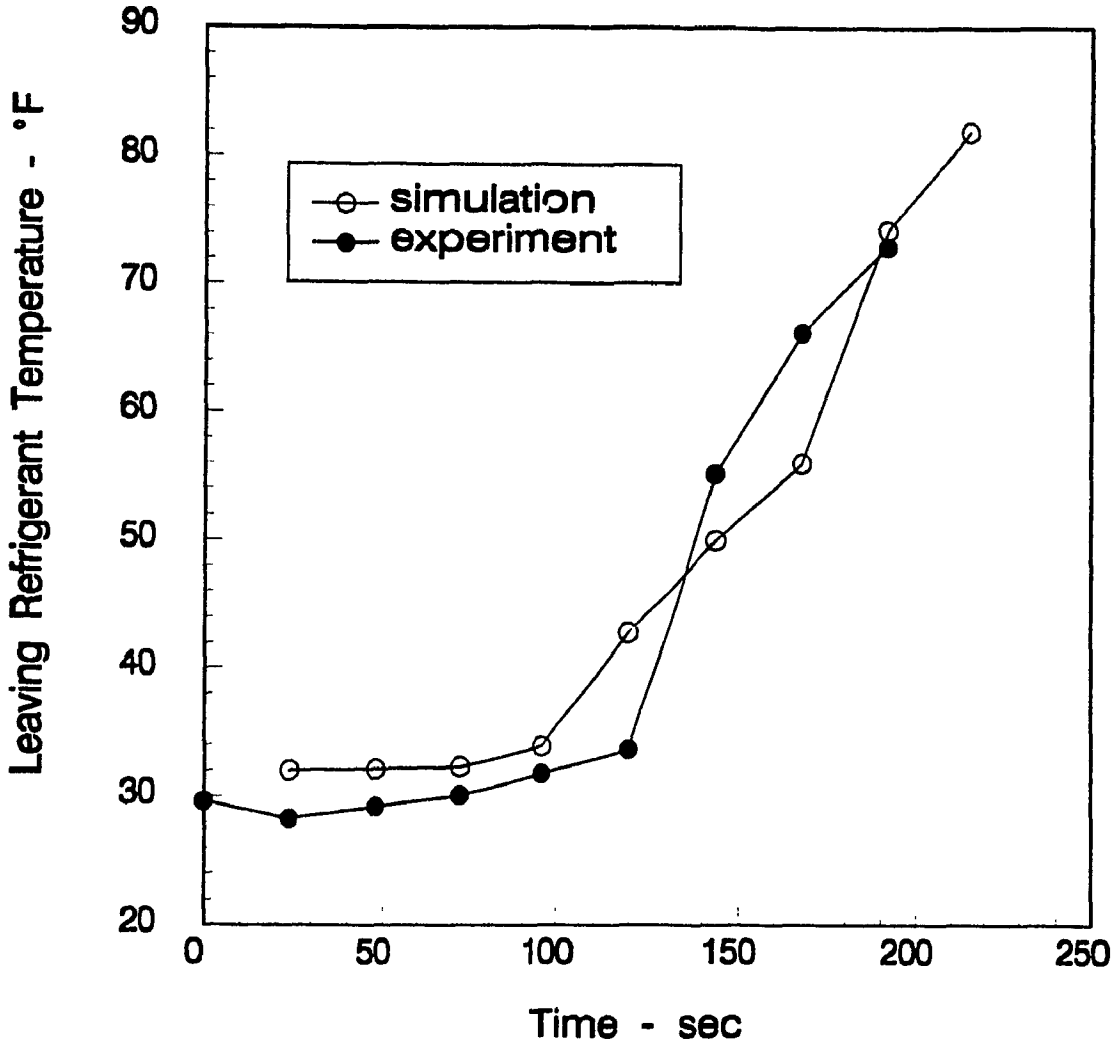

Figure 10.2 Temperature Comparison of Data Set 2

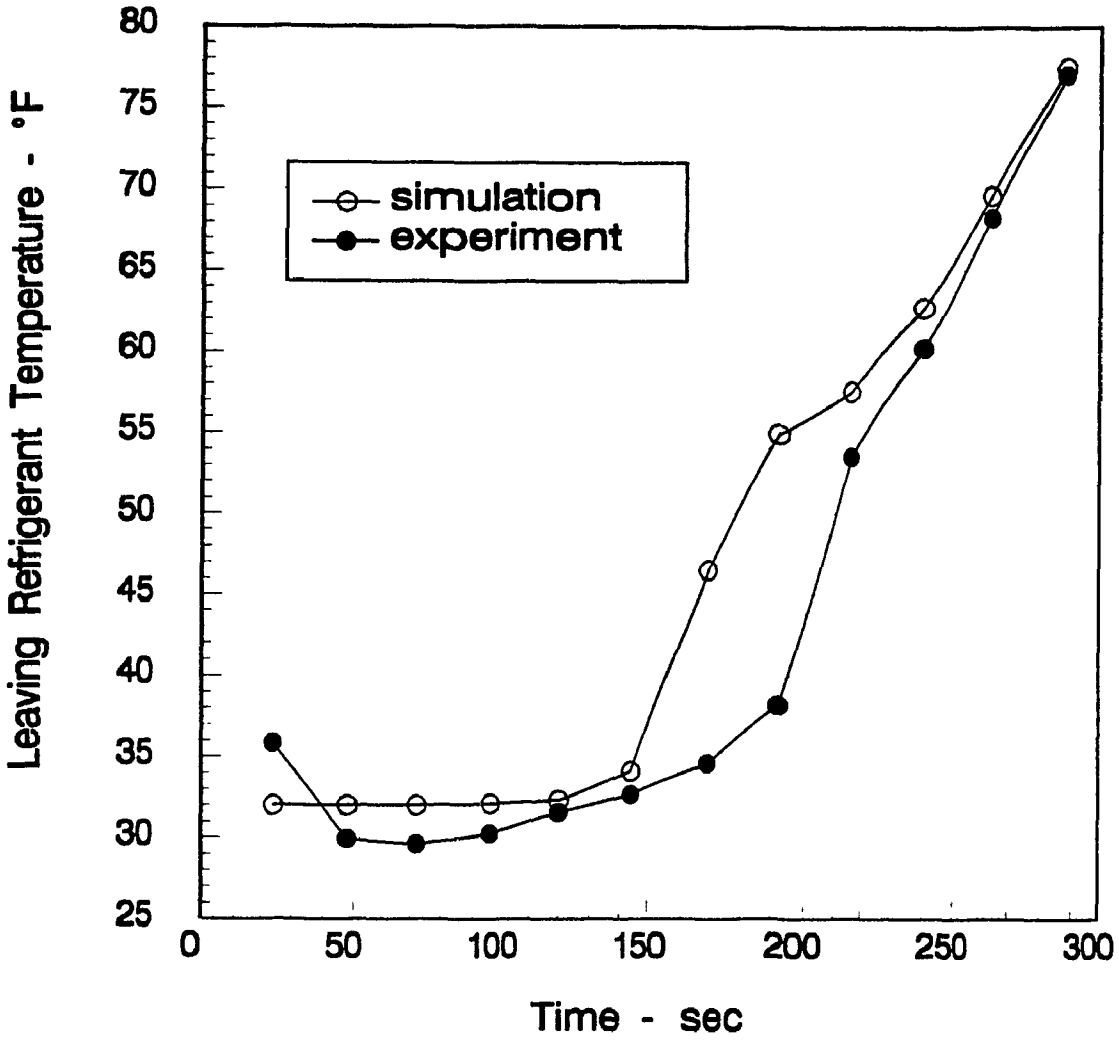

Figure 10.3 Temperature Comparison of Data Set 3

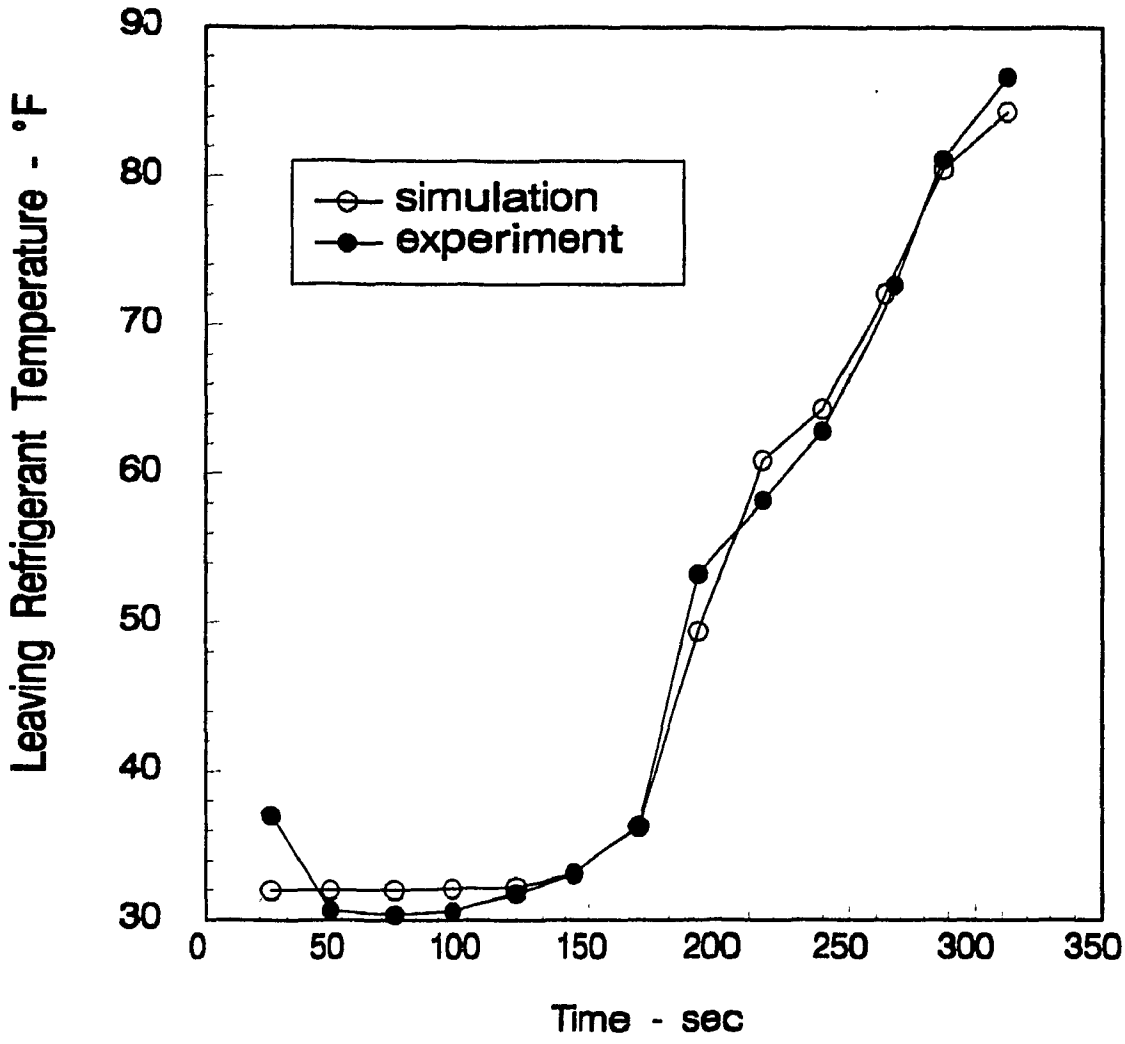

Figure 10.4 Temperature Comparison of Data Set 4

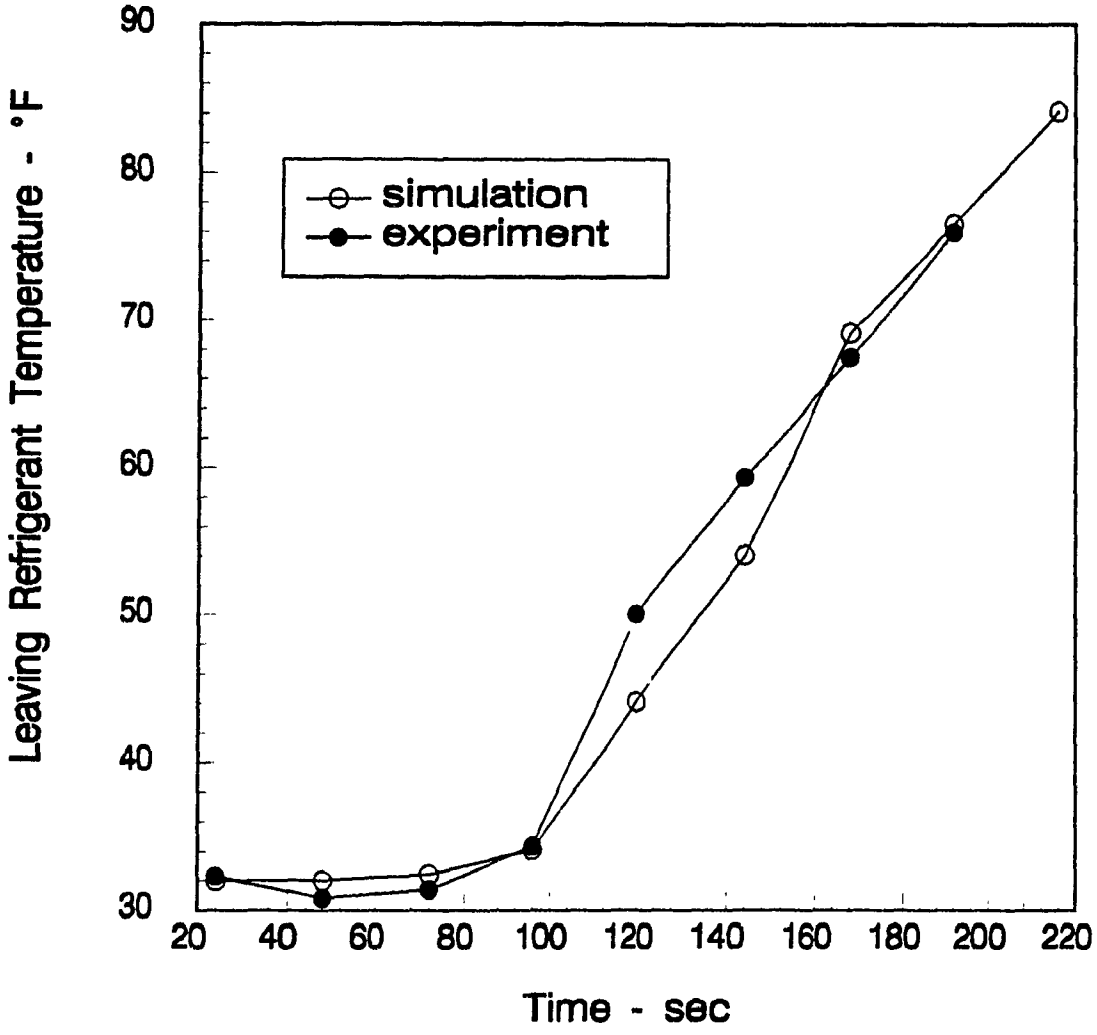

Figure 10.5 Temperature Comparison of Data Set 5

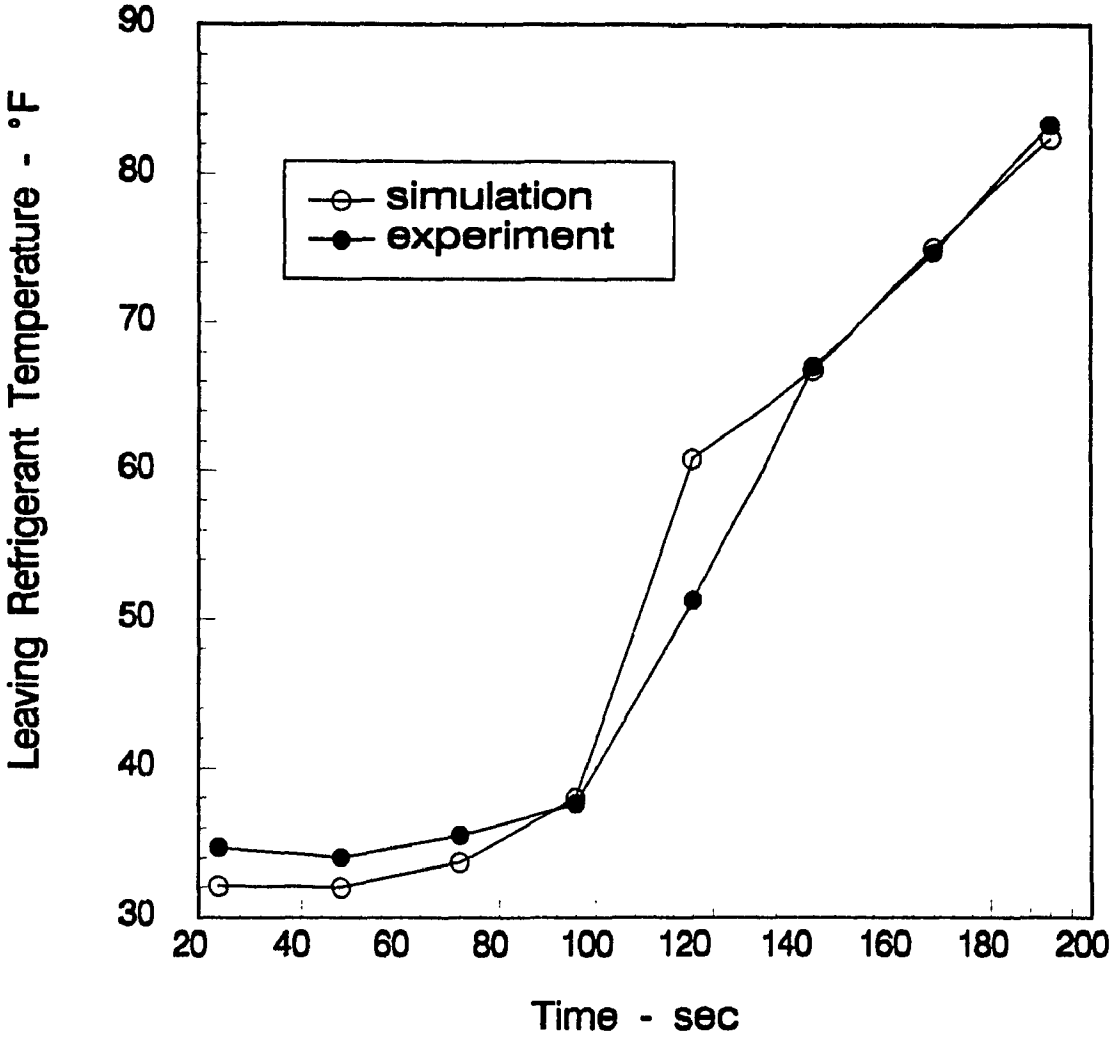

Figure 10.6 Temperature Comparison of Data Set 6

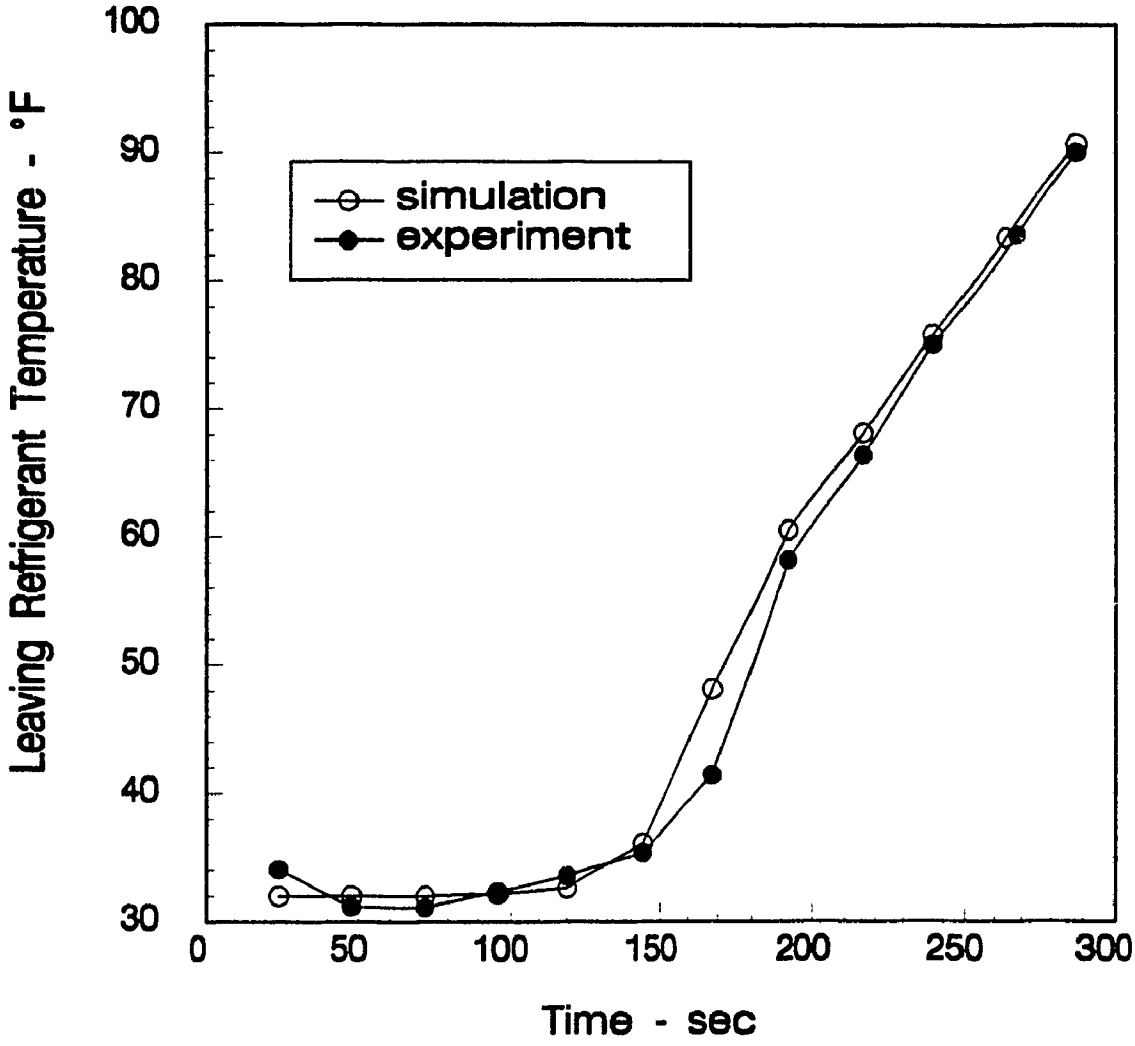

Figure 10.7 Temperature Comparison of Data Set 7

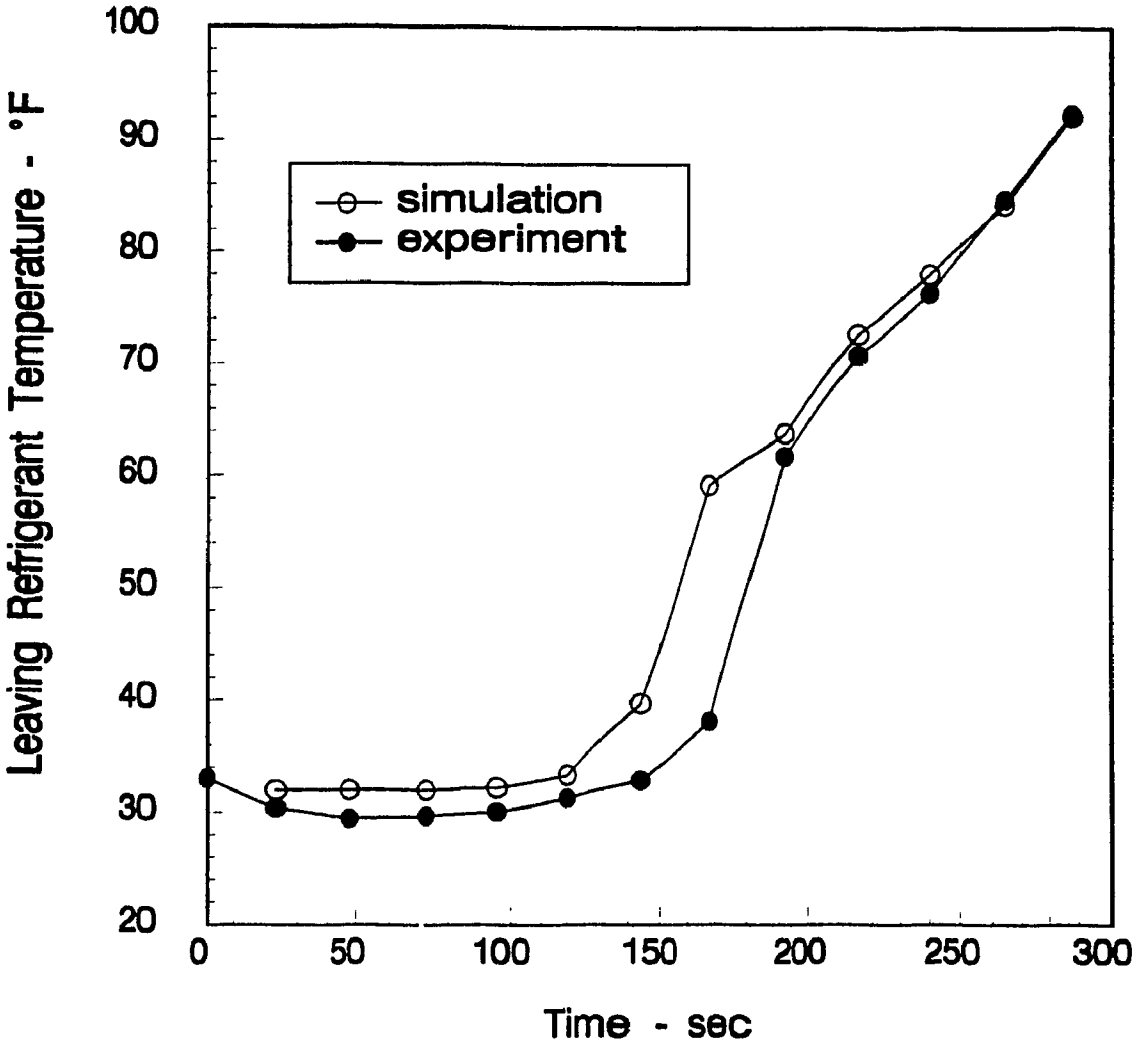

Figure 10.8 Temperature Comparison of Data Set 8

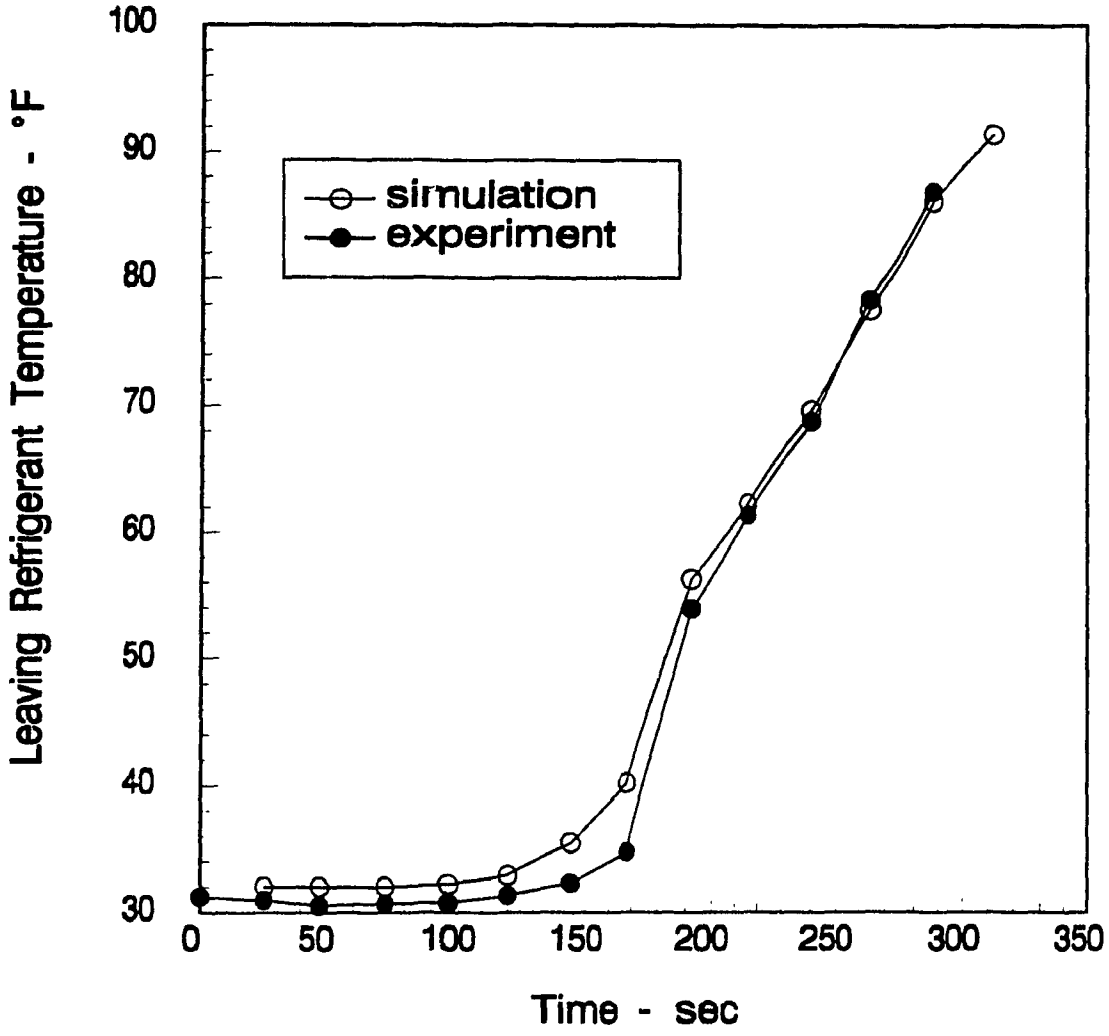

Figure 10.9 Temperature Comparison of Data Set 9

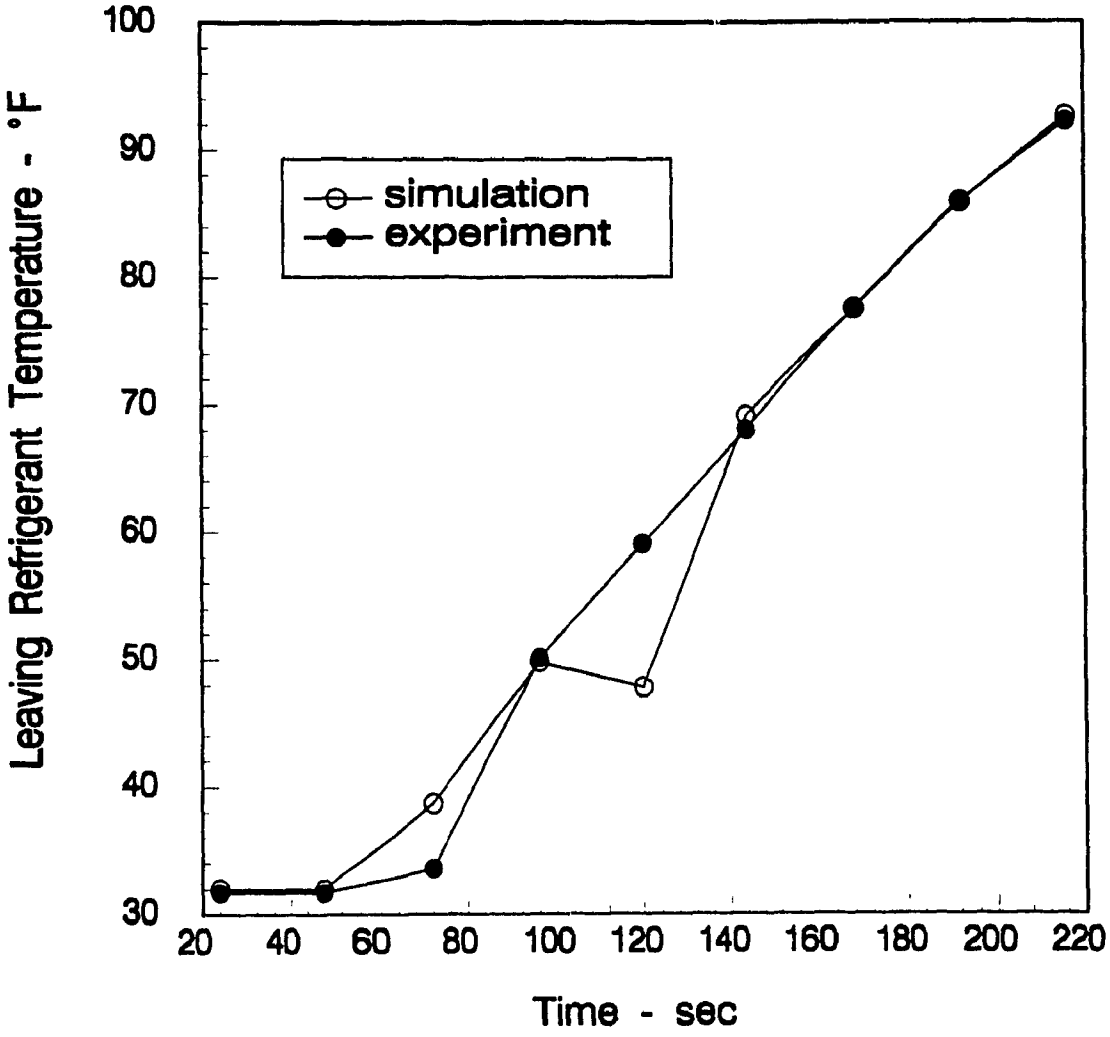

Figure 10.10 Temperature Comparison of Data Set 10

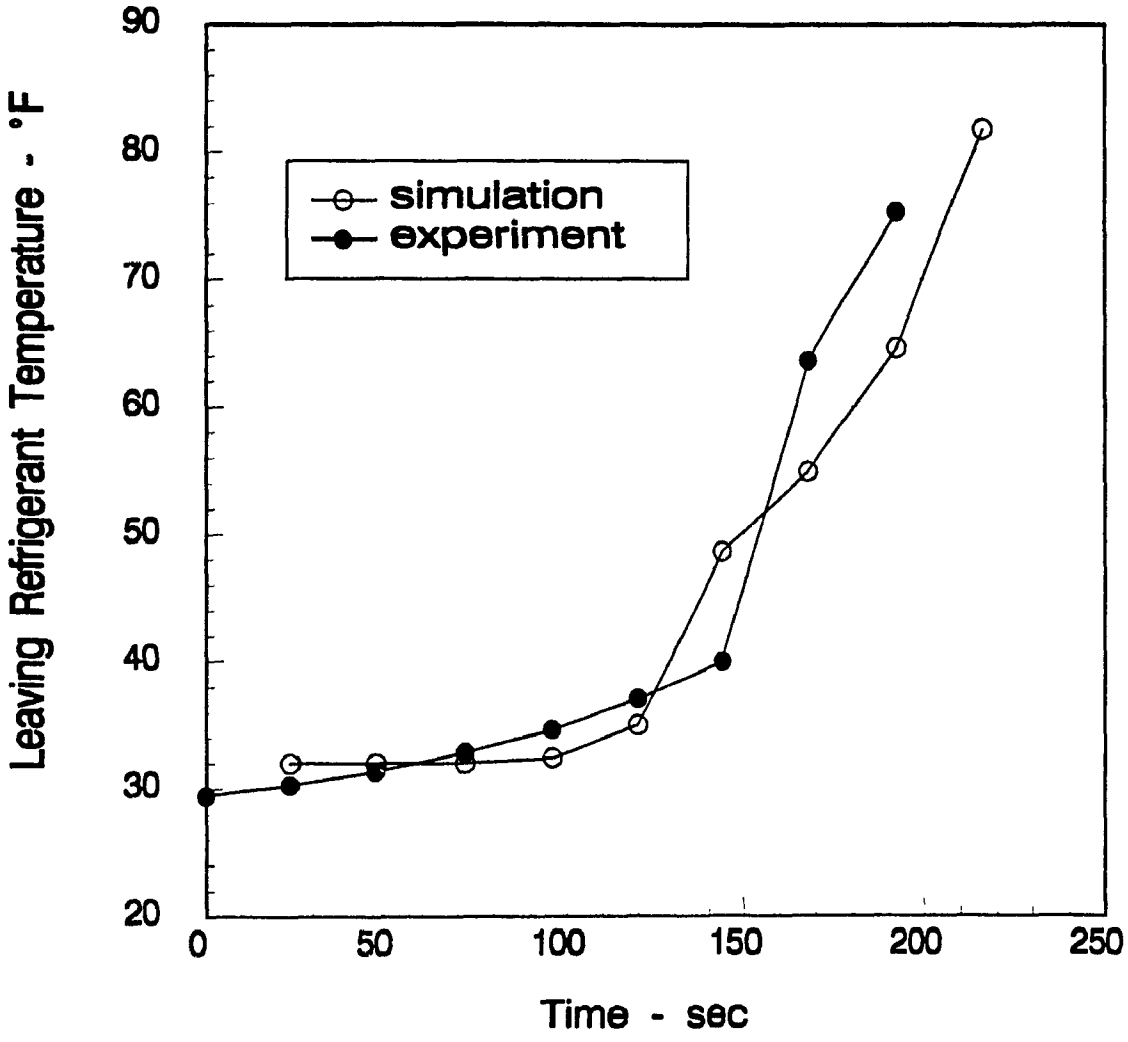

Figure 10.11 Temperature Comparison of Data Set 11

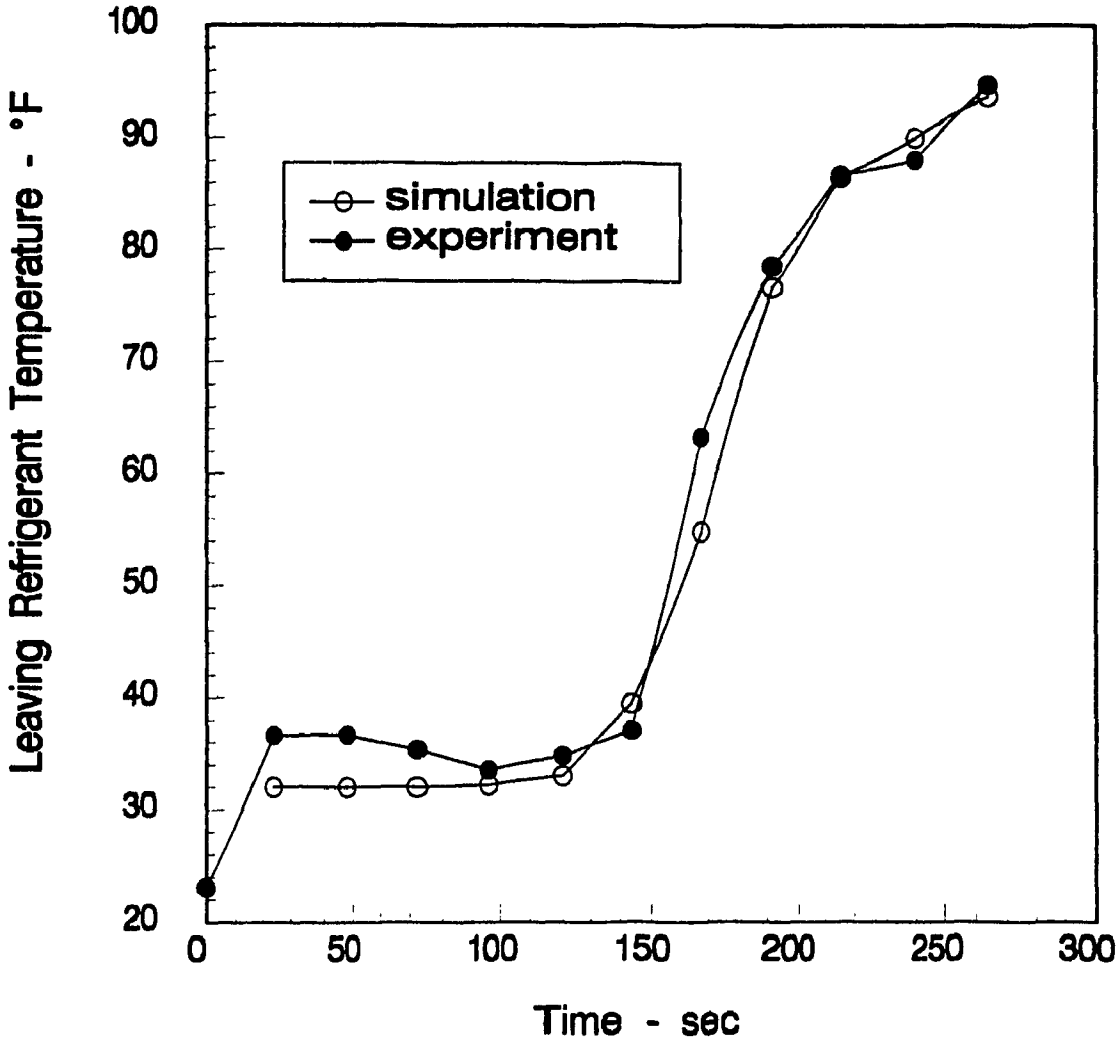

Figure 10.12 Temperature Comparison of Data Set 12

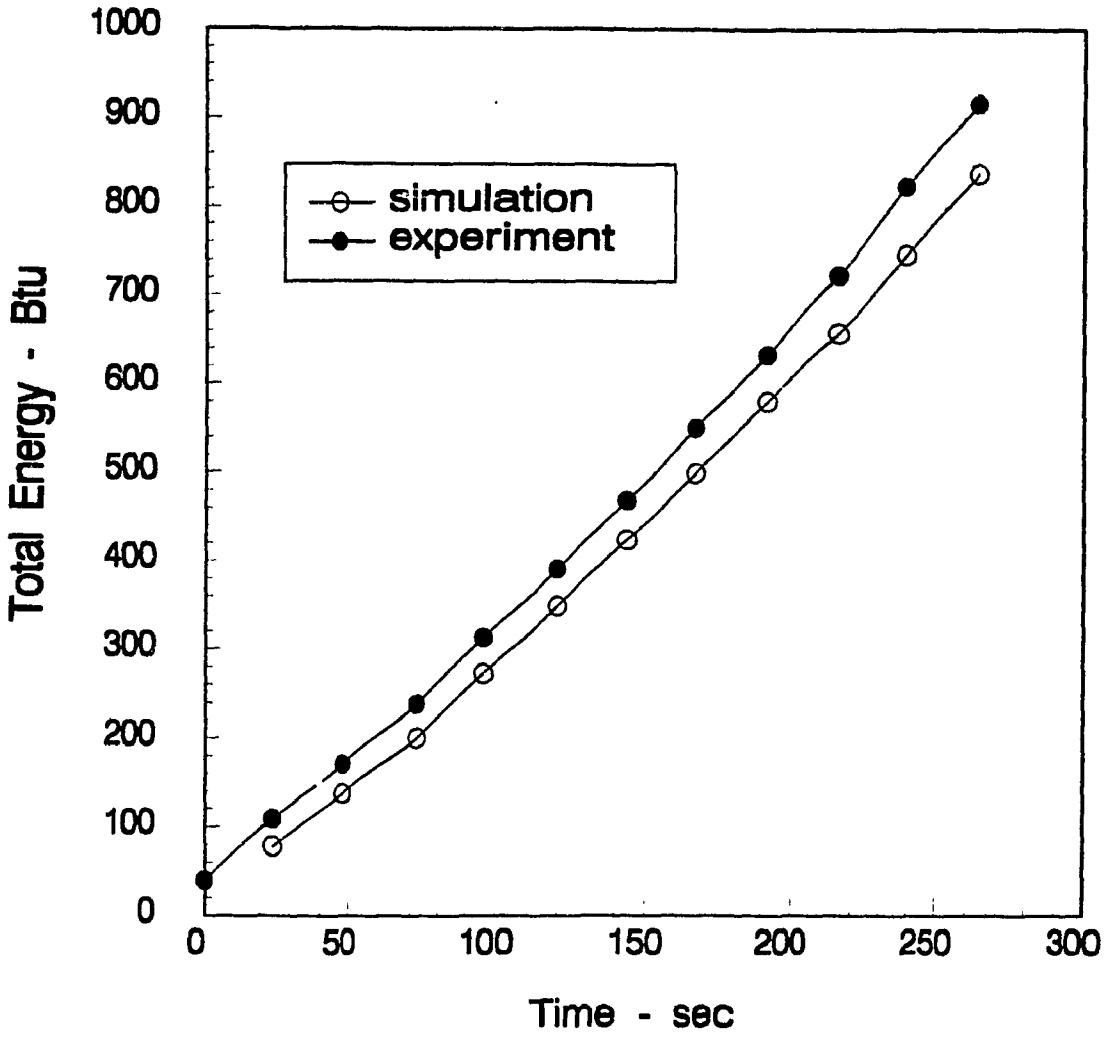

Figure 10.13 Energy Comparison of Data Set 1

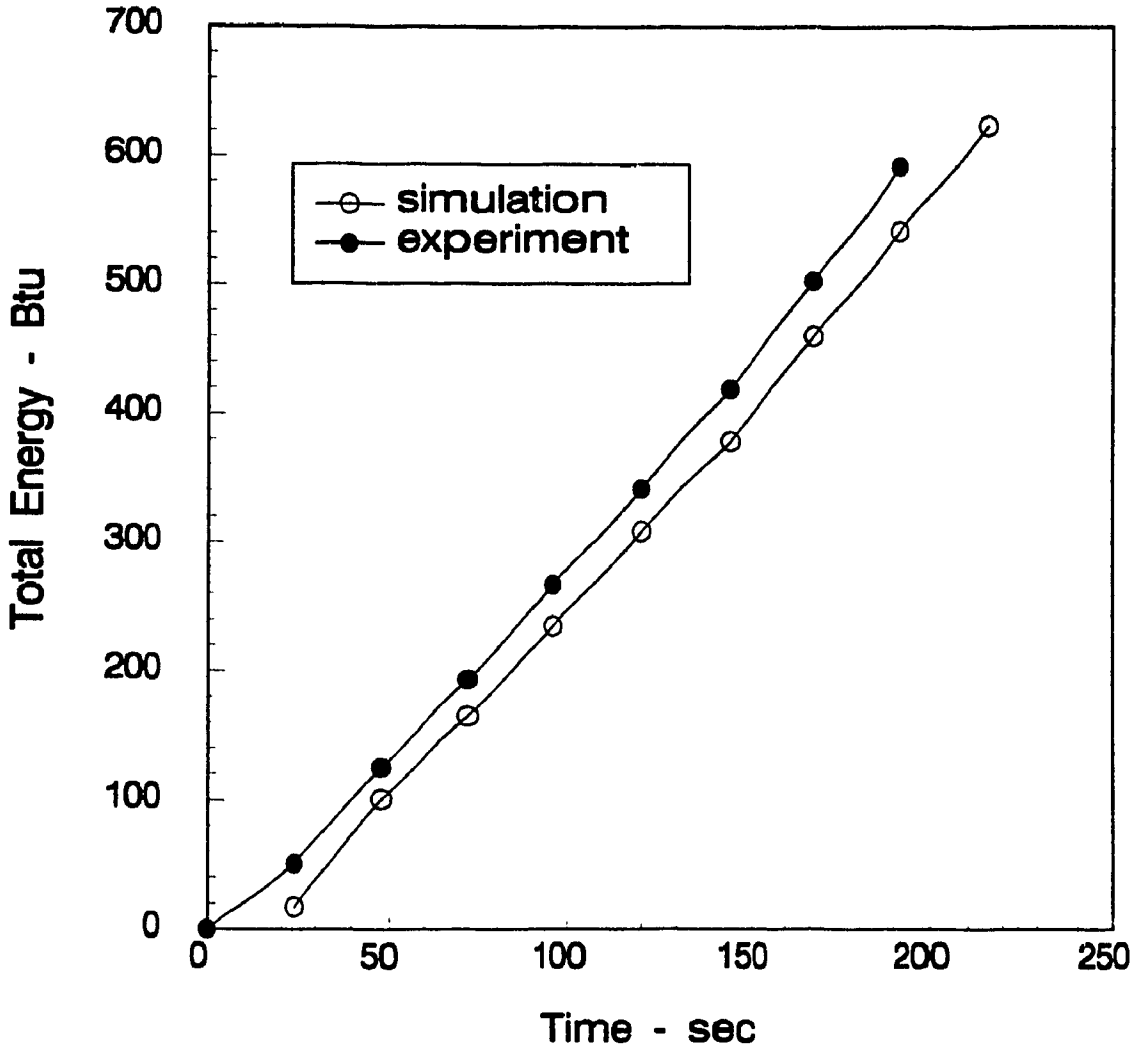

Figure 10.14 Energy Comparison of Data Set 2

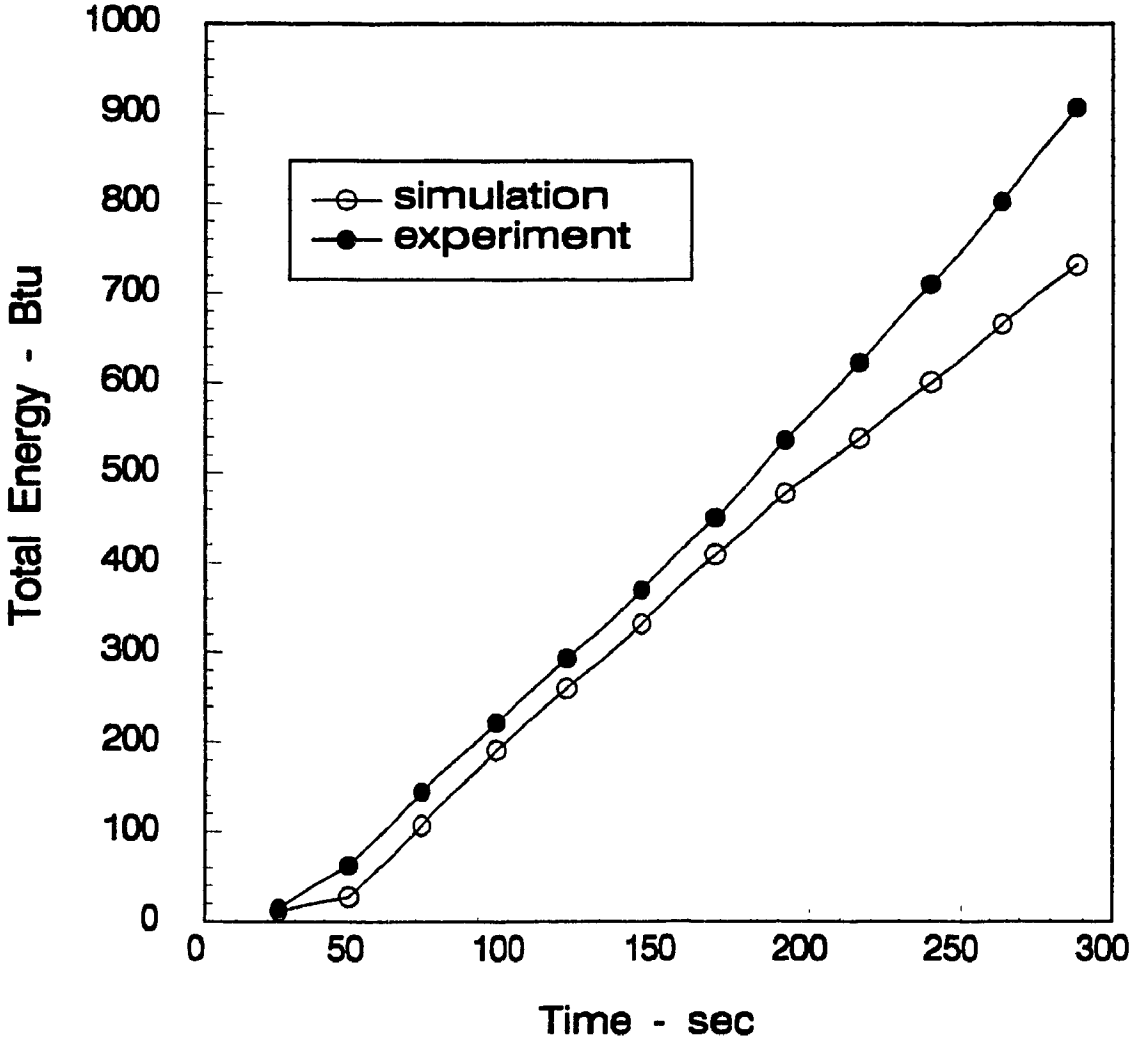

Figure 10.15 Energy Comparison of Data Set 3

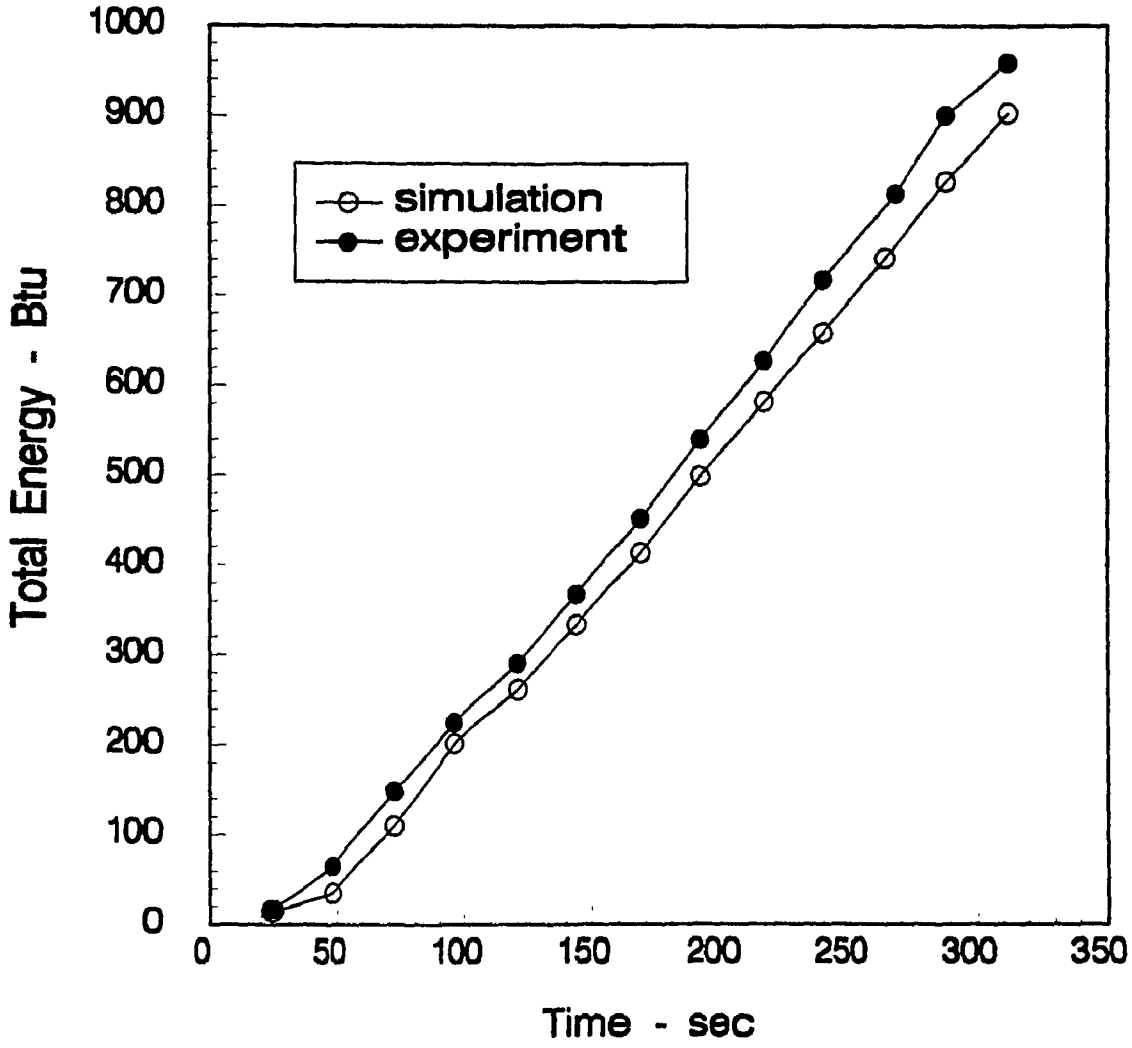

Figure 10.16 Energy Comparison of Data Set 4

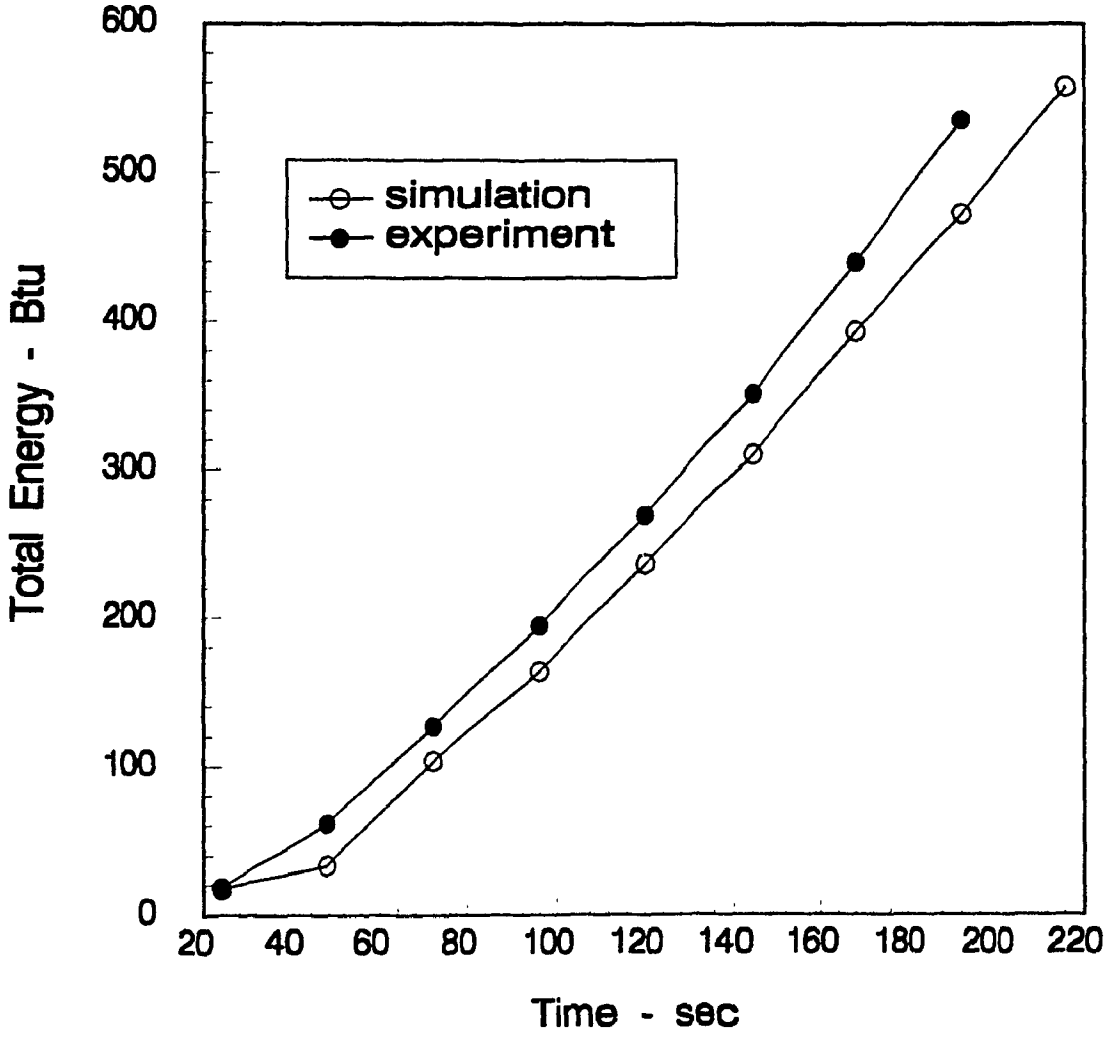

Figure 10.17 Energy Comparison of Data Set 5

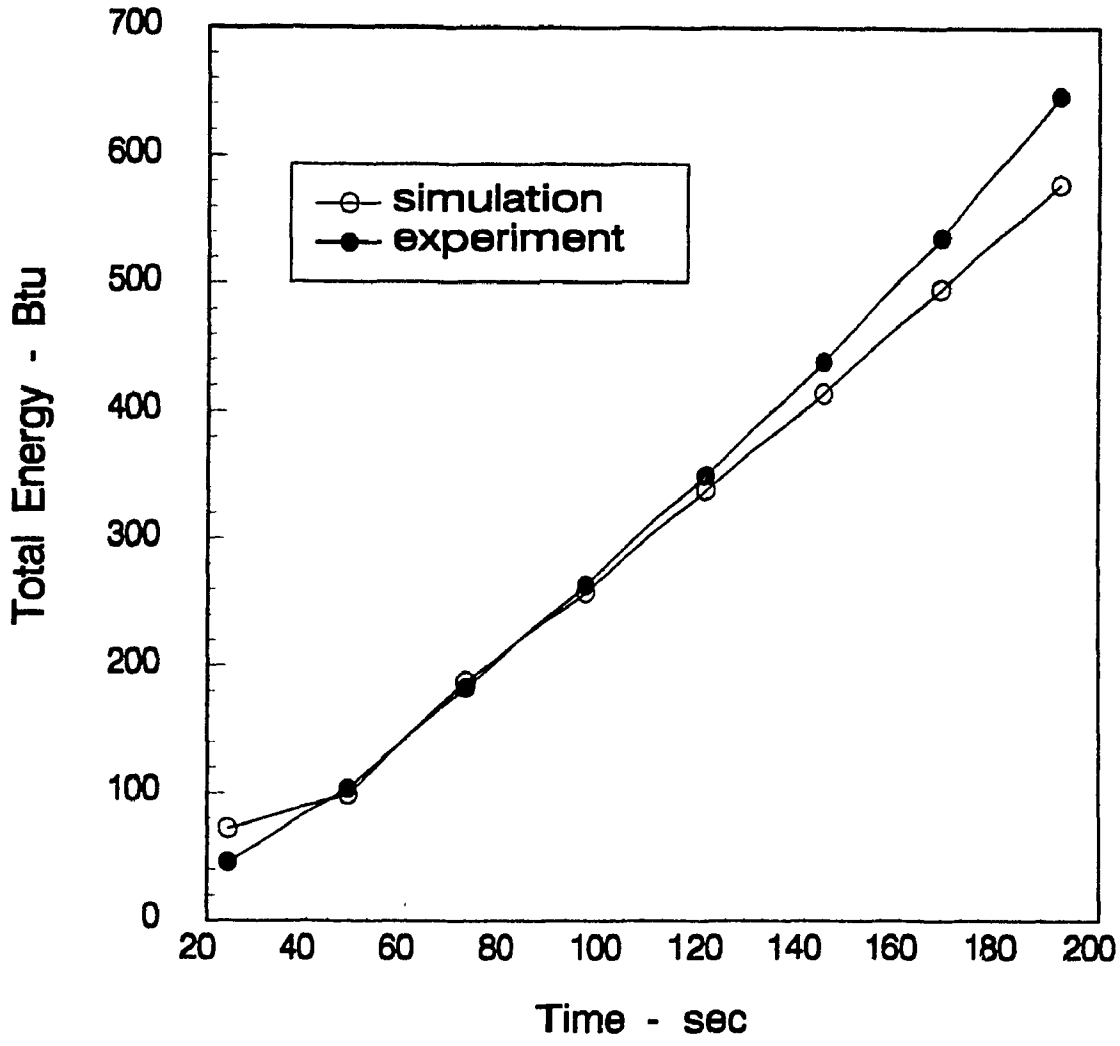

Figure 10.18 Energy Comparison of Data Set 6

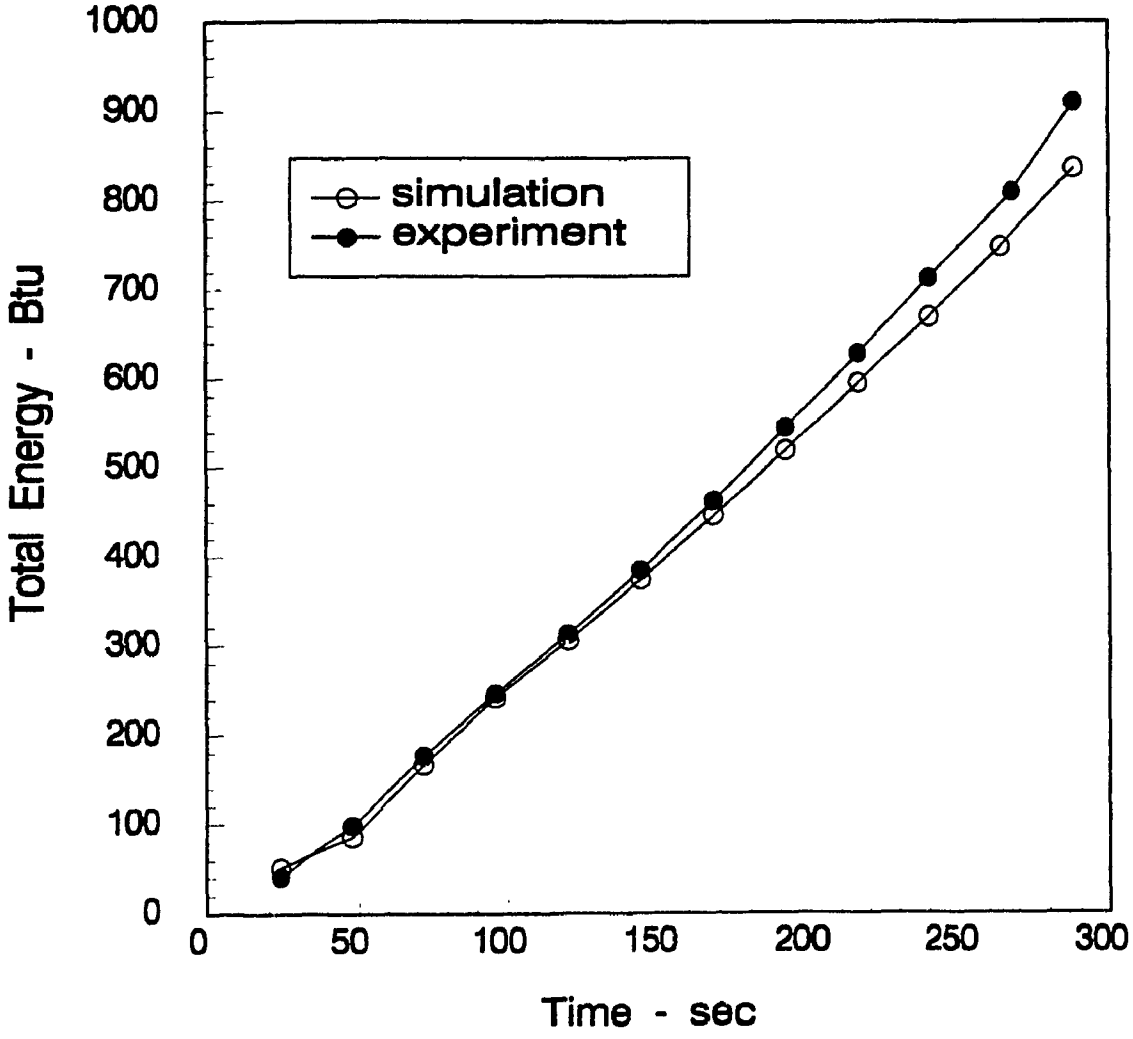

Figure 10.19 Energy Comparison of Data Set 7

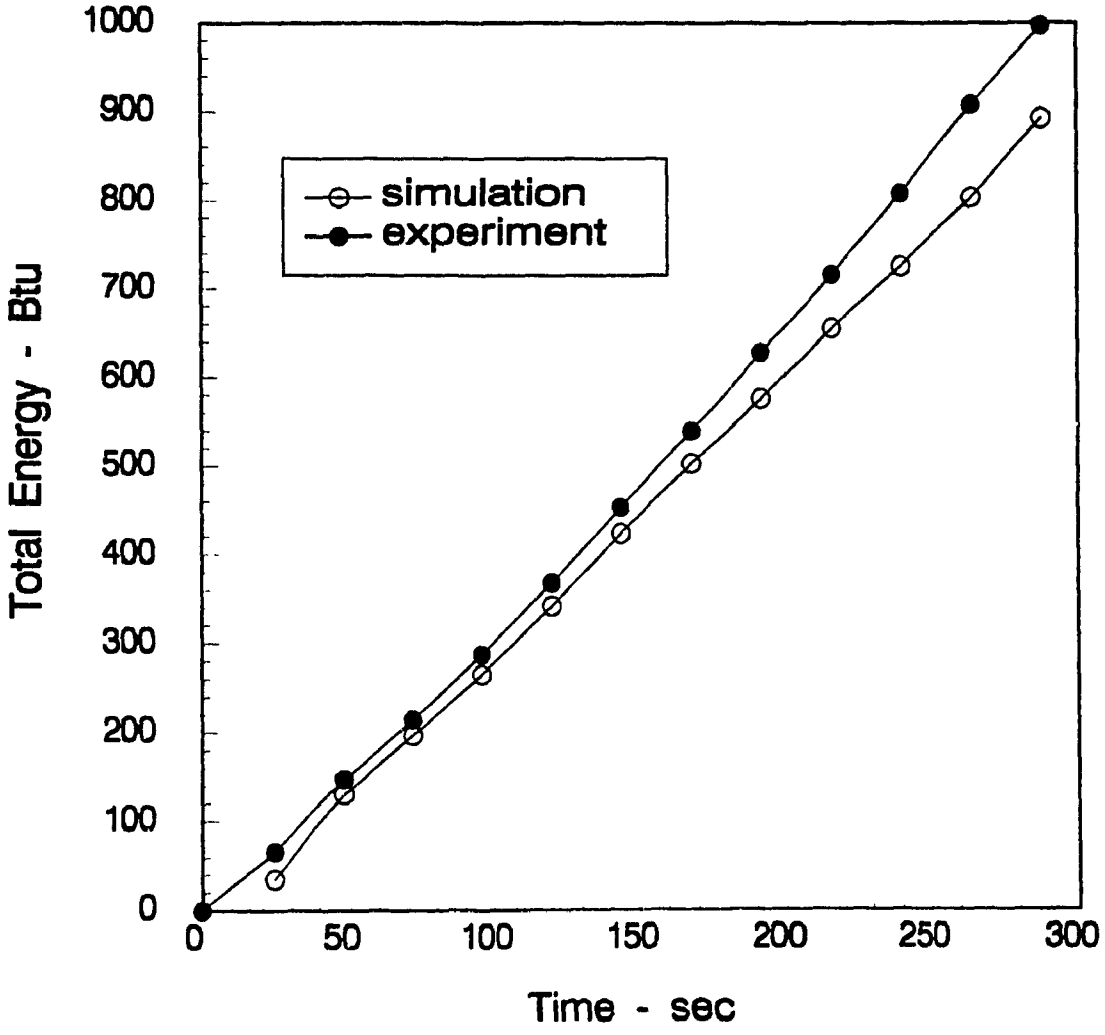

Figure 10.20 Energy Comparison of Data Set 8

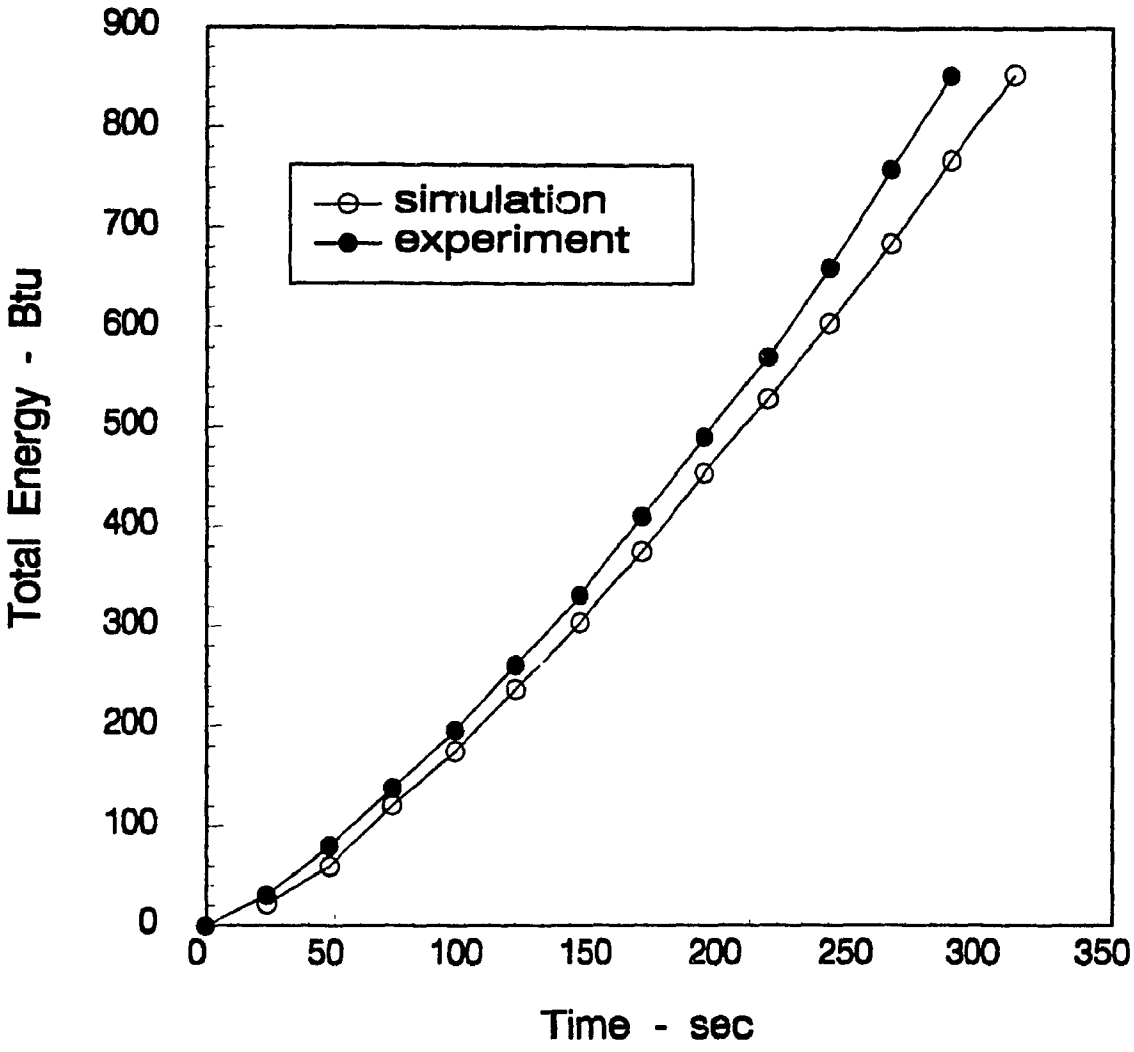

Figure 10.21 Energy Comparison of Data Set 9

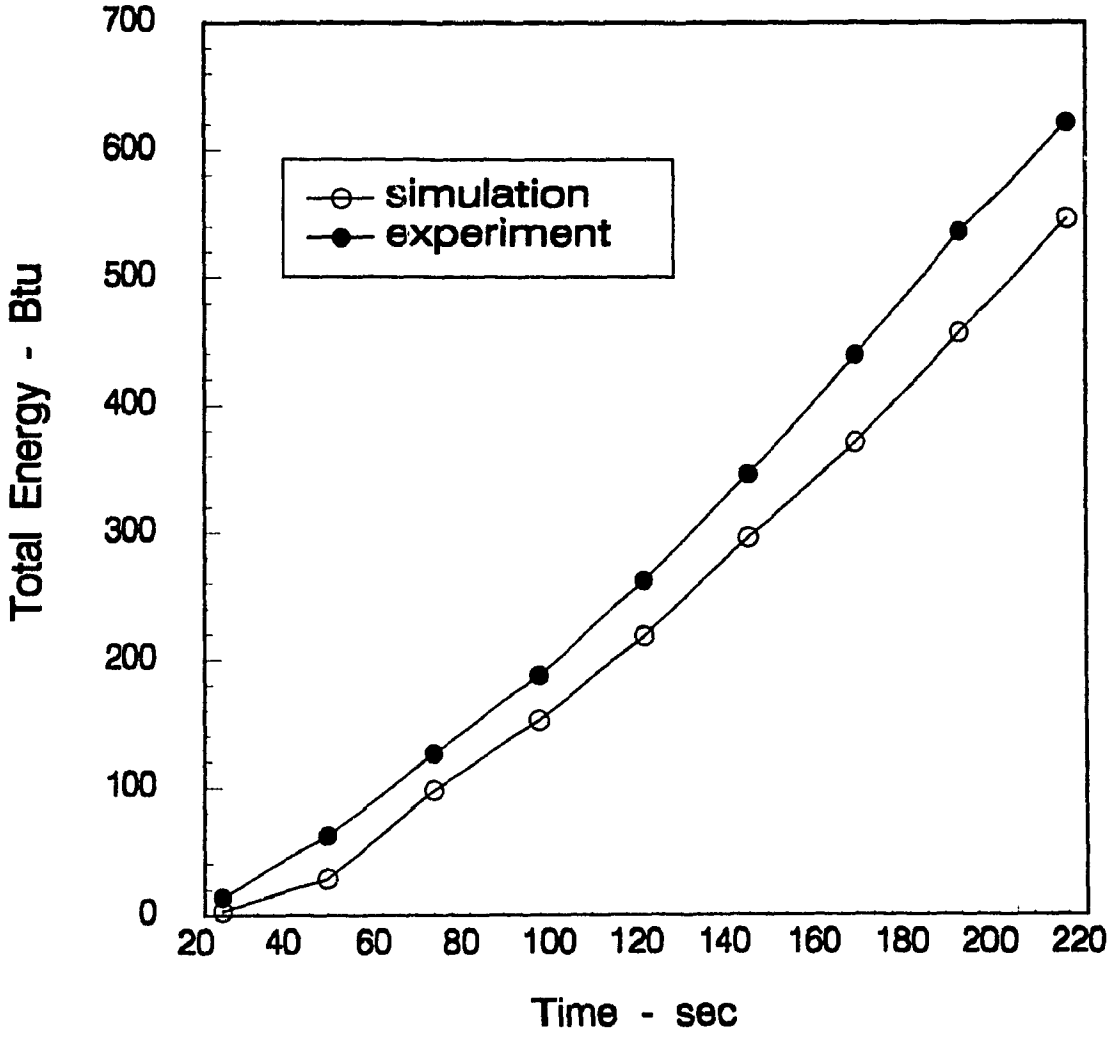

Figure 10.22 Energy Comparison of Data Set 10

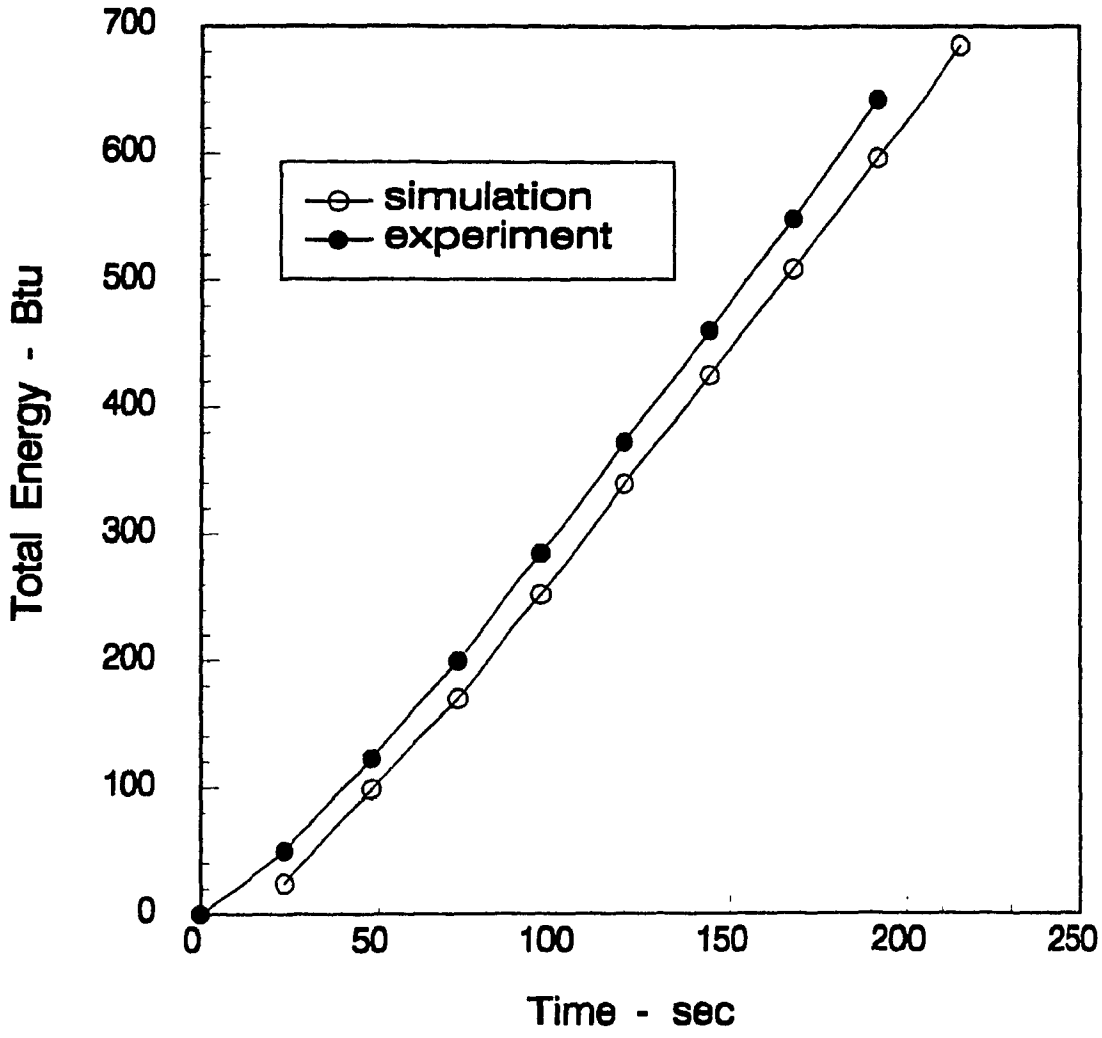

Figure 10.23 Energy Comparison of Data Set 11

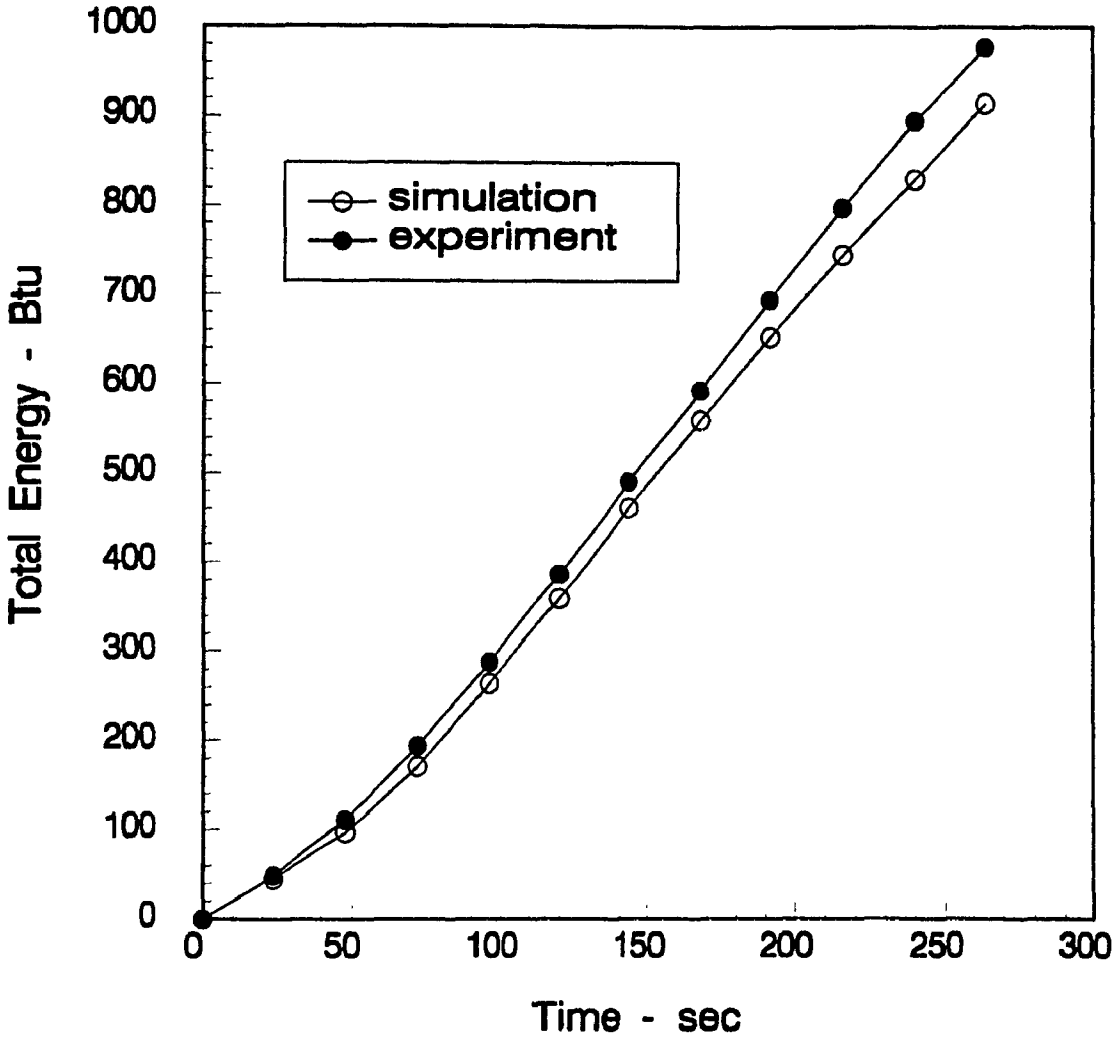

Figure 10.24 Energy Comparison of Data Set 12

Table 10.1

Comparison of Simulation Results with Experimental Data

Refrigerant Pressure Drop in the Evaporator, dP (psi)

Data Set	Simulation	Experiment	Deviation
1	1.1	2.5	-1.4
2	0.7	3.0	-2.3
3	0.7	3.6	-2.9
4	0.7	0.9	-0.2
5	0.7	2.6	-1.9
6	0.8	2.7	-1.9
7	1.2	2.8	-1.6
8	1.1	2.1	-1.0
9	1.0	2.3	-1.3
10	1.0	2.1	-1.1
11	0.6	3.3	-2.7
12	1.0	1.5	-0.5

Table 10.2

Comparison of Simulation Results with Experimental Data

Refrigerant Leaving State

Amount of Subcooling, $T_r - T_s$ (°F), and Quality, x

Data Set	Simulation		Experiment	
	$T_r - T_s$	x	$T_r - T_s$	x
1	0.0	0.08	-4.95	0.0
2	0.0	0.03	-7.60	0.0
3	0.0	0.10	-4.75	0.0
4	0.0	0.0	-0.26	0.0
5	0.0	0.10	-7.10	0.0
6	0.0	0.19	-6.45	0.0
7	0.0	0.14	-6.06	0.0
8	0.0	0.10	-5.43	0.0
9	0.0	0.16	-5.85	0.0
10	0.0	0.01	-6.21	0.0
11	-0.9	0.0	-4.81	0.0
12	0.0	0.04	-5.94	0.0

Table 10.3

Comparison of Simulation Results with Experimental Data

Total Mass of Vaporized Surface Water, m_v (lbm)

Data Set	Simulation	Experiment	Deviation
1	0.21	0.53	-0.32
2	0.09	0.22	-0.13
3	0.10	0.60	-0.50
4	0.14	0.40	-0.26
5	0.11	0.54	-0.44
6	0.11	0.33	-0.22
7	0.16	0.59	-0.43
8	0.19	0.09	0.10
9	0.16	0.22	-0.06
10	0.21	0.18	0.03
11	0.09	0.78	-0.69
12	0.26	0.92	-0.66

CHAPTER 11

CONCLUSIONS

A hot gas defrosting model of evaporators and a computer program for simulating defrosting processes of evaporators have been developed in this thesis. The defrosting process of evaporators has been idealized to undergo four stages: preheating, melting frost, wet surface and dry surface. From the theoretical analysis, computer simulation and experimental determination, the following conclusions have been reached.

This four surface stage defrosting model and computer simulation program have been validated and shown to yield satisfied results for modelling and simulating defrosting processes. The theoretical model well approaches the real defrosting process. The program well performs the two dimensional dynamic defrosting process simulation involving time and space. The predictions of defrosting process characteristics, energy, time, heat and mass transfer, etc., by using this computer program, are successful. The deviation of predicting total required energy for defrosting process is 5 % to 9 %. Deviations of predicting other characteristic parameters are satisfactory.

Two empirical correlations and six coefficients for the heat and mass transfer of evaporator outside surface during

the defrosting process are obtained. These correlations and coefficients are based on the combination of theoretical analysis and experimental determination. These correlations and coefficients make a complete and accurate simulation of defrosting processes possible.

This defrosting model and simulation program can be used to predict the required time and energy for the hot gas defrosting process of evaporators, and to study the behaviour of evaporators under the defrosting conditions.

The computer program can also be used as an aid to optimize the defrosting process, to increase the defrosting efficiency, and further to improve the system performance.

The coefficients for the heat and mass transfer of evaporator outside surface can be used for the defrosting process simulation of other evaporators with similar configurations.

The complete model and simulation program presented in this work provides useful fundamentals for the development of heat pumps and refrigeration systems.

REFERENCES

Anand, N.K., Tree, D.R., 1982, "Steady State Simulation of a Single Tube-Finned Condenser Heat Exchanger", ASHRAE Transactions, Vol.88, Part 2.

ASHRAE, 1981. ASHRAE Handbook 1981 Fundamentals, American Society of Heating, Refrigeration, and Air Conditioning Engineers, Inc.

Bouma, J.W.J., 1979, "Frosting and Defrosting Behaviour of Outdoor Coils of Air-Source Heat Pumps", New Ways to Save Energy, Commission of the European Communities, International Seminar, Brussels, 23-25 October, D.Reidel Publishing Company.

Domanski, P., 1982, Computer Modelling and Prediction of an Air Source Heat Pump with a Capillary Tube, Ph.D. dissertation, The Catholic University of America.

Ellison, R.D., Creswick, F.A., Fischer, S.K., Jackson, W.L., 1981, "A computer Model for Air-Cooled Refrigerant Condensers with Specified Refrigerant Circuiting", ASHRAE Transactions, Vol.87, Part 1.

Hiller, C.C., Glicksman, L.R., 1976, Improving Heat Pump Performance via Compressor Capacity Control --- Analysis and Test, Report 24525-96, Heat Transfer Laboratory, Massachusetts Institute of Technology, Cambridge, Massachusetts.

Kartsonnes, G.T., Earth, R.A., 1971, "Computer Calculation of the Thermodynamics Properties of Refrigerants 12, 22, and 502", ASHRAE Transactions, Vol.77, Part 2.

Lockhard, R.W., Martinelli, R.C., 1949, "Proposed Correlation of Data for Isothermal Two-Phase, Two-Component Flow in Pipes", Chemical Engineering Progress, Vol.45, No.1.

McAdams, W.H., 1954, Heat Transmission, McGraw - Hill Book Company.

McQuiston, F.C., 1975, "Fin Efficiency with Combined Heat and Mass Transfer", ASHRAE Transactions, Vol.81, Part 1.

Miller, W.A., 1987, "Laboratory Examination and Seasonal Analysis of Frosting and Defrosting for an Air-to-Air Heat Pump", ASHRAE Transactions, Vol.93, Part 1.

Miller, W.A., 1984, "Frosting Experiment for a Heat Pump Having a One-Row Spine-Fin Outdoor Coil", ASHRAE Transactions, Vol.90, Part 1B.

Miller, W.A., 1982, Laboratory Evaluation of the Heating Capacity and Efficiency of a High-Efficiency, Air-to-Air Heat Pump with Emphasis on Frosting / Defrosting Operation, ORNL / CON-69, Oak Ridge, TN: Oak Ridge National Laboratory, December.

Niederer, D.H., 1976, "Frosting and Defrosting Effects on Coil Heat Transfer", ASHRAE Transactions, Vol.82, Part 1.

Oskarsson, S.P., Krakow, K.I., Lin, S., 1990, "Evaporator Models for Operation with Dry, Wet, and Frosted Finned Surface --- Part I: Heat Transfer and Fluid Flow Theory, Part II: Evaporator Models and Verification", ASHRAE Transactions, Vol.96, Part 1.

Pierre, B., 1964, "Flow Resistance with Boiling Refrigerants", ASHRAE Journal, Part I: September, Part II: October.

Sanders, C.T., 1974, Frost Formation --- The Influence of Frost Formation and Defrosting on the Performance of Air Coolers, Ph.D. Thesis, Technische Hogeschool, Delft, Netherlands.

Stoecker, W.F., Lux, J.J.Jr, Kooy, R.J., 1983, "Energy Consideration in Hot-Gas Defrosting of Industrial Refrigeration Coil", ASHRAE Transactions, Vol.89, Part 2A.

Tantakitti, C., Howell, R.H., 1986, "Air-to-Air Heat Pumps Operating under frosting conditions on the Outdoor Coil", ASHRAE Transactions, Vol.92, Part 1B.

Traviss, D.P., Baron, A.B., Rohsenow, W.M., 1971, Forced-Convection Condensation Inside Tubes, Report DSR72591-94, Heat Transfer Laboratory, Massachusetts Institute of Technology, Cambridge, Massachusetts.

BIBLIOGRAPHY

Baxter, V.D., Moyers, J.C., 1985, "Field-Measured Cycling, Frosting, and Defrosting Losses for a High-Efficiency Air-Source Heat Pump" ASHRAE Transactions, Vol.91, Part 2B.

Eckert, E.R.G., Drake, R.M.Jr., 1972, Analysis of Heat and Mass Transfer, McGraw-Hill Book Company.

Incropera, F.P., DeWitt, D.P., 1981, Fundamentals of Heat Transfer, Jone Wiley & Sons, Inc.

Kays, W.M., London, A.L., 1964, Compact Heat Exchangers, McGraw - Hill Book Company.

Krakow, K.I., Lin, S., 1987, "A Numerical Model of Heat Pumps Having Various Means of Refrigerant Flow Control and Capacity Control", ASHRAE Transactions, Vol.93, Part 2.

Malhammar, A., 1986, Frostpaslag vid flansade ytor, Doktorsavhandling, Kungliga Teknisla Hogskolan, Stockholm, Sweden.

McQuiston, F.C., Parker, J.D., 1988, Heating, Ventilation, and

Air Conditioning Analysis and Design, John Wiley & Sons, Inc.

Merrill, P., 1981, "Heat Pumps 'on-off' Capacity Control and Defrost Performance Using Demand and Time-Temperature Defrost Controls", ASHRAE Transactions, Vol.87, Part 1.

Stamm, R.H., 1985, "Industrial Refrigeration: Frost Removal", Heating, Piping and Air Conditioning, Vol.57, April.

Strong, A.P., 1988, "Hot Gas Defrosting for Industrial Refrigeration", Heating, Piping and Air Conditioning, Vol.60, July.

Wallis, G.B., 1969, One-dimensional Two-phase Flow, McGraw - Hill Book Company.

APPENDIX I

COMPUTER PROGRAM LISTINGS

```
      PROGRAM DFRST


      DIMENSION T(101),TS(101),P(101),X(101),V(101),H(101),
     #HR(101),ESUM(101),TWO(101),TWI(101),TWF(101),IHTM(101),
     #MFRST(101),MLIQ(101),PATH(101),DTMX(101)
      COMMON/HT/IMAX
      REAL MFO,MFOE,MFR,MFRE,MFRST,MLIQ,MLIQO,MLIQE,MELT,MVAP,
     #MTUB,MFIN,Z
      CHARACTER*20 FNAME1,FNAME2,FNAME3
      DATAPI,DCU,DAL,CTUB,CFIN,CFO,CWAT,HIFW,HFGW/3.1415926,
     #556,171,0.092,0.214,0.4872,1.0,143.33,1069.48/
C
C     Q = HEAT TRANSFER RATE - BTU/HR
C     E = HEAT TRANSFERRED - BTU
C     IHTM(I) = HEAT TRANSFER MODE  1 = PREHEAT TO 32 F
C                                   2 = MELT FROSTED SURFACE
C                                   3 = WET SURFACE
C                                   4 = DRY SURFACE
C     E1 = HEAT TRANSFERRED DURING TIME INTERVAL - MODE 1
C     E2 = HEAT TRANSFERRED DURING TIME INTERVAL - MODE 2
C     E3 = HEAT TRANSFERRED DURING TIME INTERVAL - MODE 3
C     E4 = HEAT TRANSFERRED DURING TIME INTERVAL - MODE 4
C     ESUM = E1 + E2 + E3 + E4
C
C     EMX IS NOT USED FOR IHTM = 1
C     TWO IS NOT USED FOR CALCULATIONS BUT ONLY FOR REFERENCE
C     D3 IS NOT USED
C*****************************************************************
C     INPUT
C*****************************************************************
      OPEN(UNIT=5,FILE='CON')
      OPEN(UNIT=6,FILE='LPT1')
      WRITE(5,5)
    5 FORMAT(4X,'INPUT FILE NAME ?     '$)
      READ(5,10) FNAME1
   10 FORMAT(A10)
      OPEN(UNIT=1,FILE=FNAME1,STATUS='OLD')
      WRITE(5,15)
   15 FORMAT(4X,'OUTPUT FILE1 NAME ?   '$)
      READ(5,10) FNAME2
      OPEN(UNIT=2,FILE=FNAME2,STATUS='NEW')
      WRITE(5,20)
   20 FORMAT(4X,'OUTPUT FILE2 NAME ?   '$)
      READ(5,10) FNAME3
      OPEN(UNIT=3,FILE=FNAME3,STATUS='NEW')
      WRITE(2,25) FNAME1,FNAME2,FNAME3
```

```
   25 FORMAT(/,10X,3A20)
C       CALL IDATE(IMO,IDA,IYR)
C       CALL TIME(CTIME)
C       WRITE(2,30)
C    30 FORMAT(/,6X,'YR  MO  DA      TIME'
C      #10X,'PROGRAM: DFRST + DFSUBS - 1989 DEC
C      #11',/,4X,3I4,2X,A8)
        WRITE(2,30)
   30 FORMAT(/,10X,'PROGRAM: DFRST + DFSUBS - 1989 DEC 11')
        READ(1,*) DIN,DOUT,D1,D2,THK,FPI,ZMX
        WRITE(2,35) DIN,DOUT,D1,D2,THK,FPI,ZMX
   35 FORMAT(/,7X,'DIN     DOUT       D1       D2',
      #'      THK      FPI      ZMX',/,2X,7F8.3,/)
        READ(1,*) NTMX,NEL,NTUB,DTI,TCOIL,XMX,FBO,IMAX
        WRITE(2,40) NTMX,NEL,NTUB,DTI,TCOIL,XMX,FBO,IMAX
   40 FORMAT(/,6X,'NTMX      NEL     NTUB      DTI    TCOIL',
      #'      XMX      FBO     IMAX',/,2X,3I8,2F8.1,2F8.3,I8/)
        READ(1,*) MFO,MFR,MLIQO,HA,SECO,SEEX,CWR,CWMX
        WRITE(2,45) MFO,MFR,MLIQO,HA,SECO,SEEX,CWR,CWMX
   45 FORMAT(/,7X,'MFO      MFR    MLIQO       HA     SECO',
      #'     SEEX      CWR     CWMX',/,2X,8F8.2,/)
C*****************************************************************
C       DIVIDE ELEMENT
C*****************************************************************
        NCHK=(NEL/2)*2
        IF(NEL.NE.NCHK) STOP
        NPL=NEL+1
        NELT=NEL/NTUB
C
        CALL DATAR
        CALL DATAV
        CALL DATASH
        CALL DATAK
C
        DIN=DIN/12
        DOUT=DOUT/12
        D1=D1/12
        D2=D2/12
        THK=THK/12
        ZE=ZMX/NEL/12
        ZF=1/(FPI*12)-THK
        FPE=ZE*FPI*12
        ARSD=PI*DIN*ZE
        AX=PI*DIN**2/4
        VTUB=PI*(DOUT**2-DIN**2)/4*ZE
        VFINL=(D1*D2-PI*DOUT**2/4)*THK*FPE
        VFINR=PI*((DOUT+THK)**2-DOUT**2)/4*ZF*FPE
        VFIN=VFINL+VFINR
        MTUB=DCU*VTUB
        MFIN=DAL*VFIN
        MFOE=MFO/NEL
        MFRE=MFR/NEL
```

```
      MLIQE=MLIQO/NEL
      CCOI=MTUB*CTUB+MFIN*CFIN
      CTOT=CCOI+MFOE*CFO
C*****************************************************************
C     INITIALIZE
C*****************************************************************
      ICONT=1
C     ICONT=0 STOP
      NTDROP=0
      DPAC=0
      TEPF=0
      TEF=0
      ET=0
      TOTT=0
      TMELT=0
      TMVAP=0
      IHTM0=1
      IF(TCOIL.GT.31.999) IHTM0=2
      DO 50 I=1,NPL-1
      TW0(I)=TCOIL
      TWI(I)=TCOIL
      IHTM(I)=IHTM0
      PATH(I)=0
      MFRST(I)=MFOE
      MLIQ(I)=0
   50 CONTINUE
C*****************************************************************
C     TIME INTERVAL LOOP
C*****************************************************************
      DO 160 NT=1,NTMX
      READ(1,*) PPHR,PO,TO,XO,TAMB,RHA,PNXT
   55 FORMAT(1H1,/,6X,'PPHR      PO      TO      XO    TAMB',
     #'     RHA    PNXT',/,2X,7F8.2,/)
      IF(NT.EQ.1) THEN
          EPRE=CTOT*NEL*(32.0-TAMB)
          EDFR=MFO*HIFW
          TWMX=-999
          WRITE(2,60) CCOI,CTOT,EPRE,EDFR
   60     FORMAT(4(/),8X,'CCOI      CTOT      EPRE      EDFR'
     #    ,/,2X,2F10.4,2F10.1,/)
      END IF
      WRITE(2,55) PPHR,PO,TO,XO,TAMB,RHA,PNXT
C*****************************************************************
C     REFRIGERANT INITIAL CONDITION
C*****************************************************************
      G=PPHR/AX
      T(1)=TO
      P(1)=PO
      TS(1)=TSAT(1,P(1))
      TWMAX=TWMX
      TWMX=TSAT(1,PNXT)
      IF(TWMX.LT.TWMAX) TWMX=TWMAX
```

```
      IF(T(1).GT.TS(1)) THEN
          CALL VAPOR(1,T(1),P(1),V(1),H(1))
          X(1)=1
      ELSE
          CALL SATPRP(1,T(1),PSAT,VF,VG,HF,HFG,HG)
          X(1)=XO
          V(1)=VF+X(1)*(VG-VF)
          H(1)=HF+X(1)*HFG
      END IF
      QHP=0
      NB=1
C*************************************************************
C     SPACE ELEMENT LOOP
C*************************************************************
      DO 95 I=2,NPL
      K=I-1
      WRITE(5,*) '  NT I IHTM', NT,I,IHTM(K)
      E1=0
      E2=0
      E3=0
      E4=0
      ESUM(K)=0
      DT1=0
      DT2=0
      DT3=0
      DT4=0
      DTX=DTI
      GO TO (65,70,75,80), IHTM(K)
C*************************************************************
C     IHTM=1 PREHEAT FROSTED SURFACE TO 32 F
C*************************************************************
   65 IF(TS(K).LT.TWI(K)) THEN
          ICONT=0
C         NOGO CONDITION = TSAT < TWALL FOR IHTM=1
          WRITE(2,*) 'STOP AT NOGO CONDITION - TSAT<TWALL,
     #    IHTM=1'
          GOTO 100
      END IF
C
      CALL FINEF2(D1,D2,DOUT,THK,HA,FEF)
      AASD=(2*(D1*D2-PI*DOUT**2/4)*FEF+PI*DOUT*ZF)*FPE
      HAAS=HA*AASD
      CALL HTCRE(T(K),TS(K),TWI(K),X(K),XMX,G,DIN,
     #     HR(K),KHTM,IHTM(K))
      HARS=HR(K)*ARSD
CCC       EMX=CTOT*(32.0-TWI(K))
      CTOT=CCOI+MFRST(K)*CFO
      A=(HARS+HAAS)/CTOT
      TWB=(HARS*T(K)+HAAS*TAMB)/(HARS+HAAS)
      DT1=DTX
      TW1=TWI(K)
      POW=-A*DT1/3600
```

```
      EPOW=EXP(POW)
      D=1-EPOW
      F=(TWB-TW1)*D
      TW2=TWB*(1-EPOW)+TW1*EPOW
C
      IF(TW2.LT.32) THEN
           EC=HAAS*((TWB-TAMB)*DT1/3600-F/A)
           ES=CTOT*F
           EPF=MFRST(K)*CFO*F
           TEPF=TEPF+EPF
           ER1=ES+EC
CC           ER1=HARS*((T(K)-TWB)*DT1/3600+F/A)
CC           ECHK=ABS(ER1-ES-EC)/ER1
CC           IF(ECHK.GT.0.001) THEN
CC              WRITE(2,*) '  NT I ITRC=11',NT,I,' ECHK',ECHK
CC               WRITE(2,*) '  ER1, ES, EC ', ER1, ES, EC
CC           END IF
           E1=ER1
           TWF(K)=TW2
           PATH(K)=PATH(K)+1
           GOTO 85
      ELSE
           F1=(TWB-32)/(TWB-TW1)
           DT1=-3600*ALOG(F1)/A
           POW=-A*DT1/3600
           EPOW=EXP(POW)
C          TW2 = TWB*(1-EPOW)+TW1*EPOW = 32
           D=1-EPOW
           F=(TWB-TW1)*D
C
           EC=HAAS*((TWB-TAMB)*DT1/3600-F/A)
           ES=CTOT*F
           EPF=MFRST(K)*CFO*F
           TEPF=TEPF+EPF
           ER1=ES+EC
CC           ER1=HARS*((T(K)-TWB)*DT1/3600+F/A)
CC           ECHK=ABS(ER1-ES-EC)/ER1
CC           IF(ECHK.GT.0.001) THEN
CC              WRITE(2,*) '  NT I ITRC=12',NT,I,' ECHK',ECHK
CC               WRITE(2,*) '  ER1, ES, EC ', ER1, ES, EC
CC           END IF
           E1=ER1
           TWI(K)=32.0
           DTX=DTX-DT1
           PATH(K)=PATH(K)+10
           IHTM(K)=2
      END IF
      WRITE(5,*) '  NT I IHTM', NT,I,IHTM(K)
C*************************************************************
C     IHTM=2 MELT FROSTED SURFACE
C*************************************************************
   70 DENOM=1-MFRST(K)/MFRE
```

```
      IF(DENOM.LT.0.00001) DENOM=0.00001
      CW=CWR/DENOM
      IF(CW.GT.CWMX) CW=CWMX
C
      CALL FINEF2(D1,D2,DOUT,THK,CW,FEF)
      AASD=(2*(D1*D2-PI*DOUT**2/4)*FEF+PI*DOUT*ZF)*FPE
      HAWF=CW*AASD
      CALL HTCRE(T(K),TS(K),TWI(K),X(K),XMX,G,DIN,
     #     HR(K),KHTM,IHTM(K))
      HARS=HR(K)*ARSD
      EMX=MFRST(K)*HIFW
CCC      CTOT=CCOI+MFRST(K)*CFO
      A=(HARS+HAWF)/CCOI
      TWB=(HARS*T(K)+HAWF*32.0)/(HARS+HAWF)
      DT2=DTX
      TW1=TWI(K)
      POW=-A*DT2/3600
      EPOW=EXP(POW)
      D=1-EPOW
      F=(TWB-TW1)*D
      TW2=TWB*(1-EPOW)+TW1*EPOW
C
      DTCF=1
      DTCFC=0
      DTLM=999
      DTMX(K)=DTLM
      IF((KHTM.EQ.2).AND.(TW2.GT.TWMX)) THEN
          DTLM=3600*ALOG((TWB-TW1)/(TWB-TWMX))/A
          DTMX(K)=DTLM
          DTCF=DTLM/DT2
          DTCFC=1-DTCF
          IF(DTLM.LT.0) THEN
              DTLM=0
              WRITE(2,*) ' DTLM < 0   I, IHTM = ',I,IHTM(K)
          END IF
          POW=-A*DTLM/3600
          EPOW=EXP(POW)
          D=1-EPOW
          F=(TWB-TW1)*D
          TW2=TWB*(1-EPOW)+TW1*EPOW
C     TW2=TWMX
      END IF
C
      EF=HAWF*((TWB-32.0)*DT2*DTCF/3600-F/A)
     #  +HAWF*(TW2-32.0)*DT2*DTCFC/3600
      IF(EF.LT.EMX) THEN
          ES=CCOI*F
          ER2=EF+ES
CC          ER2=HARS*((T(K)-TWB)*DT2*DTCF/3600+F/A)
CC     #        +HARS*(T(K)-TW2)*DT2*DTCFC/3600
CC          ECHK=ABS(ER2-EF-ES)/ER2
CC          IF((ECHK.GT.0.005).AND.(ER2.GT.0.01)) THEN
```

```
CC              WRITE(2,*) '  NT I ITRC=21',NT,I,' ECHK',ECHK
CC               WRITE(2,*) '  ER2, ES, EF ', ER2, ES, EF
CC            END IF
              E2=ER2
              TWF(K)=TW2
              MELT=EF/HIFW
              MFRST(K)=MFRST(K)-MELT
              TMELT=TMELT+MELT
              TEF=TEF+EF
              PATH(K)=PATH(K)+100
              GOTO 85
           ELSE
              DT2=DT2*EMX/EF
              AA=TWB-32
              BB=(TWB-TW1)/A
              CC=A
              DD=EMX/HAWF+BB
              CALL DTQ(DT2,AA,BB,CC,DD)
              DTCF=1
              DTCFC=0
              IF(DT2.GT.DTLM) THEN
                 TW232=TW2-32
                 F1=EMX/HAWF/TW232
                 POW=-A*DTLM/3600
                 EPOW=EXP(POW)
                 F2=(TWB-TW1)*(1-EPOW)/TW232/A
                 F3=(TWB-TW2)*DTLM/TW232
                 DT2=3600*(F1+F2)-F3
                 DTCF=DTLM/DT2
                 DTCFC=1-DTCF
              END IF
              POW=-A*DT2*DTCF/3600
              EPOW=EXP(POW)
              D=1-EPOW
              F=(TWB-TW1)*D
              TW2=TWB*(1-EPOW)+TW1*EPOW
C
              EF=HAWF*((TWB-32.0)*DT2*DTCF/3600-F/A)
     #          +HAWF*(TW2-32.0)*DT2*DTCFC/3600
              ES=CCOI*F
              ER2=EF+ES
CC            ER2=HARS*((T(K)-TWB)*DT2*DTCF/3600+F/A)
CC            ECHK=ABS(ER2-EF-ES)/ER2
CC            IF((ECHK.GT.0.005).AND.(ER2.GT.0.01)) THEN
CC               WRITE(2,*) '  NT I ITRC=22',NT,I,' ECHK',ECHK
CC               WRITE(2,*) '  ER2, ES, EF ', ER2, ES, EF
CC            END IF
              E2=ER2
              TWI(K)=TW2
              MELT=EF/HIFW
              MFRST(K)=MFRST(K)-MELT
              TMELT=TMELT+MELT
```

```
            TEF=TEF+EF
            MLIQ(K)=MLIQE
            DTX=DTX-DT2
            PATH(K)=PATH(K)+1000
            IHTM(K)=3
            WRITE(5,*) '  NT I IHTM', NT,I,IHTM(K)
        END IF
C*****************************************************************
C       IHTM=3 WET SURFACE
C*****************************************************************
   75   CALL FINEF2(D1,D2,DOUT,THK,HA,FEF)
        AASD=(2*(D1*D2-PI*DOUT**2/4)*FEF+PI*DOUT*ZF)*FPE
        HAAS=HA*AASD
        CALL HTCRE(T(K),TS(K),TWI(K),X(K),XMX,G,DIN,
       #     HR(K),KHTM,IHTM(K))
        HARS=HR(K)*ARSD
        AWET=AASD*(MLIQ(K)/MLIQE)**SEEX
        FLO=EVPPH(TWI(K),TAMB,RHA,SECO,AWET)
        QV=FLO*HFGW
        CTOT=CCOI+MLIQ(K)*CWAT
        A=(HARS+HAAS)/CTOT
        TWB=(HARS*T(K)+HAAS*TAMB-QV)/(HARS+HAAS)
C
C       AS SECO -> UP, QV -> UP, TWB -> DOWN, TW2 -> DOWN
C
        DT3=DTX
        TW1=TWI(K)
        POW=-A*DT3/3600
        EPOW=EXP(POW)
        D=1-EPOW
        F=(TWB-TW1)*D
        TW2=TWB*(1-EPOW)+TW1*EPOW
C
        DTCF=1
        DTCFC=0
        DTLM=999
        DTMX(K)=DTLM
        IF((KHTM.EQ.2).AND.(TW2.GT.TWMX)) THEN
            DTLM=3600*ALOG((TWB-TW1)/(TWB-TWMX))/A
            DTMX(K)=DTLM
            DTCF=DTLM/DT3
            DTCFC=1-DTCF
            IF(DTLM.LT.0) THEN
                DTLM=0
                WRITE(2,*) ' DTLM < 0  I, IHTM = ',I,IHTM(K)
            END IF
            POW=-A*DTLM/3600
            EPOW=EXP(POW)
            D=1-EPOW
            F=(TWB-TW1)*D
            TW2=TWB*(1-EPOW)+TW1*EPOW
C       TW2=TWMX
```

```
      END IF
C
      EMX=MLIQ(K)*HFGW
      EV=QV*DT3/3600
      IF(EV.LT.EMX) THEN
          MVAP=EV/HFGW
          MLIQ(K)=MLIQ(K)-MVAP
          EC=HAAS*((TWB-TAMB)*DT3*DTCF/3600-F/A)
     #      +HAAS*(TW2-TAMB)*DT3*DTCFC/3600
          ES=CTOT*F
          ER3=ES+EC+EV
CC          ER3=HARS*((T(K)-TWB)*DT3*DTCF/3600+F/A)
CC     #        +HARS*(T(K)-TW2)*DT3*DTCFC/3600
CC          ECHK=ABS(ER3-ES-EC-EV)/ER3
CC          IF(ECHK.GT.0.001) THEN
CC              WRITE(2,*) '  NT I ITRC=31',NT,I,' ECHK',ECHK
CC               WRITE(2,*) '  ER3, ES, EC, EV', ER3, ES, EC,
EV
CC          END IF
          E3=ER3
          TWF(K)=TW2
          IF(TW2.LT.TW1) NTDROP=NTDROP+1
          TMVAP=TMVAP+MVAP
          PATH(K)=PATH(K)+10000
          GOTO 85
      ELSE
          DT3=DT3*EMX/EV
          POW=-A*DT3/3600
          EPOW=EXP(POW)
          D=1-EPOW
          F=(TWB-TW1)*D
          TW2=TWB*(1-EPOW)+TW1*EPOW
C
          EC=HAAS*((TWB-TAMB)*DT3*DTCF/3600-F/A)
     #      +HAAS*(TW2-TAMB)*DT3*DTCFC/3600
          ES=CTOT*F
          EV=QV*DT3/3600
          MVAP=EV/HFGW
          MLIQ(K)=MLIQ(K)-MVAP
          ER3=ES+EC+EV
CC          ER3=HARS*((T(K)-TWB)*DT3/3600+F/A)
CC          ECHK=ABS(ER3-ES-EC-EV)/ER3
CC          IF(ECHK.GT.0.001) THEN
CC              WRITE(2,*) '  NT I ITRC=32',NT,I,' ECHK',ECHK
CC               WRITE(2,*) '  ER3, ES, EC, EV', ER3, ES, EC,
EV
CC          END IF
          E3=ER3
          TWI(K)=TW2
          TMVAP=TMVAP+MVAP
          DTX=DTX-DT3
          IF(TW2.LT.TW1) NTDROP=NTDROP+1
```

```
            PATH(K)=PATH(K)+100000
            IHTM(K)=4
            WRITE(5,*) '  NT I IHTM', NT,I,IHTM(K)
         END IF
C*************************************************************
C      IHTM=4 DRY SURFACE
C*************************************************************
   80 CALL FINEF2(D1,D2,DOUT,THK,HA,FEF)
      AASD=(2*(D1*D2-PI*DOUT**2/4)*FEF+PI*DOUT*ZF)*FPE
      HAAS=HA*AASD
      CALL HTCRE(T(K),TS(K),TWI(K),X(K),XMX,G,DIN,
     #     HR(K),KHTM,IHTM(K))
      HARS=HR(K)*ARSD
      A=(HARS+HAAS)/CCOI
      TWB=(HARS*T(K)+HAAS*TAMB)/(HARS+HAAS)
      TW1=TWI(K)
      DT4=DTX
      POW=-A*DT4/3600
      EPOW=EXP(POW)
      D=1-EPOW
      F=(TWB-TW1)*D
      TW2=TWB*(1-EPOW)+TW1*EPOW
C
      DTCF=1
      DTCFC=0
      DTLM=999
      DTMX(K)=DTLM
      IF((KHTM.EQ.2).AND.(TW2.GT.TWMX)) THEN
          DTLM=3600*ALOG((TWB-TW1)/(TWB-TWMX))/A
          DTMX(K)=DTLM
          DTCF=DTLM/DT4
          DTCFC=1-DTCF
          IF(DTLM.LT.0) THEN
              DTLM=0
              WRITE(2,*) ' DTLM < 0  I, IHTM = ',I,IHTM(K)
          END IF
          POW=-A*DTLM/3600
          EPOW=EXP(POW)
          D=1-EPOW
          F=(TWB-TW1)*D
          TW2=TWB*(1-EPOW)+TW1*EPOW
C     TW2=TWMX
      END IF
C
      EC=HAAS*((TWB-TAMB)*DT4*DTCF/3600-F/A)
     #  +HAAS*(TW2-TAMB)*DT4*DTCFC/3600
      ES=CCOI*F
      ER4=ES+EC
CC      ER4=HARS*((T(K)-TWB)*DT4*DTCF/3600+F/A)
CC     #    +HARS*(T(K)-TW2)*DT4*DTCFC/3600
CC      ECHK=ABS(ER4-ES-EC)/ER4
CC      IF(ECHK.GT.0.001) THEN
```

```
CC          WRITE(2,*) '  NT I ITRC=41',NT,I,' ECHK',ECHK
CC          WRITE(2,*) '  ER4, ES, EC ', ER4, ES, EC
CC        END IF
          E4=ER4
          TWF(K)=TW2
          PATH(K)=PATH(K)+1000000
C*****************************************************************
C     CHARACTERISTIC PARAMETER CALCULATION
C*****************************************************************
   85 CONTINUE
          TSUM=DT1+DT2+DT3+DT4
          DTCK=ABS(DTI-TSUM)/DTI
          IF(DTCK.GT.0.001) THEN
              WRITE(2,*) '  DTI TSUM',DTI,TSUM
              ICONT=0
              GOTO 100
          END IF
C
          ESUM(K)=E1+E2+E3+E4
C
          H(I)=H(I-1)-3600*ESUM(K)/(PPHR*DTI)
C
          Z=K/NELT
          DZ=NB-Z
          IF(DZ.LT.0.1.AND.DZ.GT.-0.1) THEN
              CALL DPLRB(T(I-1),X(I-1),G,FBO,DPLB)
              NB=NB+1
          ELSE
              DPLB=0
          END IF
CC        WRITE(5,*) 'Z DZ NB DPLB',Z,DZ,NB,DPLB
          CALL DPFRR(T(I-1),X(I-1),XMX,G,DIN,ZE,DPFR)
          P(I)=P(I-1)-DPFR+DPLB-DPAC
          DP=P(1)-P(I)
C
          TS(I)=TSAT(I,P(I))
          CALL SATPRP(I,TS(I),PSAT,VF,VG,HF,HFG,HG)
          IF(H(I).GT.HG) THEN
              X(I)=1.0
              CALL TVAP(I,P(I),H(I),TS(I),T(I),V(I))
              GOTO 90
          END IF
          IF(H(I).LE.HG.AND.H(I).GE.HF) THEN
              X(I)=(H(I)-HF)/HFG
              T(I)=TS(I)
              V(I)=VF+X(I)*(VG-VF)
              GOTO 90
          END IF
          IF(H(I).LT.HF) THEN
              X(I)=0.0
              CALL TLIQ(I,H(I),TS(I),T(I),V(I))
              GOTO 90
```

```
      END IF
C
   90 DPAC=(G/3600)**2*(V(I-1)-V(I))/32.174/144
C
   95 CONTINUE
C*****************************************************************
C     SUMMATION AND OUTPUT
C*****************************************************************
  100 CONTINUE
      EZ=0
      DO 105 K=1,NEL
      EZ=EZ+ESUM(K)
  105 CONTINUE
      QHP=EZ*3600/DTI
      ET=ET+EZ
      TOTT=TOTT+DTI
      EFFC=TEF/ET
      DFEF=(TEPF+TEF)/ET
      DHTF=QHP/(TS(1)-32.0)
      SCLVG=T(NPL)-TS(NPL)
C
      WRITE(2,110) TOTT,QHP,TEPF,TEF,EZ,ET,TMELT,TMVAP
  110 FORMAT(/,6X,'TOTT      QHP     TEPF      TEF       EZ',
     #'       ET    TMELT    TMVAP',/,2X,2F8.0,6F8.2,/)
      WRITE(2,115) DFEF,EFFC,P(NPL),DP,DHTF,SCLVG,X(NPL),
     #NTDROP
  115 FORMAT(/,6X,'DFEF     EFFC  P(NPL)       DP     DHTF',
     #SCLVG'     XLVG  NTDROP',/,
     #2X,2F8.4,2F8.3,F8.2,F8.1,F8.3,I8/)
      WRITE(2,120)
  120 FORMAT(/,5X,'I      T     TS    TWO    TWI    TWF      X',
     #'  ESUM IHTM       PATH',/,50X,'     4332211')
      DO 125 I=1,NPL
  125 WRITE(2,130) I,T(I),TS(I),TWO(I),TWI(I),TWF(I),X(I),
     #ESUM(I),IHTM(I),PATH(I)
  130 FORMAT(2X,I4,2F6.1,3F6.1,F6.3,F6.2,I5,F11.1)
      WRITE(2,135)
  135 FORMAT(/,5X,'I   MFRST     MLIQ      DTLM         P',
     #'        V       H      HR')
      DO 140 I=1,NEL
  140 WRITE(2,145) I,MFRST(I),MLIQ(I),DTMX(I),P(I),V(I),H(I),
     #HR(I)
  145 FORMAT(2X,I4,2F8.4,2F9.3,F8.4,2F7.2)
      WRITE(3,150)T(NPL),TOTT,X(NPL),H(NPL),P(NPL),DP,SCLVG,
     #QHP,ET,TMVAP
  150FORMAT(2X,F6.1,',',F6.1,',',F5.3,',',F6.2,',',F8.3,',',
     #F5.3,',',F6.1,',',F7.0,',',F7.2,',',F5.3)
C
      IF(ICONT.EQ.0) STOP
      DO 155 I=1,NPL
      TWO(I)=TWF(I)
  155 TWI(I)=TWF(I)
```

```
      NTDROP=0
  160 CONTINUE
      WRITE(2,165)
  165 FORMAT(1H1)
      END


      SUBROUTINE HTCRE(T,TS,TW,X,XMX,G,DIN,HR,KHTM,IHTM)
C     FORCED CONVECTION HEAT TRANSFER COEFFICIENT OF
C     REFRIGERANT
C     FOR ALL REGIONS INSIDE A TUBE
C     HR UNITS = BTU/(H.FT**2.F)
C
C     REVISED 30 SEPT 1989 - KTHM ADDED
C             1 OCT 1989   - TW.GT.(TS-0.2)
C             8 OCT 1989   - IHTM ADDED
C             21 OCT 1989  - NOGO STOP ADDED
C
      COMMON/HT/IMAX
C
C     NOGO CONDITION = EVAPORATION OF REFRIGERANT REQUIRED
      IF((TW.GT.T).AND.((X.GT.0.001).AND.(X.LT.0.999))) THEN
          WRITE(2,*) 'STOP AT NOGO - TWO>T - REFRIG EVAP
     #REQUIRED'
          WRITE(5,*) 'STOP AT NOGO - TWO>T - REFRIG EVAP
     #REQUIRED'
          STOP
      END IF
C
      IF(IHTM.LE.IMAX) THEN
          IF(TW.GT.(TS+0.2)) THEN
              CALL HTCV(T,G,DIN,HR)
              KHTM=1
              RETURN
          END IF
      ELSE
          IF(X.GT.0.999) THEN
              CALL HTCV(T,G,DIN,HR)
              KHTM=1
              RETURN
          END IF
      END IF
C
      IF(X.GT.XMX) THEN
          CALL HTC2P(T,XMX,G,DIN,HR)
          KHTM=2
          RETURN
      END IF
C
      IF((X.LE.XMX).AND.(X.GE.0.01)) THEN
          CALL HTC2P(T,X,G,DIN,HR)
          KHTM=2
```

```
          RETURN
        END IF
C
        IF(X.LT.0.01) THEN
          CALL HTCL(T,G,DIN,HR)
          KHTM=3
          RETURN
        END IF
C
        WRITE(2,*) ' STOP - ERROR IN HTCRE. TW TS X',TW,TS,X
        WRITE(5,*) ' STOP - ERROR IN HTCRE. TW TS X',TW,TS,X
        STOP
        END


        SUBROUTINE HTCV(T,G,DIN,HV)
C       FORCED CONVECTION HEAT TRANSFER COEFFICIENT
C       SINGLE PHASE REFRIGERANT INSIDE A TUBE (VAPOUR)
C       REFERENCE 1 "FUNDAMENTALS OF HEAT TRANSFER"
C       FRANK P. INCROPERA PAGE 406
C       REFERENCE 2 "HEAT TRANSFER" W. H. McADAMS PAGE 219
C       HV UNITS = BTU/(H.FT**2.F)
        REAL NU
        DATA A,B,C/.023,0.8,0.333/
        X1=1
        VISC=VSC(T,X1)
        CON =COND(T,X1)
        CP  =SH(T,X1)
        RE  =G*DIN/VISC
        PR  =VISC*CP/CON
        NU  =A*RE**B*PR**C
        HV  =NU*CON/DIN
        RETURN
        END


        SUBROUTINE HTC2P(T,X,G,DIN,H2P)
C       FORCED CONVECTION HEAT TRANSFER COEFFICIENT
C       TWO PHASE REFRIGERANT INSIDE A TUBE
C       REFERENCE 1 "A COMPUTER MODEL FOR AIR-COOLED
C       REFRIGERANT CONDENSERS WITH SPECIFIED REFRIGERANT
C       CIRCUITING"
C       RAYMOND D. ELLISON, FREDERICK A. CRESWICK,
C       STEVEN K. FISCHER, WILLIAM L. JACKSON
C       ASHRAE TRANSACTIONS 1981 V.87 PT.1
C       REFERENCE 2 "STEADY STATE SIMULATION OF A SINGLE TUBE-
C       FINNED CONDENSER HEAT EXCHANGER" N.K.ANAND, D.R.TREE
C       ASHRAE TRANSACTIONS 1982 V.88 PT.2
C       H2P UNITS = BTU/(H.FT**2.F)
        REAL NU
        X1=1
        X0=0
```

```
      VISCV=VSC(T,X1)
      VISCL=VSC(T,X0)
      CONV =COND(T,X1)
      CONL =COND(T,X0)
      CPV  =SH(T,X1)
      CPL  =SH(T,X0)
      REL  =G*DIN*(1-X)/VISCL
      PRL  =VISCL*CPL/CONL
      IF(REL.LT.50)
     #F2 =0.707*PRL*REL**0.5
      IF(REL.GE.50.AND.REL.LE.1125)
     #F2 =5*PRL+5*ALOG(1+PRL*(0.0963*REL**0.585-1))
      IF(REL.GT.1125)
     #F2 =5*PRL+5*ALOG(1+5*PRL)+2.5*ALOG(0.00313*REL**0.812)
      CALL SATPRP(1,T,PSAT,VF,VG,HF,HFG,HG)
      XTT=((1-X)/X)**0.9*(VF/VG)**0.5*(VISCL/VISCV)**0.1
      FXT=0.15*(1/XTT+2.85/XTT**0.476)
      IF(FXT.GT.0.1.AND.FXT.LT.1)
     #NU =FXT*PRL*REL**0.9/F2
      IF(FXT.GE.1.AND.FXT.LT.50)
     #NU =FXT**1.15*PRL*REL**0.9/F2
      IF(FXT.LE.0.1.OR.FXT.GE.50) STOP
      H2P=NU*CONL/DIN
      RETURN
      END


      SUBROUTINE HTCL(T,G,DIN,HL)
C     FORCED CONVECTION HEAT TRANSFER COEFFICIENT
C     SINGLE PHASE REFRIGERANT INSIDE A TUBE (LIQUID)
C     REFERENCE 1 "FUNDAMENTALS OF HEAT TRANSFER"
C     FRANK P. INCROPERA PAGE 406
C     REFERENCE 2 "HEAT TRANSFER" W. H. McADAMS PAGE 219
C     HL UNITS = BTU/(H.FT**2.F)
      REAL NU
      A=0.023
      B=0.8
      C=0.333
      X0=0
      VISC=VSC(T,X0)
      CON =COND(T,X0)
      CP  =SH(T,X0)
      RE  =G*DIN/VISC
      PR  =VISC*CP/CON
      NU  =A*RE**B*PR**C
      HL  =NU*CON/DIN
      RETURN
      END


      SUBROUTINE DPFRR(T,X,XMX,G,DIN,ZE,DPFR)
C     FRICTIONAL PRESSURE LOSS OF REFRIGERANT
```

```
C       FOR ALL REGIONS INSIDE A TUBE
C       DPFR UNIT = PSI
        IF(X.GT.XMX.OR.X.LT.0.01) THEN
            CALL PLMOO(T,X,G,DIN,ZE,DPF)
        ELSE
            CALL PLC2P(T,X,G,DIN,ZE,DPF)
        END IF
        DPFR=DPF
        RETURN
        END


        SUBROUTINE PLMOO(T,X,G,DIN,ZE,PLM)
C       FRICTIONAL PRESSURE LOSS
C       SINGLE PHASE IN A TUBE
C       REFERENCE 1 "STEADY STATE SIMULATION OF A SINGLE TUBE-
C       FINNED CONDENSER HEAT EXCHANGER" N.K.ANAND, D.R.TREE
C       ASHRAE TRANSACTIONS 1982 V.88 PT.2
C       MOODY EQUATION
C       PLM UNITS = PSI
        RETP=G*DIN/VSC(T,X)
        IF(RETP.LE.2500) I=1
        IF(RETP.GT.2500.AND.RETP.LT.20000) I=2
        IF(RETP.GE.20000) I=3
        GO TO (10,15,20),I
   10   F2P=64/RETP
        GO TO 25
   15   F2P=0.316/RETP**0.25
        GO TO 25
   20   F2P=0.184/RETP**0.2
        GO TO 25
   25   CALL SATPRP(1,T,PSAT,VF,VG,HF,HFG,HG)
        PLM=F2P*(G/3600)**2*ZE*VF/DIN/2
        PLM=PLM/32.174/144
        RETURN
        END


        SUBROUTINE PLC2P(T,X,G,DIN,ZE,PL2P)
C       FRICTIONAL PRESSURE LOSS
C       TWO PHASE IN A TUBE
C       REFERENCE1 "COMPUTER MODELING AND PREDICTION OF
C       PERFORMANCE OF AN AIR SOURCE HEAT PUMP WITH A
C       CAPILLARY TUBE" DOMANSKI, PIOTR PAGE 89
C       PL2P UNITS = PSI
        X1=1
        X0=0
        VISCV=VSC(T,X1)
        VISCL=VSC(T,X0)
        REL=G*DIN*(1-X)/VISCL
        F2P=0.046/REL**0.2
        CALL SATPRP(1,T,PSAT,VF,VG,HF,HFG,HG)
```

```
      XTT=((1-X)/X)**0.9*(VF/VG)**0.5*(VISCL/VISCV)**0.1
      A1 = 1.4
      A2 =-0.87917
      A3 = 0.14062
      A4 = 0.0010417
      A5 =-0.00078125
      B1 = A1
      B2 = A2*(ALOG10(XTT))
      B3 = A3*(ALOG10(XTT))**2
      B4 = A4*(ALOG10(XTT))**3
      B5 = A5*(ALOG10(XTT))**4
      FE = 10**(B1+B2+B3+B4+B5)
      PL2P=2*F2P*(G/3600*(1-X))**2*ZE*FE*VF/DIN
      PL2P=PL2P/32.174/144
      RETURN
      END


      SUBROUTINE DPLRB(T,X,G,FBO,PLB)
C     FRICTIONAL PRESSURE LOSS
C     IN RETURN BENDS
C     REFERENCE 1 "FLOW RESISTANCE WITH BOILING
C     REFRIGERANTS" PIERRE, B.
C     ASHRAE JOURNAL PT.1: SEP 1964 PT.2: OCT 1964
C     REFERENCE 2 "A COMPUTER MODEL FOR AIR-COOLED
C     REFRIGERANT CONDENSERS WITH SPECIFIED REFRIGERANT
C     CIRCUITING"
C     R.D.ELLISON, F.A.CRESWICK, S.K.FISCHER, W.L.JACKSON
C     ASHRAE TRANSACTIONS 1981 V.87 PT.1
C     PLB UNITS = PSI
      CALL SATPRP(1,T,PSAT,VF,VG,HF,HFG,HG)
      V=VF+X*(VG-VF)
      IF(X.LT.0.0001) FB1=0.7
      IF(X.GT.0.0.AND.X.LT.0.2) FB1=0.7+0.1*X/0.2
      IF(X.GT.0.2.AND.X.LT.0.4) FB1=0.8+0.2*(X-0.2)/0.2
      IF(X.GT.0.4.AND.X.LT.0.6) FB1=1.0+0.1*(X-0.4)/0.2
      IF(X.GT.0.6.AND.X.LT.0.8) FB1=1.1-0.1*(X-0.6)/0.2
      IF(X.GT.0.8.AND.X.LT.1.0) FB1=1.0-0.4*(X-0.8)/0.2
      IF(X.GT.0.9999) FB1=0.6
      FB=FBO+FB1
      PLB=FB*(G/3600)**2*V/2
      PLB=PLB/32.174/144
      RETURN
      END


      SUBROUTINE FINEF2(D1,D2,DOUT,THK,HA,FEF)
C     FIN EFFICIENCY
C     REFERENCE 1 "STEADY STEAT SIMULATION OF A SINGLE TUBE-
C     FINNED CONDENSER HEAT EXCHANGER" N.K.ANAND, D.R.TREE
C     ASHRAE TRANSACTIONS 1982 V.88 PT.2
C     REFERENCE 2 "FIN EFFICIENCY WITH COMBINED HEAT AND
```

```
C     MASS TRANSFER"
C     F.C.McQUISTON ASHRAE TRANSACTIONS 1975 V.81 PT.1
      CONFIN=128
      DEQ=2.0*(D1*D2/3.14159265)**0.5
      YEQ=(DEQ-DOUT)/2.0
      DEQIN=DEQ*12
      YEQIN=YEQ*12
      R=DEQ/DOUT
      X=YEQ*(2.0*HA/(CONFIN*THK))**0.5
      TANH=(EXP(X)-EXP(-X))/(EXP(X)+EXP(-X))
      FEF=TANH/X
      RETURN
      END


      SUBROUTINE DTQ(T,A,B,C,D)
      T=T/3600
      K=0
    5 IF(T.LT.0) T=0
      F=A*T+B*EXP(-C*T)
      K=K+1
      DEL=ABS(D-F)
      IF(DEL.LT.0.0002) GOTO 15
      IF(K.EQ.16) WRITE(2,*) '  SOLV K=16 '
      IF(K.GT.16) GOTO 15
      IF(K.GE.2) GOTO 10
      T1=T
      F1=F
      IF(F.GT.D) T=T/1.1
      IF(F.LT.D) T=T*1.1
      GOTO 5
   10 T2=T
      F2=F
      T=T2+(D-F2)*(T2-T1)/(F2-F1)
      T1=T2
      F1=F2
      GOTO 5
   15 T=3600*T
      RETURN
      END


      FUNCTION EVPPH(TW,TA,RHA,SECO,A)
      DATA RHW/1/
      DENSA=RHO(TA,RHA)
      DENSS=RHO(TW,RHW)
      EVPPH=SECO*A*(DENSS-DENSA)
      IF(EVPPH.LT.0) EVPPH=0
      RETURN
      END
```

```
      FUNCTION RHO(T,RH)
      TFREZ=491.67
      TA=T+459.67
      TR=TFREZ/TA
      RTR=1.0/TR
      IF(T.LT.32.0) GO TO 5
      ALOGP=10.79586*(1.0-TR) + 5.02808*ALOG10(TR) +
     #1.50474E-4*(1.0-10.0**(8.29692*(1.0-RTR))) +
     #0.42873E-3*(10.0**(4.76955*(1.0-TR))-1.0) - 2.219583
      GO TO 10
    5 ALOGP=-9.096936*(TR-1.0) - 3.56654*ALOG10(TR) +
     #0.876817*(1.0-RTR) - 2.2195983
   10 PVAP=10.**ALOGP
      RHO=RH*2116.224*PVAP/85.778/TA
      RETURN
      END
```

APPENDIX II

COMPUTER UTILITIES LISTINGS

```
      SUBROUTINE DATAR
C     R 12
      COMMON/QRS/
     1        AVP,BVP,CVP,DVP,EVP,FVP,
     2        ACV,BCV,CCV,DCV,ECV,FCV,
     3        AL,BL,CL,DL,EL,
     4        R,B,A2,B2,C2,A3,B3,C3,A4,B4,
     5        C4,A5,B5,C5,A6,B6,C6,K,ALPHA,
     6        X,Y,CPR,TFR,PC,TC,VC,AA,BB
      REAL K
      AL=34.84
      BL=0.02696
      CL=0.834921
      DL=6.02683
      EL=-0.655549E-5
      AVP=39.88381727
      BVP=-3436.632228
      CVP=-12.47152228
      DVP=0.004730442442
      EVP=0.0
      FVP=0.0
      R=0.088734
      B=0.0065093886
      A2=-3.409727134
      B2=0.00159434848
      C2=-56.7627671
      A3=0.06023944654
      B3=-1.879618431E-5
      C3=1.311399484
      A4=-0.000548737007
      B4=0.0
      C4=0.0
      A5=0.0
      B5=3.468834E-9
      C5=-2.54390678E-5
      A6=0.0
      B6=0.0
      C6=0.0
      K=5.475
      ALPHA=0.0
      ACV=0.0080945
      BCV=0.000332662
      CCV=-2.413896E-7
      DCV=6.72363E-11
      ECV=0.0
      FCV=0.0
      X= 39.55655122
      Y=-0.0165379361
```

```
      PC=596.9
      TC=693.3
      VC=0.02870
      CPR=0.0
      TFR=459.7
      AA=120.
      BB=312.
      RETURN
      END


      FUNCTION TSAT(ITR,PSAT)
      COMMON/QRS/
     1        AVP,BVP,CVP,DVP,EVP,FVP,
     2        ACV,BCV,CCV,DCV,ECV,FCV,
     3        AL,BL,CL,DL,EL,
     4        R,B,A2,B2,C2,A3,B3,C3,A4,B4,
     5        C4,A5,B5,C5,A6,B6,C6,K,ALPHA,
     6        X,Y,CPR,TFR,PC,TC,VC,AA,BB
      REAL LE10,K
      DATA LE10/2.302585093/
      IF(PSAT.LE.0.0) GOTO 15
      PLOG=ALOG10(PSAT)
      TR=AA*PLOG+BB
      ITER=0
    5 TR0=TR
      ITER=ITER+1
      IF(ITER.GT.10) GOTO 10
      C=ALOG10(ABS(FVP-TR0))
      F=AVP+BVP/TR0+CVP*ALOG10(TR0)+DVP*TR0+EVP*((FVP-
     #TR0)/TR0)*C-PLOG
      FP=-BVP/TR0**2+CVP/(LE10*TR0)+DVP-EVP*(1./(LE10*TR0)+
     #FVP*C/TR0**2)
      TR=TR0-F/FP
      IF(ABS(TR-TR0).GT..01) GOTO 5
      TSAT=TR-TFR
      RETURN
   10 TSAT=TR-TFR
      WRITE(2,20) ITR,ITER,PSAT
      RETURN
   15 TSAT=0
      WRITE(2,20) ITR,ITER,PSAT
   20 FORMAT(/,10X,'ERROR - TSAT'
     #,/,/,12X,'ITR ITER          PSAT',/,10X,2I5,F14.3,/)
      RETURN
      END


      FUNCTION SPVOL(ITR,TF,PPSIA)
      COMMON/QRS/
     1        AVP,BVP,CVP,DVP,EVP,FVP,
     2        ACV,BCV,CCV,DCV,ECV,FCV,
```

```
     3        AL,BL,CL,DL,EL,
     4        R,B,A2,B2,C2,A3,B3,C3,A4,B4,
     5        C4,A5,B5,C5,A6,B6,C6,K,ALPHA,
     6        X,Y,CPR,TFR,PC,TC,VC,AA,BB
      REAL K
      T=TF+TFR
      IF(T.LE.0.0) GOTO 15
      TFSAT=TSAT(ITR,PPSIA)
      IF(TF.LT.(TFSAT-0.002)) GOTO 15
      IF(PPSIA.LE.0.0) GOTO 15
      ARG=-K*T/TC
      IF (ARG .LT. -100) ARG=-100
      ES0=EXP(ARG)
      ES1=PPSIA
      ES2=R*T
      ES3=A2+B2*T+C2*ES0
      ES4=A3+B3*T+C3*ES0
      ES5=A4+B4*T+C4*ES0
      ES6=A5+B5*T+C5*ES0
      ES7=A6+B6*T+C6*ES0
      ES32=2.*ES3
      ES43=3.*ES4
      ES54=4.*ES5
      ES65=5.*ES6
      VN=R*T/PPSIA
      ITER=0
    5 ITER=ITER+1
      IF(ITER.GT.30) GOTO 10
      V=VN
      V2=V**2
      V3=V**3
      V4=V**4
      V5=V**5
      V6=V**6
      ARG=-ALPHA*(V+B)
      IF (ARG.LT.-100) THEN
       ITR=ARG
       ARG=-100
      END IF
      EMAV=EXP(ARG)
      F=ES1-ES2/V-ES3/V2-ES4/V3-ES5/V4-ES6/V5-ES7*EMAV
      FV=ES2/V2+ES32/V3+ES43/V4+ES54/V5+ES65/V6+
     #ES7*ALPHA*EMAV
      VN=V-F/FV
      IF(ABS((VN-V)/V).GT.1.E-06) GOTO 5
      SPVOL=VN+B
      RETURN
   10 SPVOL=VN+B
      WRITE(2,20) ITR,ITER,T,TF,PPSIA
      RETURN
   15 SPVOL=0
      WRITE(2,20) ITR,ITER,T,TF,PPSIA
```

```
20 FORMAT(/,10X,'ERROR - SPVOL'
  #,/,12X,'ITR ITER              T              TF'
  #,9X,'PPSIA',/,10X,2I5,3F14.3,/)
   RETURN
   END


   SUBROUTINE SATPRP(ITR,TF,PSAT,VF,VG,HF,HFG,HG)
   COMMON/QRS/
  1        AVP,BVP,CVP,DVP,EVP,FVP,
  2        ACV,BCV,CCV,DCV,ECV,FCV,
  3        AL,BL,CL,DL,EL,
  4        R,B,A2,B2,C2,A3,B3,C3,A4,B4,
  5        C4,A5,B5,C5,A6,B6,C6,K,ALPHA,
  6        X,Y,CPR,TFR,PC,TC,VC,AA,BB
   REAL J,KTDTC,LE10,K,L10E
   DATA J,LE10/0.185053,2.302585093/
   L10E=0.4342944819
   T=TF+TFR
   IF(T.LE.0.0) GOTO 10
   IF(T.GE.TC) GOTO 10
   DEL = TC -T
   PSAT=10.**(AVP+BVP/T+CVP*ALOG10(T)+DVP*T)
   VG=SPVOL(ITR,TF,PSAT)
   TCMT=TC-T
   VF=1./(AL+BL*TCMT+CL*TCMT**(1./2.)+DL*TCMT**(1./3.)+
  #EL*TCMT**2)
   HFG=(VG-VF)*PSAT*LE10*(-BVP/T+CVP/LE10+DVP*T)*J
   T2=T**2
   T3=T**3
   T4=T**4
   VR=VG-B
   VR2=2.*VR**2
   VR3=3.*VR**3
   VR4=4.*VR**4
   KTDTC=K*T/TC
   ARG=-KTDTC
   IF (ARG .LT. -100) ARG=-100
   EKTDTC=EXP(ARG)
   ARG=-ALPHA*VG
   IF (ARG .LT. -100) ARG=-100
   EMAV=EXP(ARG)
   H1=ACV*T+BCV*T2/2.+CCV*T3/3.+DCV*T4/4.-FCV/T
   H2=J*PSAT*VG
   H3=A2/VR+A3/VR2+A4/VR3+A5/VR4
   H4=C2/VR+C3/VR2+C4/VR3+C5/VR4
   HG=H1+H2+J*H3+J*EKTDTC*(1.+KTDTC)*H4+X
   HF=HG-HFG
   IF (DEL.GT.10.) RETURN
   WRITE(2,5) ITR,DEL,VF,VG,HF,HG
 5 FORMAT(10X,'CAUTION TCRIT-T < 10F',/,17X,'ITR',5X,
  #'DEL',8X,'VF',8X,'VG',8X,'HF',8X,'HG',/,10X,I5,5F10.5)
```

```
      RETURN
   10 WRITE(2,15) ITR,T,TF
   15 FORMAT(/,10X,'ERROR - SATPRP'
     #,/,12X,'ITR              T              TF'
     #,/,10X,I5,2F14.3,/)
      RETURN
      END


      SUBROUTINE VAPOR(ITR,TF,PPSIA,VVAP,HVAP)
      COMMON/QRS/
     1        AVP,BVP,CVP,DVP,EVP,FVP,
     2        ACV,BCV,CCV,DCV,ECV,FCV,
     3        AL,BL,CL,DL,EL,
     4        R,B,A2,B2,C2,A3,B3,C3,A4,B4,
     5        C4,A5,B5,C5,A6,B6,C6,K,ALPHA,
     6        X,Y,CPR,TFR,PC,TC,VC,AA,BB
      REAL J,KTDTC,LE10,K
      J=0.185053
      T=TF+TFR
      IF(T.LE.0.0) GOTO 5
      TFSAT=TSAT(ITR,PPSIA)
      IF(TF.LT.(TFSAT-0.002)) GOTO 5
      IF(PPSIA.LE.0.0) GOTO 5
      VVAP=SPVOL(ITR,TF,PPSIA)
      T2=T**2
      T3=T**3
      T4=T**4
      VR=VVAP-B
      VR2=2.*VR**2
      VR3=3.*VR**3
      VR4=4.*VR**4
      KTDTC=K*T/TC
      ARG=-KTDTC
      IF (ARG .LT. -100) ARG=-100
      EKTDTC=EXP(ARG)
      ARG=-ALPHA*VVAP
      IF (ARG .LT. -100) ARG=-100
      EMAV=EXP(ARG)
      H1=ACV*T+BCV*T2/2.+CCV*T3/3.+DCV*T4/4.-FCV/T
      H2=J*PPSIA*VVAP
      H3=A2/VR+A3/VR2+A4/VR3+A5/VR4
      H4=C2/VR+C3/VR2+C4/VR3+C5/VR4
      HVAP=H1+H2+J*H3+J*EKTDTC*(1.+KTDTC)*H4+X
      RETURN
    5 WRITE(2,10) ITR,T,TF,PPSIA,TFSAT
   10 FORMAT(/,10X,'ERROR - VAPOR'
     #,/,12X,'ITR              T              TF'
     #,9X,'PPSIA         TFSAT',/,10X,I5,5F14.3,/)
      RETURN
      END
```

```
      SUBROUTINE TVAP(ITR,P,H,TMIN,T,V)
      K=0
    5 IF(T.LT.TMIN) T=TMIN
      CALL VAPOR(ITR,T,P,V,HV)
      K=K+1
      DEL=ABS(H-HV)
      IF(DEL.LT.0.0002) RETURN
      IF(K.GT.16) RETURN
      IF(K.GE.2) GOTO 10
      T1=T
      H1=HV
      IF(HV.GT.H) T=T-2
      IF(HV.LT.H) T=T+2
      GOTO 5
   10 T2=T
      H2=HV
      DH=H2-H1
      IF(ABS(DH).GT.0.00001) THEN
          T=T2+(H-H2)*(T2-T1)/DH
      ELSE
          WRITE(2,15) ITR,K,T,TMIN
          RETURN
      END IF
      T1=T2
      H1=H2
      GOTO 5
   15 FORMAT(/,2X,'TVAP ERROR',/,3X,'ITR   K       T
     #    TMIN',/,2X,2I4,2F8.3,/)
      END


      SUBROUTINE TLIQ(ITR,H,TMAX,T,VF)
      K=0
    5 IF(T.GT.TMAX) T=TMAX
      CALL SATPRP(ITR,T,PSAT,VF,VG,HF,HFG,HG)
      K=K+1
      DEL=ABS(H-HF)
      IF(DEL.LT.0.0002) RETURN
      IF(K.GT.16) RETURN
      IF(K.GE.2) GOTO 10
      T1=T
      H1=HF
      IF(HF.GT.H) T=T-2
      IF(HF.LT.H) T=T+2
      GOTO 5
   10 T2=T
      H2=HF
      T=T2+(H-H2)*(T2-T1)/(H2-H1)
      T1=T2
      H1=H2
      GOTO 5
      END
```

```
      FUNCTION VSC(T,X)
C     VISCOSITY  UNITS = LBM/(FT.HR)
      COMMON/AV/CWF(14),CWG(14)
      COMMON/BV/TW(12)
      VSCF=WV(CWF,T)
      IF(X.GT.0.0001) GOTO 5
      VSC=VSCF
C      VSC=VSCF/3600.
      RETURN
    5 VSCG=WV(CWG,T)
      ITR=999
      CALL SATPRP(ITR,T,PSAT,VF,VG,HF,HFG,HG)
      VSC=(1.-X)*VF*VSCF+X*VG*VSCG
      VM=VF+X*(VG-VF)
      VSC=VSC/VM
C
C      MCADAMS EQUATION AS PER WALLIS
C      RVSC=(1-X)/VSCF + X/VSCG
C      VSC=1/RVSC
C
C      VSC=VSC/3600.
      RETURN
      END


      FUNCTION WV(C,T)
C     EVALUATE FUNCTION USING COEFFICIENTS DETERMINED BY
C     SPLINE FIT INTERPOLATION
      DIMENSION C(14)
      COMMON/BV/TW(12)
      WV=0.
      DO 5 I=1,11
    5 WV=WV+USF(T,TW(I))*C(I)*(T-TW(I))**3
      WV=WV+C(12)*T**2+C(13)*T+C(14)
      RETURN
      END


      FUNCTION COND(T,X)
C     CONDUCTIVITY UNITS = BTU/(H.FT.F)
      COMMON/AK/CWF(14),CWG(14)
      COMMON/BK/TW(12)
      CONDF=WK(CWF,T)
      IF(X.GT.0.0001) GOTO 5
      COND=CONDF
      RETURN
    5 CONDG=WK(CWG,T)
      COND=(1.-X)*CONDF+X*CONDG
      RETURN
      END
```

```
      FUNCTION WK(C,T)
C     EVALUATE FUNCTION USING COEFFICIENTS DETERMINED BY
C     SPLINE FIT INTERPOLATION
      DIMENSION C(14)
      COMMON/BK/TW(12)
      WK=0.
      DO 5 I=1,11
    5 WK=WK+USF(T,TW(I))*C(I)*(T-TW(I))**3
      WK=WK+C(12)*T**2+C(13)*T+C(14)
      RETURN
      END


      FUNCTION SH(T,X)
C     SPECIFIC HEAT UNITS = BTU/(LBM.F)
      COMMON/ASH/CWF(14),CWG(14)
      COMMON/BSH/TW(12)
      SHF=WSH(CWF,T)
      IF(X.GT.0.0001) GOTO 5
      SH=SHF
      RETURN
    5 SHG=WSH(CWG,T)
      SH=(1.-X)*SHF+X*SHG
      RETURN
      END


      FUNCTION WSH(C,T)
C     EVALUATE FUNCTION USING COEFFICIENTS DETERMINED BY
C     SPLINE FIT INTERPOLATION
      DIMENSION C(14)
      COMMON/BSH/TW(12)
      WSH=0.
      DO 5 I=1,11
    5 WSH=WSH+USF(T,TW(I))*C(I)*(T-TW(I))**3
      WSH=WSH+C(12)*T**2+C(13)*T+C(14)
      RETURN
      END


      SUBROUTINE DATAV
C     R 12 VISCOSITY
      DIMENSION WF(12),WG(12)
      COMMON/AV/CWF(14),CWG(14)
      COMMON/BV/TW(12)
C     DATA TW/-20.,0.,20.,40.,60.,80.,100.,120.,140.,160.
C    #,180.,200/
      DATA WF/.866,.767,.687,.620,.564,.517,.477,.441,.409
     #,.370,.329,.273/
      DATA WG/.0249,.0265,.0279,.0291,.0301,.0311,.0324
     #,.0339,.0359,.0384,.0417,.0458/
      DO 5 I=1,12
```

```
    5 TW(I)=-20.+20.*(I-1)
      CALL COEF(TW,WF,CWF)
      CALL COEF(TW,WG,CWG)
      RETURN
      END


      SUBROUTINE DATAK
C     R 12 CONDUCTIVITY
      DIMENSION WF(12),WG(12)
      COMMON/AK/CWF(14),CWG(14)
      COMMON/BK/TW(12)
C     DATA TW/-20.,0.,20.,40.,60.,80.,100.,120.,140.,160.
C    #,180.,200/
      DATAWF/.0514,.0490,.0467,.0443,.0420,.0397,.0373,.0350
     #,.0326,.0302,.0276,.0246/
      DATAWG/.0040,.0043,.0046,.0050,.0053,.0056,.0060,.0064
     #,.0068,.0072,.0076,.0083/
      DO 5 I=1,12
    5 TW(I)=-20.+20.*(I-1)
      CALL COEF(TW,WF,CWF)
      CALL COEF(TW,WG,CWG)
      RETURN
      END


      SUBROUTINE DATASH
C     R 12 SPECIFIC HEAT
      DIMENSION WF(12),WG(12)
      COMMON/ASH/CWF(14),CWG(14)
      COMMON/BSH/TW(12)
C     DATA TW/-20.,0.,20.,40.,60.,80.,100.,120.,140.,160.
C    #,180.,200/
      DATA WF/.214,.217,.220,.224,.229,.234,.240,.251,.266
     #,.288,.317,.356/
      DATA WG/.139,.145,.150,.157,.164,.174,.185,.199,.216
     #,.235,.290,.362/
      DO 5 I=1,12
    5 TW(I)=-20.+20.*(I-1)
      CALL COEF(TW,WF,CWF)
      CALL COEF(TW,WG,CWG)
      RETURN
      END


      SUBROUTINE COEF(X,Y,C)
      DIMENSION A(14,15),C(14),X(12),Y(12)
C     NP=12  NE=NP+2=14  NPM=NP-1=11  NPP=NP+1=13
C     NY=NE+1=15
C     E=3  E*(E-1)=6  E-2=1
      DO 15 J=1,12
      DO 5 I=1,11
```

```
    5 A(J,I)=USF(X(J),X(I))*(X(J)-X(I))**3
      DO 10 I=12,13
   10 A(J,I)=X(J)**(14-I)
      A(J,14)=1.
   15 A(J,15)=Y(J)
      DO 30 J=13,14
      K=1
      IF(J.EQ.14) K=12
      DO 20 I=1,11
   20 A(J,I)=USF(X(K),X(I))*6.*(X(K)-X(I))
      DO 25 I=12,14
   25 A(J,I)=(14-I)*(13-I)
   30 A(J,15)=0.
      CALL SIMEQ(14,A,C)
      RETURN
      END


      FUNCTION USF(X,XI)
C     UNIT STEP FUNCTION
      USF=0.
      IF(X.GT.XI) USF=1.
      RETURN
      END


      SUBROUTINE SIMEQ(N,A,X)
C     SUBROUTINE TO SOLVE A SYSTEM OF N LINEAR SIMULTANEOUS
C     EQUATIONS
C     GIVEN BY THE ARRAY A(J,I) WHERE I=J+1
C     SOLUTION IS X(J)
C     ZERO  ABS VALUES LESS THAN ZERO ARE TAKEN AS 0
C     IER  IF IER IS POSITIVE SOLUTION IS VALID
C          IF IER IS NEGATIVE SOLUTION IS INVALID
      DIMENSION A(14,15),X(14)
      ZERO=1.E-6
      NP=N+1
      NM=N-1
      DO 25 I=1,NM
      IR=I
      IP=I+1
      DO 5 J=IP,N
      IF(ABS(A(IR,I)).GE.ABS(A(J,I))) GO TO 5
      IR=J
    5 CONTINUE
      IF(IR.EQ.I) GO TO 15
      DO 10 J=1,NP
      HH=A(I,J)
      A(I,J)=A(IR,J)
      A(IR,J)=HH
   10 CONTINUE
   15 IF(ABS(A(I,I)).LE.ZERO) GO TO 30
```

```
      DO 20 J=IP,N
      HH=A(J,I)
      DO 20 K=IP,NP
      A(J,K)=A(J,K)-(A(I,K)/A(I,I))*HH
   20 CONTINUE
   25 CONTINUE
      IF(ABS(A(N,N)).GT.ZERO) GO TO 40
   30 CONTINUE
C     IER=-1
      WRITE(2,35)
   35 FORMAT(/,2X,'SUBROUTINE SIMEQ - SOLUTION INVALID',/)
      RETURN
   40 DO 55 IK=1,N
      I=N+1-IK
      X(I)=A(I,NP)
      IF(I.EQ.N) GO TO 50
      IP=I+1
      DO 45 J=IP,N
   45 X(I)=X(I)-X(J)*A(I,J)
   50 X(I)=X(I)/A(I,I)
   55 CONTINUE
C     IER=1
      RETURN
      END
```

APPENDIX III

SAMPLE COMPUTER OUTPUT FILE

PROGRAM: DFRST + DFSUBS - 1989 DEC 11

INPUT DATA

DIN	DOUT	D1	D2	THK	FPI	ZMX
.485	.537	1.250	1.200	.006	8.000	640.000

NTMX	NEL	NTUB	DTI	TCOIL	XMX	FBO	IMAX
13	40	20	24.0	32.0	.950	.300	3

MFO	MFR	MLIQO	HA	SECO	SEEX	CWR	CWMX
4.01	4.01	1.00	.54	55.00	.50	3.70	500.00

OUTPUT DATA

CCOI	CTOT	EPRE	EDFR
.0421	.0910	44.4	574.8

PPHR	PO	TO	XO	TAMB	RHA	PNXT
31.50	68.70	53.16	1.00	19.80	.62	69.60

TOTT	QHP	TEPF	TEF	EZ	ET	TMELT	TMVAP
24.	2118.	.00	13.86	14.12	14.12	.10	.00

DFEF	EFFC	P(NPL)	DP	DHTF	SCLVG	XLVG	NTDROP
.9818	.9818	68.686	.014	85.57	-24.7	.000	0

I	T	TS	TWO	TWI	TWF	X	ESUM	IHTM	PATH
									4332211
1	53.2	56.8	32.0	32.0	34.0	1.000	4.60	2	100.0
2	56.8	56.8	32.0	32.0	33.3	.641	2.99	2	100.0
3	56.8	56.8	32.0	32.0	33.0	.412	2.21	2	100.0
4	56.7	56.7	32.0	32.0	32.7	.242	1.63	2	100.0
5	56.7	56.7	32.0	32.0	32.5	.117	1.14	2	100.0
6	56.7	56.7	32.0	32.0	32.3	.030	.58	2	100.0
7	52.6	56.7	32.0	32.0	32.1	.000	.31	2	100.0
8	45.9	56.7	32.0	32.0	32.1	.000	.21	2	100.0
9	41.4	56.7	32.0	32.0	32.1	.000	.14	2	100.0
10	38.3	56.7	32.0	32.0	32.0	.000	.10	2	100.0
11	36.3	56.7	32.0	32.0	32.0	.000	.06	2	100.0
12	34.9	56.7	32.0	32.0	32.0	.000	.04	2	100.0
13	34.0	56.7	32.0	32.0	32.0	.000	.03	2	100.0
14	33.3	56.7	32.0	32.0	32.0	.000	.02	2	100.0
15	32.9	56.7	32.0	32.0	32.0	.000	.01	2	100.0
16	32.6	56.7	32.0	32.0	32.0	.000	.01	2	100.0
17	32.4	56.7	32.0	32.0	32.0	.000	.01	2	100.0
18	32.3	56.7	32.0	32.0	32.0	.000	.00	2	100.0
19	32.2	56.7	32.0	32.0	32.0	.000	.00	2	100.0
20	32.1	56.7	32.0	32.0	32.0	.000	.00	2	100.0
21	32.1	56.7	32.0	32.0	32.0	.000	.00	2	100.0
22	32.1	56.7	32.0	32.0	32.0	.000	.00	2	100.0
23	32.0	56.7	32.0	32.0	32.0	.000	.00	2	100.0
24	32.0	56.7	32.0	32.0	32.0	.000	.00	2	100.0
25	32.0	56.7	32.0	32.0	32.0	.000	.00	2	100.0
26	32.0	56.7	32.0	32.0	32.0	.000	.00	2	100.0
27	32.0	56.7	32.0	32.0	32.0	.000	.00	2	100.0
28	32.0	56.7	32.0	32.0	32.0	.000	.00	2	100.0
29	32.0	56.7	32.0	32.0	32.0	.000	.00	2	100.0
30	32.0	56.7	32.0	32.0	32.0	.000	.00	2	100.0
31	32.0	56.7	32.0	32.0	32.0	.000	.00	2	100.0
32	32.0	56.7	32.0	32.0	32.0	.000	.00	2	100.0
33	32.0	56.7	32.0	32.0	32.0	.000	.00	2	100.0
34	32.0	56.7	32.0	32.0	32.0	.000	.00	2	100.0
35	32.0	56.7	32.0	32.0	32.0	.000	.00	2	100.0
36	32.0	56.7	32.0	32.0	32.0	.000	.00	2	100.0
37	32.0	56.7	32.0	32.0	32.0	.000	.00	2	100.0
38	32.0	56.7	32.0	32.0	32.0	.000	.00	2	100.0
39	32.0	56.7	32.0	32.0	32.0	.000	.00	2	100.0
40	32.0	56.7	32.0	32.0	32.0	.000	.00	2	100.0
41	32.0	56.7	.0	.0	.0	.000	.00	0	.0

I	MFRST	MLIQ	DTLM	P	V	H	HR
1	.0687	.0000	999.000	68.700	.6227	82.74	212.23
2	.0798	.0000	999.000	68.700	.3813	60.84	112.79
3	.0851	.0000	999.000	68.697	.2492	46.60	82.34
4	.0891	.0000	999.000	68.693	.1514	36.07	60.15
5	.0924	.0000	999.000	68.691	.0793	28.29	41.61
6	.0963	.0000	999.000	68.689	.0289	22.86	21.06
7	.0981	.0000	999.000	68.688	.0118	20.09	13.64
8	.0988	.0000	999.000	68.687	.0117	18.59	13.57
9	.0993	.0000	999.000	68.687	.0116	17.58	13.51
10	.0996	.0000	999.000	68.687	.0116	16.91	13.48
11	.0998	.0000	999.000	68.687	.0115	16.45	13.45
12	.1000	.0000	999.000	68.687	.0115	16.14	13.44
13	.1000	.0000	999.000	68.687	.0115	15.93	13.43
14	.1001	.0000	999.000	68.687	.0115	15.79	13.42
15	.1002	.0000	999.000	68.687	.0115	15.70	13.41
16	.1002	.0000	999.000	68.687	.0115	15.63	13.41
17	.1002	.0000	999.000	68.687	.0115	15.59	13.41
18	.1002	.0000	999.000	68.687	.0115	15.56	13.40
19	.1002	.0000	999.000	68.687	.0115	15.54	13.40
20	.1002	.0000	999.000	68.687	.0115	15.53	13.40
21	.1002	.0000	999.000	68.687	.0115	15.52	13.40
22	.1002	.0000	999.000	68.687	.0115	15.51	13.40
23	.1002	.0000	999.000	68.687	.0115	15.51	13.40
24	.1002	.0000	999.000	68.687	.0115	15.51	13.40
25	.1002	.0000	999.000	68.687	.0115	15.50	13.40
26	.1002	.0000	999.000	68.687	.0115	15.50	13.40
27	.1002	.0000	999.000	68.687	.0115	15.50	13.40
28	.1002	.0000	999.000	68.686	.0115	15.50	13.40
29	.1002	.0000	999.000	68.686	.0115	15.50	13.40
30	.1002	.0000	999.000	68.686	.0115	15.50	13.40
31	.1002	.0000	999.000	68.686	.0115	15.50	13.40
32	.1002	.0000	999.000	68.686	.0115	15.50	13.40
33	.1002	.0000	999.000	68.686	.0115	15.50	13.40
34	.1002	.0000	999.000	68.686	.0115	15.50	13.40
35	.1002	.0000	999.000	68.686	.0115	15.50	13.40
36	.1003	.0000	999.000	68.686	.0115	15.50	13.40
37	.1003	.0000	999.000	68.686	.0115	15.50	13.40
38	.1003	.0000	999.000	68.686	.0115	15.50	13.40
39	.1003	.0000	999.000	68.686	.0115	15.50	13.40
40	.1003	.0000	999.000	68.686	.0115	15.50	13.40
41	.0000	.0000	.000	68.686	.0115	15.50	.00

PPHR	PO	TO	XO	TAMB	RHA	PNXT
45.70	69.60	62.37	1.00	20.20	.65	71.40

TOTT	QHP	TEPF	TEF	EZ	ET	TMELT	TMVAP
48.	3129.	.00	32.61	20.86	34.98	.23	.00

DFEF	EFFC	P(NPL)	DP	DHTF	SCLVG	XLVG	NTDROP
.9323	.9323	69.569	.031	122.47	-25.5	.000	0

I	T	TS	TWO	TWI	TWF	X	ESUM	IHTM	PATH
									4332211
1	62.4	57.5	34.0	34.0	51.0	1.000	3.65	2	200.0
2	57.5	57.5	33.3	33.3	43.8	.820	3.10	2	200.0
3	57.5	57.5	33.0	33.0	41.0	.655	2.96	2	200.0
4	57.5	57.5	32.7	32.7	38.7	.499	2.74	2	200.0
5	57.5	57.5	32.5	32.5	36.6	.354	2.42	2	200.0
6	57.5	57.5	32.3	32.3	34.5	.225	2.06	2	200.0
7	57.5	57.5	32.1	32.1	33.3	.116	1.55	2	200.0
8	57.5	57.5	32.1	32.1	32.6	.035	.87	2	200.0
9	54.4	57.5	32.1	32.1	32.2	.000	.46	2	200.0
10	47.7	57.5	32.0	32.0	32.1	.000	.32	2	200.0
11	43.0	57.5	32.0	32.0	32.1	.000	.22	2	200.0
12	39.7	57.5	32.0	32.0	32.1	.000	.16	2	200.0
13	37.4	57.5	32.0	32.0	32.0	.000	.11	2	200.0
14	35.8	57.5	32.0	32.0	32.0	.000	.08	2	200.0
15	34.6	57.5	32.0	32.0	32.0	.000	.05	2	200.0
16	33.8	57.5	32.0	32.0	32.0	.000	.04	2	200.0
17	33.3	57.5	32.0	32.0	32.0	.000	.03	2	200.0
18	32.9	57.5	32.0	32.0	32.0	.000	.02	2	200.0
19	32.6	57.5	32.0	32.0	32.0	.000	.01	2	200.0
20	32.4	57.5	32.0	32.0	32.0	.000	.01	2	200.0
21	32.3	57.5	32.0	32.0	32.0	.000	.01	2	200.0
22	32.2	57.5	32.0	32.0	32.0	.000	.00	2	200.0
23	32.2	57.5	32.0	32.0	32.0	.000	.00	2	200.0
24	32.1	57.5	32.0	32.0	32.0	.000	.00	2	200.0
25	32.1	57.5	32.0	32.0	32.0	.000	.00	2	200.0
26	32.1	57.5	32.0	32.0	32.0	.000	.00	2	200.0
27	32.0	57.5	32.0	32.0	32.0	.000	.00	2	200.0
28	32.0	57.5	32.0	32.0	32.0	.000	.00	2	200.0
29	32.0	57.5	32.0	32.0	32.0	.000	.00	2	200.0
30	32.0	57.5	32.0	32.0	32.0	.000	.00	2	200.0
31	32.0	57.5	32.0	32.0	32.0	.000	.00	2	200.0
32	32.0	57.5	32.0	32.0	32.0	.000	.00	2	200.0
33	32.0	57.5	32.0	32.0	32.0	.000	.00	2	200.0
34	32.0	57.5	32.0	32.0	32.0	.000	.00	2	200.0
35	32.0	57.5	32.0	32.0	32.0	.000	.00	2	200.0
36	32.0	57.5	32.0	32.0	32.0	.000	.00	2	200.0
37	32.0	57.5	32.0	32.0	32.0	.000	.00	2	200.0
38	32.0	57.5	32.0	32.0	32.0	.000	.00	2	200.0
39	32.0	57.5	32.0	32.0	32.0	.000	.00	2	200.0
40	32.0	57.5	32.0	32.0	32.0	.000	.00	2	200.0
41	32.0	57.5	.0	.0	.0	.000	.00	0	.0

I	MFRST	MLIQ	DTLM	P	V	H	HR
1	.0483	.0000	999.000	69.600	.5888	83.97	248.65
2	.0612	.0000	999.000	69.600	.4779	71.99	186.79
3	.0668	.0000	999.000	69.599	.3845	61.82	152.38
4	.0717	.0000	999.000	69.592	.2954	52.11	125.79
5	.0768	.0000	999.000	69.588	.2129	43.11	101.03
6	.0826	.0000	999.000	69.582	.1401	35.17	78.79
7	.0876	.0000	999.000	69.578	.0781	28.42	56.42
8	.0929	.0000	999.000	69.573	.0315	23.35	30.89
9	.0961	.0000	999.000	69.572	.0118	20.49	18.39
10	.0974	.0000	999.000	69.571	.0117	18.98	18.30
11	.0983	.0000	999.000	69.571	.0116	17.93	18.22
12	.0989	.0000	999.000	69.571	.0116	17.20	18.17
13	.0993	.0000	999.000	69.571	.0115	16.69	18.13
14	.0996	.0000	999.000	69.571	.0115	16.33	18.11
15	.0998	.0000	999.000	69.571	.0115	16.08	18.09
16	.0999	.0000	999.000	69.571	.0115	15.91	18.08
17	.1000	.0000	999.000	69.571	.0115	15.78	18.07
18	.1001	.0000	999.000	69.571	.0115	15.70	18.06
19	.1001	.0000	999.000	69.571	.0115	15.64	18.06
20	.1002	.0000	999.000	69.570	.0115	15.60	18.06
21	.1002	.0000	999.000	69.570	.0115	15.57	18.05
22	.1002	.0000	999.000	69.570	.0115	15.55	18.05
23	.1002	.0000	999.000	69.570	.0115	15.53	18.05
24	.1002	.0000	999.000	69.570	.0115	15.52	18.05
25	.1002	.0000	999.000	69.570	.0115	15.52	18.05
26	.1002	.0000	999.000	69.570	.0115	15.51	18.05
27	.1002	.0000	999.000	69.570	.0115	15.51	18.05
28	.1002	.0000	999.000	69.570	.0115	15.51	18.05
29	.1002	.0000	999.000	69.570	.0115	15.50	18.05
30	.1002	.0000	999.000	69.570	.0115	15.50	18.05
31	.1002	.0000	999.000	69.570	.0115	15.50	18.05
32	.1002	.0000	999.000	69.570	.0115	15.50	18.05
33	.1002	.0000	999.000	69.570	.0115	15.50	18.05
34	.1002	.0000	999.000	69.570	.0115	15.50	18.05
35	.1002	.0000	999.000	69.570	.0115	15.50	18.05
36	.1002	.0000	999.000	69.570	.0115	15.50	18.05
37	.1003	.0000	999.000	69.570	.0115	15.50	18.05
38	.1003	.0000	999.000	69.570	.0115	15.50	18.05
39	.1003	.0000	999.000	69.570	.0115	15.50	18.05
40	.1003	.0000	999.000	69.569	.0115	15.50	18.05
41	.0000	.0000	.000	69.569	.0115	15.50	.00

PPHR	PO	TO	XO	TAMB	RHA	PNXT
159.30	71.40	77.36	1.00	20.50	.68	69.20

TOTT	QHP	TEPF	TEF	EZ	ET	TMELT	TMVAP
72.	11282.	.00	102.34	75.21	110.19	.71	.00

DFEF	EFFC	P(NPL)	DP	DHTF	SCLVG	XLVG	NTDROP
.9287	.9287	71.085	.315	416.08	-26.8	.000	0

I	T	TS	TWO	TWI	TWF	X	ESUM	IHTM	PATH
									4332211
1	77.4	59.1	51.0	51.0	59.1	1.000	3.24	2	300.0
2	59.1	59.1	43.8	43.8	54.7	.999	3.54	2	300.0
3	59.2	59.2	41.0	41.0	54.1	.945	3.98	2	300.0
4	59.1	59.1	38.7	38.7	52.8	.884	4.29	2	300.0
5	59.2	59.2	36.6	36.6	51.6	.819	4.72	2	300.0
6	59.1	59.1	34.5	34.5	49.7	.747	5.32	2	300.0
7	59.1	59.1	33.3	33.3	47.5	.666	5.96	2	300.0
8	59.1	59.1	32.6	32.6	44.1	.575	6.76	2	300.0
9	59.1	59.1	32.2	32.2	40.8	.472	7.15	2	300.0
10	59.0	59.0	32.1	32.1	38.6	.363	6.73	2	300.0
11	59.0	59.0	32.1	32.1	36.8	.261	6.04	2	300.0
12	58.9	58.9	32.1	32.1	35.3	.169	5.16	2	300.0
13	58.9	58.9	32.0	32.0	34.0	.091	3.96	2	300.0
14	58.9	58.9	32.0	32.0	33.0	.030	2.39	2	300.0
15	57.2	58.9	32.0	32.0	32.6	.000	1.39	2	300.0
16	51.4	58.9	32.0	32.0	32.5	.000	1.07	2	300.0
17	46.9	58.9	32.0	32.0	32.4	.000	.82	2	300.0
18	43.5	58.9	32.0	32.0	32.3	.000	.63	2	300.0
19	40.8	58.9	32.0	32.0	32.2	.000	.48	2	300.0
20	38.8	58.9	32.0	32.0	32.2	.000	.37	2	300.0
21	37.2	58.9	32.0	32.0	32.1	.000	.28	2	300.0
22	36.0	58.9	32.0	32.0	32.1	.000	.22	2	300.0
23	35.1	58.9	32.0	32.0	32.1	.000	.17	2	300.0
24	34.4	58.9	32.0	32.0	32.1	.000	.13	2	300.0
25	33.8	58.9	32.0	32.0	32.0	.000	.10	2	300.0
26	33.4	58.9	32.0	32.0	32.0	.000	.08	2	300.0
27	33.1	58.9	32.0	32.0	32.0	.000	.06	2	300.0
28	32.8	58.9	32.0	32.0	32.0	.000	.05	2	300.0
29	32.6	58.9	32.0	32.0	32.0	.000	.03	2	300.0
30	32.5	58.9	32.0	32.0	32.0	.000	.03	2	300.0
31	32.4	58.9	32.0	32.0	32.0	.000	.02	2	300.0
32	32.3	58.8	32.0	32.0	32.0	.000	.02	2	300.0
33	32.2	58.8	32.0	32.0	32.0	.000	.01	2	300.0
34	32.2	58.8	32.0	32.0	32.0	.000	.01	2	300.0
35	32.1	58.8	32.0	32.0	32.0	.000	.01	2	300.0
36	32.1	58.8	32.0	32.0	32.0	.000	.01	2	300.0
37	32.1	58.8	32.0	32.0	32.0	.000	.00	2	300.0
38	32.1	58.8	32.0	32.0	32.0	.000	.00	2	300.0
39	32.0	58.8	32.0	32.0	32.0	.000	.00	2	300.0
40	32.0	58.8	32.0	32.0	32.0	.000	.00	2	300.0
41	32.0	58.8	.0	.0	.0	.000	.00	0	.0

I	MFRST	MLIQ	DTLM	P	V	H	HR
1	.0281	.0000	.744	71.400	.5967	86.33	548.06
2	.0397	.0000	999.000	71.399	.5658	83.28	627.91
3	.0429	.0000	999.000	71.456	.5354	79.94	616.50
4	.0459	.0000	999.000	71.425	.5020	76.19	535.77
5	.0482	.0000	999.000	71.456	.4656	72.16	496.40
6	.0499	.0000	999.000	71.405	.4261	67.71	462.48
7	.0503	.0000	999.000	71.419	.3810	62.70	426.71
8	.0491	.0000	999.000	71.356	.3310	57.09	387.39
9	.0487	.0000	999.000	71.348	.2739	50.72	341.21
10	.0524	.0000	999.000	71.280	.2137	43.99	289.25
11	.0575	.0000	999.000	71.250	.1568	37.65	239.19
12	.0638	.0000	999.000	71.193	.1059	31.97	192.38
13	.0723	.0000	999.000	71.162	.0622	27.11	140.51
14	.0832	.0000	999.000	71.129	.0288	23.39	82.02
15	.0903	.0000	999.000	71.113	.0119	21.13	50.05
16	.0926	.0000	999.000	71.107	.0118	19.82	49.83
17	.0944	.0000	999.000	71.107	.0117	18.82	49.65
18	.0958	.0000	999.000	71.105	.0116	18.05	49.51
19	.0968	.0000	999.000	71.105	.0116	17.46	49.39
20	.0976	.0000	999.000	71.104	.0116	17.01	49.31
21	.0983	.0000	999.000	71.103	.0115	16.66	49.24
22	.0987	.0000	999.000	71.102	.0115	16.39	49.19
23	.0991	.0000	999.000	71.102	.0115	16.18	49.15
24	.0993	.0000	999.000	71.100	.0115	16.03	49.11
25	.0996	.0000	999.000	71.100	.0115	15.91	49.09
26	.0997	.0000	999.000	71.098	.0115	15.81	49.07
27	.0998	.0000	999.000	71.098	.0115	15.74	49.06
28	.0999	.0000	999.000	71.096	.0115	15.68	49.05
29	.1000	.0000	999.000	71.096	.0115	15.64	49.04
30	.1001	.0000	999.000	71.095	.0115	15.61	49.03
31	.1001	.0000	999.000	71.094	.0115	15.58	49.03
32	.1001	.0000	999.000	71.093	.0115	15.56	49.02
33	.1002	.0000	999.000	71.093	.0115	15.55	49.02
34	.1002	.0000	999.000	71.091	.0115	15.54	49.02
35	.1002	.0000	999.000	71.091	.0115	15.53	49.01
36	.1002	.0000	999.000	71.089	.0115	15.52	49.01
37	.1002	.0000	999.000	71.089	.0115	15.52	49.01
38	.1002	.0000	999.000	71.087	.0115	15.51	49.01
39	.1002	.0000	999.000	71.087	.0115	15.51	49.01
40	.1002	.0000	999.000	71.086	.0115	15.51	49.01
41	.0000	.0000	.000	71.085	.0115	15.51	.00

PPHR	PO	TO	XO	TAMB	RHA	PNXT
183.70	69.20	99.29	1.00	20.80	.71	67.10

TOTT	QHP	TEPF	TEF	EZ	ET	TMELT	TMVAP
96.	13677.	.00	185.54	91.18	201.37	1.29	.00

DFEF	EFFC	P(NPL)	DP	DHTF	SCLVG	XLVG	NTDROP
.9214	.9214	68.807	.393	542.78	-24.6	.000	0

I	T	TS	TWO	TWI	TWF	X	ESUM	IHTM	PATH
									4332211
1	99.3	57.2	59.1	59.1	61.3	1.000	2.36	2	400.0
2	87.4	57.2	54.7	54.7	59.1	1.000	2.71	2	400.0
3	73.9	57.2	54.1	54.1	59.1	1.000	2.86	2	400.0
4	59.6	57.2	52.8	52.8	56.4	1.000	2.65	2	400.0
5	57.3	57.3	51.6	51.6	54.3	.971	2.49	2	400.0
6	57.3	57.3	49.7	49.7	54.1	.938	2.61	2	400.0
7	57.3	57.3	47.5	47.5	53.9	.904	2.67	2	400.0
8	57.3	57.3	44.1	44.1	53.8	.869	2.72	2	400.0
9	57.3	57.3	40.8	40.8	53.7	.833	2.81	2	400.0
10	57.3	57.3	38.6	38.6	53.3	.796	2.99	2	400.0
11	57.3	57.3	36.8	36.8	52.9	.757	3.24	2	400.0
12	57.3	57.3	35.3	35.3	52.1	.714	3.54	2	400.0
13	57.3	57.3	34.0	34.0	50.9	.667	4.06	2	400.0
14	57.2	57.2	33.0	33.0	48.3	.614	5.06	2	400.0
15	57.2	57.2	32.6	32.6	45.3	.547	6.04	2	400.0
16	57.1	57.1	32.5	32.5	43.4	.468	6.22	2	400.0
17	57.1	57.1	32.4	32.4	41.5	.386	6.19	2	400.0
18	57.1	57.1	32.3	32.3	39.6	.305	5.90	2	400.0
19	57.0	57.0	32.2	32.2	38.0	.227	5.50	2	400.0
20	57.0	57.0	32.2	32.2	36.5	.155	4.86	2	400.0
21	56.9	56.9	32.1	32.1	35.1	.091	3.96	2	400.0
22	56.9	56.9	32.1	32.1	33.9	.039	2.75	2	400.0
23	56.9	56.9	32.1	32.1	32.9	.003	1.52	2	400.0
24	52.3	56.9	32.1	32.1	32.6	.000	1.24	2	400.0
25	47.8	56.9	32.0	32.0	32.4	.000	.96	2	400.0
26	44.2	56.9	32.0	32.0	32.3	.000	.75	2	400.0
27	41.5	56.9	32.0	32.0	32.3	.000	.58	2	400.0
28	39.4	56.9	32.0	32.0	32.2	.000	.45	2	400.0
29	37.7	56.9	32.0	32.0	32.2	.000	.35	2	400.0
30	36.4	56.9	32.0	32.0	32.1	.000	.27	2	400.0
31	35.5	56.9	32.0	32.0	32.1	.000	.21	2	400.0
32	34.7	56.9	32.0	32.0	32.1	.000	.16	2	400.0
33	34.1	56.9	32.0	32.0	32.1	.000	.13	2	400.0
34	33.6	56.9	32.0	32.0	32.0	.000	.10	2	400.0
35	33.3	56.9	32.0	32.0	32.0	.000	.08	2	400.0
36	33.0	56.9	32.0	32.0	32.0	.000	.06	2	400.0
37	32.8	56.9	32.0	32.0	32.0	.000	.05	2	400.0
38	32.6	56.9	32.0	32.0	32.0	.000	.04	2	400.0
39	32.5	56.9	32.0	32.0	32.0	.000	.03	2	400.0
40	32.4	56.9	32.0	32.0	32.0	.000	.02	2	400.0
41	32.3	56.8	.0	.0	.0	.000	.00	0	.0

I	MFRST	MLIQ	DTLM	P	V	H	HR
1	.0123	.0000	999.000	69.200	.6540	90.01	54.20
2	.0221	.0000	.262	69.199	.6348	88.08	566.92
3	.0244	.0000	.525	69.248	.6119	85.87	627.15
4	.0285	.0000	999.000	69.239	.5876	83.54	697.28
5	.0317	.0000	999.000	69.316	.5664	81.37	709.57
6	.0330	.0000	999.000	69.307	.5477	79.33	682.25
7	.0335	.0000	999.000	69.364	.5277	77.21	628.35
8	.0329	.0000	999.000	69.317	.5080	75.03	597.37
9	.0329	.0000	999.000	69.364	.4871	72.80	573.93
10	.0358	.0000	999.000	69.304	.4664	70.51	552.87
11	.0397	.0000	999.000	69.343	.4437	68.06	531.68
12	.0440	.0000	999.000	69.274	.4198	65.42	510.18
13	.0489	.0000	999.000	69.297	.3930	62.53	486.81
14	.0524	.0000	999.000	69.219	.3629	59.21	460.57
15	.0519	.0000	999.000	69.225	.3248	55.08	427.22
16	.0525	.0000	999.000	69.140	.2798	50.15	386.50
17	.0539	.0000	999.000	69.119	.2331	45.07	342.25
18	.0568	.0000	999.000	69.037	.1867	40.02	295.30
19	.0602	.0000	999.000	69.000	.1423	35.20	253.83
20	.0650	.0000	999.000	68.934	.1010	30.71	209.39
21	.0715	.0000	999.000	68.898	.0643	26.74	160.30
22	.0800	.0000	999.000	68.856	.0345	23.51	105.70
23	.0887	.0000	999.000	68.835	.0137	21.26	56.09
24	.0909	.0000	999.000	68.826	.0118	20.02	55.89
25	.0929	.0000	999.000	68.825	.0117	19.00	55.69
26	.0946	.0000	999.000	68.823	.0117	18.22	55.52
27	.0959	.0000	999.000	68.823	.0116	17.61	55.39
28	.0969	.0000	999.000	68.821	.0116	17.13	55.29
29	.0976	.0000	999.000	68.821	.0116	16.77	55.21
30	.0982	.0000	999.000	68.819	.0115	16.48	55.15
31	.0987	.0000	999.000	68.819	.0115	16.26	55.10
32	.0990	.0000	999.000	68.817	.0115	16.09	55.06
33	.0993	.0000	999.000	68.816	.0115	15.96	55.03
34	.0995	.0000	999.000	68.814	.0115	15.86	55.01
35	.0997	.0000	999.000	68.814	.0115	15.78	54.99
36	.0998	.0000	999.000	68.812	.0115	15.72	54.98
37	.0999	.0000	999.000	68.812	.0115	15.67	54.96
38	.1000	.0000	999.000	68.810	.0115	15.63	54.96
39	.1000	.0000	999.000	68.810	.0115	15.60	54.95
40	.1001	.0000	999.000	68.808	.0115	15.58	54.94
41	.0000	.0000	.000	68.807	.0115	15.56	.00

PPHR	PO	TO	XO	TAMB	RHA	PNXT
117.30	67.10	115.45	1.00	21.10	.75	66.30

TOTT	QHP	TEPF	TEF	EZ	ET	TMELT	TMVAP
120.	9044.	.00	242.55	60.29	261.66	1.69	.00

DFEF	EFFC	P(NPL)	DP	DHTF	SCLVG	XLVG	NTDROP
.9270	.9270	66.857	.243	387.75	-22.5	.000	0

I	T	TS	TWO	TWI	TWF	X	ESUM	IHTM	PATH
									4332211
1	115.4	55.3	61.3	65.2	67.5	1.000	2.27	3	11400.0
2	97.5	55.3	59.1	59.1	56.3	1.000	1.72	2	500.0
3	84.0	55.3	59.1	59.1	50.9	1.000	1.26	2	500.0
4	74.0	55.3	56.4	56.4	46.7	1.000	.99	2	500.0
5	66.3	55.4	54.3	54.3	59.1	1.000	2.44	2	500.0
6	55.4	55.4	54.1	54.1	52.4	.979	1.66	2	500.0
7	55.4	55.4	53.9	53.9	52.3	.945	1.67	2	500.0
8	55.4	55.4	53.8	53.8	52.1	.910	1.63	2	500.0
9	55.4	55.4	53.7	53.7	51.9	.877	1.61	2	500.0
10	55.4	55.4	53.3	53.3	51.6	.844	1.66	2	500.0
11	55.4	55.4	52.9	52.9	51.3	.810	1.74	2	500.0
12	55.4	55.4	52.1	52.1	50.9	.774	1.85	2	500.0
13	55.4	55.4	50.9	50.9	50.5	.736	1.99	2	500.0
14	55.3	55.3	48.3	48.3	50.0	.695	2.14	2	500.0
15	55.3	55.3	45.3	45.3	49.9	.651	2.20	2	500.0
16	55.3	55.3	43.4	43.4	49.6	.606	2.24	2	500.0
17	55.3	55.3	41.5	41.5	49.3	.560	2.30	2	500.0
18	55.3	55.3	39.6	39.6	48.7	.513	2.39	2	500.0
19	55.3	55.3	38.0	38.0	48.0	.464	2.47	2	500.0
20	55.2	55.2	36.5	36.5	47.0	.413	2.58	2	500.0
21	55.2	55.2	35.1	35.1	45.6	.360	2.74	2	500.0
22	55.2	55.2	33.9	33.9	43.2	.304	2.96	2	500.0
23	55.2	55.2	32.9	32.9	40.0	.243	3.22	2	500.0
24	55.2	55.2	32.6	32.6	38.4	.177	2.99	2	500.0
25	55.1	55.1	32.4	32.4	36.8	.116	2.63	2	500.0
26	55.1	55.1	32.3	32.3	35.2	.062	2.07	2	500.0
27	55.1	55.1	32.3	32.3	33.6	.019	1.26	2	500.0
28	53.3	55.1	32.2	32.2	33.0	.000	.90	2	500.0
29	48.2	55.1	32.2	32.2	32.6	.000	.68	2	500.0
30	44.3	55.1	32.1	32.1	32.4	.000	.52	2	500.0
31	41.3	55.1	32.1	32.1	32.3	.000	.39	2	500.0
32	39.0	55.1	32.1	32.1	32.2	.000	.30	2	500.0
33	37.3	55.1	32.1	32.1	32.1	.000	.23	2	500.0
34	36.0	55.1	32.0	32.0	32.1	.000	.17	2	500.0
35	35.0	55.1	32.0	32.0	32.1	.000	.13	2	500.0
36	34.3	55.1	32.0	32.0	32.0	.000	.10	2	500.0
37	33.7	55.1	32.0	32.0	32.0	.000	.07	2	500.0
38	33.3	55.1	32.0	32.0	32.0	.000	.06	2	500.0
39	33.0	55.1	32.0	32.0	32.0	.000	.04	2	500.0
40	32.7	55.1	32.0	32.0	32.0	.000	.03	2	500.0
41	32.6	55.1	.0	.0	.0	.000	.00	0	.0

I	MFRST	MLIQ	DTLM	P	V	H	HR
1	.0000	.0249	999.000	67.100	.7027	92.72	39.30
2	.0093	.0000	999.000	67.099	.6737	89.82	37.70
3	.0132	.0000	999.000	67.115	.6510	87.62	36.50
4	.0188	.0000	999.000	67.111	.6341	86.01	35.69
5	.0161	.0000	1.730	67.137	.6205	84.75	472.47
6	.0209	.0000	999.000	67.134	.5886	81.63	513.02
7	.0214	.0000	999.000	67.168	.5682	79.52	501.98
8	.0211	.0000	999.000	67.151	.5482	77.38	455.58
9	.0211	.0000	999.000	67.172	.5282	75.29	427.54
10	.0237	.0000	999.000	67.148	.5089	73.23	406.80
11	.0271	.0000	999.000	67.165	.4887	71.11	390.68
12	.0308	.0000	999.000	67.137	.4678	68.88	376.89
13	.0349	.0000	999.000	67.150	.4454	66.52	362.91
14	.0379	.0000	999.000	67.118	.4215	63.97	348.47
15	.0379	.0000	999.000	67.124	.3955	61.23	333.07
16	.0387	.0000	999.000	67.089	.3691	58.42	317.43
17	.0402	.0000	999.000	67.089	.3420	55.55	301.30
18	.0428	.0000	999.000	67.053	.3143	52.61	284.57
19	.0459	.0000	999.000	67.046	.2854	49.56	266.75
20	.0501	.0000	999.000	67.011	.2556	46.40	247.80
21	.0555	.0000	999.000	66.999	.2244	43.10	227.17
22	.0621	.0000	999.000	66.966	.1913	39.59	204.27
23	.0684	.0000	999.000	66.950	.1555	35.81	181.64
24	.0717	.0000	999.000	66.922	.1165	31.70	154.82
25	.0759	.0000	999.000	66.905	.0803	27.87	124.84
26	.0810	.0000	999.000	66.885	.0484	24.51	91.19
27	.0875	.0000	999.000	66.874	.0233	21.86	51.80
28	.0908	.0000	999.000	66.865	.0118	20.25	39.07
29	.0930	.0000	999.000	66.864	.0117	19.10	38.91
30	.0947	.0000	999.000	66.863	.0117	18.23	38.78
31	.0960	.0000	999.000	66.862	.0116	17.56	38.68
32	.0970	.0000	999.000	66.862	.0116	17.06	38.61
33	.0977	.0000	999.000	66.861	.0115	16.68	38.55
34	.0983	.0000	999.000	66.860	.0115	16.39	38.50
35	.0988	.0000	999.000	66.860	.0115	16.17	38.47
36	.0991	.0000	999.000	66.859	.0115	16.00	38.44
37	.0994	.0000	999.000	66.859	.0115	15.88	38.42
38	.0996	.0000	999.000	66.858	.0115	15.79	38.41
39	.0998	.0000	999.000	66.858	.0115	15.72	38.40
40	.0999	.0000	999.000	66.857	.0115	15.66	38.39
41	.0000	.0000	.000	66.857	.0115	15.62	.00

PPHR	PO	TO	XO	TAMB	RHA	PNXT
137.30	66.30	123.69	1.00	21.40	.80	66.30

TOTT	QHP	TEPF	TEF	EZ	ET	TMELT	TMVAP
144.	10719.	.00	306.77	71.46	333.12	2.14	.00

DFEF	EFFC	P(NPL)	DP	DHTF	SCLVG	XLVG	NTDROP
.9209	.9209	65.988	.312	474.33	-20.0	.000	0

I	T	TS	TWO	TWI	TWF	X	ESUM	IHTM	PATH
									4332211
1	123.7	54.6	67.5	67.5	83.4	1.000	2.41	3	21400.0
2	107.4	54.6	56.3	63.8	67.6	1.000	2.22	3	11500.0
3	92.4	54.6	50.9	50.9	59.1	1.000	2.13	2	600.0
4	78.0	54.6	46.7	46.7	59.1	1.000	2.41	2	600.0
5	61.8	54.6	59.1	59.1	44.8	1.000	.57	2	600.0
6	58.0	54.6	52.4	52.4	55.4	1.000	1.80	2	600.0
7	54.7	54.7	52.3	52.3	52.4	.977	1.48	2	600.0
8	54.7	54.7	52.1	52.1	52.4	.951	1.49	2	600.0
9	54.7	54.7	51.9	51.9	52.3	.925	1.48	2	600.0
10	54.7	54.7	51.6	51.6	52.1	.899	1.52	2	600.0
11	54.7	54.7	51.3	51.3	51.9	.873	1.57	2	600.0
12	54.7	54.7	50.9	50.9	51.6	.845	1.63	2	600.0
13	54.7	54.7	50.5	50.5	51.4	.816	1.71	2	600.0
14	54.7	54.7	50.0	50.0	51.2	.786	1.78	2	600.0
15	54.7	54.7	49.9	49.9	51.1	.755	1.77	2	600.0
16	54.7	54.7	49.6	49.6	50.9	.724	1.78	2	600.0
17	54.7	54.7	49.3	49.3	50.8	.693	1.81	2	600.0
18	54.6	54.6	48.7	48.7	50.5	.661	1.87	2	600.0
19	54.6	54.6	48.0	48.0	50.2	.629	1.94	2	600.0
20	54.6	54.6	47.0	47.0	49.7	.595	2.06	2	600.0
21	54.6	54.6	45.6	45.6	49.2	.559	2.23	2	600.0
22	54.6	54.6	43.2	43.2	48.3	.520	2.48	2	600.0
23	54.6	54.6	40.0	40.0	47.3	.476	2.76	2	600.0
24	54.5	54.5	38.4	38.4	46.4	.428	2.87	2	600.0
25	54.5	54.5	36.8	36.8	45.3	.378	3.01	2	600.0
26	54.5	54.5	35.2	35.2	43.6	.325	3.17	2	600.0
27	54.4	54.4	33.6	33.6	41.1	.270	3.42	2	600.0
28	54.4	54.4	33.0	33.0	39.3	.210	3.38	2	600.0
29	54.4	54.4	32.6	32.6	37.6	.151	3.14	2	600.0
30	54.4	54.4	32.4	32.4	36.1	.096	2.71	2	600.0
31	54.3	54.3	32.3	32.3	34.6	.048	2.07	2	600.0
32	54.3	54.3	32.2	32.2	33.2	.012	1.14	2	600.0
33	52.2	54.3	32.1	32.1	32.9	.000	.97	2	600.0
34	47.5	54.3	32.1	32.1	32.6	.000	.74	2	600.0
35	43.9	54.3	32.1	32.1	32.4	.000	.57	2	600.0
36	41.1	54.3	32.0	32.0	32.2	.000	.44	2	600.0
37	38.9	54.3	32.0	32.0	32.2	.000	.33	2	600.0
38	37.3	54.3	32.0	32.0	32.1	.000	.25	2	600.0
39	36.0	54.3	32.0	32.0	32.1	.000	.19	2	600.0
40	35.1	54.3	32.0	32.0	32.1	.000	.15	2	600.0
41	34.3	54.3	.0	.0	.0	.000	.00	0	.0

I	MFRST	MLIQ	DTLM	P	V	H	HR
1	.0000	.0241	999.000	66.300	.7252	94.08	45.42
2	.0000	.0248	999.000	66.299	.6989	91.45	43.76
3	.0007	.0000	.492	66.317	.6739	89.02	437.48
4	.0056	.0000	1.050	66.312	.6496	86.70	487.20
5	.0079	.0000	999.000	66.343	.6210	84.06	39.50
6	.0093	.0000	999.000	66.337	.6142	83.44	565.75
7	.0111	.0000	999.000	66.384	.5941	81.47	580.21
8	.0108	.0000	999.000	66.380	.5787	79.85	580.23
9	.0109	.0000	999.000	66.431	.5627	78.23	535.14
10	.0133	.0000	999.000	66.407	.5474	76.61	505.32
11	.0163	.0000	999.000	66.436	.5314	74.95	482.42
12	.0196	.0000	999.000	66.405	.5152	73.24	464.50
13	.0232	.0000	999.000	66.430	.4980	71.46	450.45
14	.0259	.0000	999.000	66.394	.4804	69.58	436.99
15	.0259	.0000	999.000	66.415	.4617	67.64	423.59
16	.0266	.0000	999.000	66.373	.4435	65.71	410.89
17	.0280	.0000	999.000	66.387	.4248	63.76	398.21
18	.0303	.0000	999.000	66.343	.4062	61.78	385.64
19	.0329	.0000	999.000	66.351	.3866	59.74	372.57
20	.0365	.0000	999.000	66.305	.3666	57.62	359.10
21	.0410	.0000	999.000	66.307	.3451	55.37	344.61
22	.0463	.0000	999.000	66.260	.3221	52.94	328.84
23	.0512	.0000	999.000	66.254	.2962	50.23	310.85
24	.0540	.0000	999.000	66.207	.2676	47.21	290.39
25	.0574	.0000	999.000	66.194	.2376	44.08	268.28
26	.0613	.0000	999.000	66.148	.2063	40.79	244.14
27	.0659	.0000	999.000	66.129	.1731	37.32	219.01
28	.0691	.0000	999.000	66.089	.1374	33.59	193.11
29	.0726	.0000	999.000	66.068	.1020	29.89	163.29
30	.0769	.0000	999.000	66.037	.0692	26.46	129.90
31	.0822	.0000	999.000	66.020	.0408	23.51	92.48
32	.0893	.0000	999.000	66.003	.0192	21.25	47.76
33	.0912	.0000	999.000	65.995	.0118	20.00	44.27
34	.0933	.0000	999.000	65.993	.0117	18.94	44.11
35	.0949	.0000	999.000	65.993	.0116	18.13	43.97
36	.0961	.0000	999.000	65.991	.0116	17.51	43.87
37	.0971	.0000	999.000	65.991	.0116	17.03	43.78
38	.0978	.0000	999.000	65.990	.0115	16.67	43.72
39	.0984	.0000	999.000	65.990	.0115	16.39	43.67
40	.0989	.0000	999.000	65.988	.0115	16.18	43.63
41	.0000	.0000	.000	65.988	.0115	16.02	.00

PPHR	PO	TO	XO	TAMB	RHA	PNXT
152.60	66.30	129.62	1.00	21.70	.84	67.70

TOTT	QHP	TEPF	TEF	EZ	ET	TMELT	TMVAP
168.	11853.	.00	373.51	79.02	412.14	2.61	.00

DFEF	EFFC	P(NPL)	DP	DHTF	SCLVG	XLVG	NTDROP
.9063	.9063	65.927	.373	524.52	-13.8	.000	1

I	T	TS	TWO	TWI	TWF	X	ESUM	IHTM	PATH
									4332211
1	129.6	54.6	83.4	83.4	89.0	1.000	2.43	3	31400.0
2	114.9	54.6	67.6	67.6	80.4	1.000	2.18	3	21500.0
3	101.6	54.6	59.1	60.1	71.6	1.000	1.88	3	11600.0
4	90.2	54.6	59.1	58.8	63.0	1.000	1.56	3	11600.0
5	80.8	54.6	44.8	59.1	59.8	1.000	2.08	3	11600.0
6	68.1	54.6	55.4	55.4	48.3	1.000	.87	2	700.0
7	62.9	54.7	52.4	59.1	58.2	1.000	1.89	3	11600.0
8	54.7	54.7	52.4	52.4	52.8	.992	1.35	2	700.0
9	54.7	54.7	52.3	52.3	52.8	.970	1.36	2	700.0
10	54.7	54.7	52.1	52.1	52.8	.949	1.40	2	700.0
11	54.8	54.8	51.9	51.9	52.6	.927	1.44	2	700.0
12	54.7	54.7	51.6	51.6	52.4	.904	1.48	2	700.0
13	54.8	54.8	51.4	51.4	52.3	.881	1.54	2	700.0
14	54.7	54.7	51.2	51.2	52.1	.857	1.57	2	700.0
15	54.8	54.8	51.1	51.1	52.0	.832	1.57	2	700.0
16	54.7	54.7	50.9	50.9	51.9	.807	1.58	2	700.0
17	54.8	54.8	50.8	50.8	51.8	.782	1.60	2	700.0
18	54.7	54.7	50.5	50.5	51.7	.757	1.64	2	700.0
19	54.7	54.7	50.2	50.2	51.5	.731	1.69	2	700.0
20	54.7	54.7	49.7	49.7	51.3	.704	1.76	2	700.0
21	54.7	54.7	49.2	49.2	51.0	.676	1.87	2	700.0
22	54.7	54.7	48.3	48.3	50.5	.647	2.00	2	700.0
23	54.7	54.7	47.3	47.3	50.1	.616	2.15	2	700.0
24	54.6	54.6	46.4	46.4	49.8	.582	2.23	2	700.0
25	54.6	54.6	45.3	45.3	49.3	.547	2.35	2	700.0
26	54.6	54.6	43.6	43.6	48.7	.510	2.50	2	700.0
27	54.6	54.6	41.1	41.1	48.0	.470	2.70	2	700.0
28	54.5	54.5	39.3	39.3	47.2	.428	2.83	2	700.0
29	54.5	54.5	37.6	37.6	46.4	.383	2.95	2	700.0
30	54.4	54.4	36.1	36.1	45.1	.337	3.09	2	700.0
31	54.4	54.4	34.6	34.6	43.4	.288	3.28	2	700.0
32	54.4	54.4	33.2	33.2	40.6	.237	3.61	2	700.0
33	54.4	54.4	32.9	32.9	39.2	.180	3.43	2	700.0
34	54.3	54.3	32.6	32.6	37.5	.126	3.15	2	700.0
35	54.3	54.3	32.4	32.4	35.9	.077	2.66	2	700.0
36	54.3	54.3	32.2	32.2	34.4	.035	1.94	2	700.0
37	54.3	54.3	32.2	32.2	33.2	.004	1.15	2	700.0
38	50.4	54.3	32.1	32.1	32.8	.000	.96	2	700.0
39	46.2	54.3	32.1	32.1	32.6	.000	.74	2	700.0
40	43.0	54.3	32.1	32.1	32.4	.000	.57	2	700.0
41	40.4	54.3	.0	.0	.0	.000	.00	0	.0

I	MFRST	MLIQ	DTLM	P	V	H	HR
1	.0000	.0227	999.000	66.300	.7346	95.04	50.07
2	.0000	.0240	999.000	66.299	.7110	92.66	48.45
3	.0000	.0244	999.000	66.319	.6892	90.52	46.98
4	.0000	.0247	999.000	66.313	.6703	88.67	45.72
5	.0000	.0248	999.000	66.346	.6539	87.14	44.72
6	.0011	.0000	999.000	66.341	.6322	85.09	43.51
7	.0000	.0250	999.000	66.387	.6224	84.24	43.07
8	.0014	.0000	999.000	66.384	.6028	82.38	628.41
9	.0015	.0000	999.000	66.444	.5896	81.05	628.15
10	.0037	.0000	999.000	66.440	.5768	79.71	625.48
11	.0065	.0000	999.000	66.483	.5632	78.34	582.83
12	.0095	.0000	999.000	66.454	.5500	76.92	553.82
13	.0127	.0000	999.000	66.492	.5358	75.47	530.83
14	.0152	.0000	999.000	66.456	.5217	73.96	513.51
15	.0152	.0000	999.000	66.489	.5066	72.41	499.56
16	.0159	.0000	999.000	66.447	.4922	70.86	487.00
17	.0171	.0000	999.000	66.477	.4771	69.31	474.80
18	.0192	.0000	999.000	66.430	.4624	67.74	463.20
19	.0215	.0000	999.000	66.453	.4469	66.12	451.42
20	.0247	.0000	999.000	66.402	.4314	64.46	439.76
21	.0285	.0000	999.000	66.419	.4147	62.73	427.54
22	.0330	.0000	999.000	66.365	.3975	60.90	414.92
23	.0371	.0000	999.000	66.375	.3787	58.93	401.18
24	.0394	.0000	999.000	66.319	.3588	56.82	386.56
25	.0422	.0000	999.000	66.321	.3378	54.62	371.06
26	.0454	.0000	999.000	66.264	.3161	52.31	354.71
27	.0490	.0000	999.000	66.257	.2926	49.86	336.84
28	.0517	.0000	999.000	66.201	.2675	47.20	317.17
29	.0545	.0000	999.000	66.186	.2409	44.43	295.82
30	.0579	.0000	999.000	66.132	.2134	41.53	272.81
31	.0619	.0000	999.000	66.111	.1843	38.48	247.45
32	.0663	.0000	999.000	66.062	.1536	35.26	224.24
33	.0691	.0000	999.000	66.037	.1196	31.72	195.25
34	.0728	.0000	999.000	65.997	.0873	28.34	163.02
35	.0774	.0000	999.000	65.974	.0577	25.25	126.82
36	.0833	.0000	999.000	65.948	.0326	22.63	85.83
37	.0894	.0000	999.000	65.935	.0144	20.73	48.26
38	.0914	.0000	999.000	65.929	.0118	19.60	48.11
39	.0934	.0000	999.000	65.928	.0117	18.66	47.95
40	.0949	.0000	999.000	65.927	.0116	17.93	47.81
41	.0000	.0000	.000	65.927	.0116	17.37	.00

PPHR	PO	TO	XO	TAMB	RHA	PNXT
167.30	67.70	134.30	1.00	22.10	.88	73.90

TOTT	QHP	TEPF	TEF	EZ	ET	TMELT	TMVAP
192.	12442.	.00	436.86	82.95	495.09	3.05	.01

DFEF	EFFC	P(NPL)	DP	DHTF	SCLVG	XLVG	NTDROP
.8824	.8824	67.334	.366	521.39	.0	.010	3

I	T	TS	TWO	TWI	TWF	X	ESUM	IHTM	PATH
									4332211
1	134.3	55.9	89.0	89.0	93.5	1.000	2.62	3	41400.0
2	119.8	55.9	80.4	80.4	85.2	1.000	2.18	3	31500.0
3	107.8	55.9	71.6	71.6	78.1	1.000	1.88	3	21600.0
4	97.4	55.9	63.0	63.0	71.4	1.000	1.67	3	21600.0
5	88.2	55.9	59.8	59.8	65.8	1.000	1.38	3	21600.0
6	80.6	55.9	48.3	61.2	61.7	1.000	1.64	3	11700.0
7	71.6	55.9	58.2	58.2	56.4	1.000	.77	3	21600.0
8	67.4	55.9	52.8	61.2	55.2	1.000	1.00	3	11700.0
9	61.9	56.0	52.8	59.2	52.2	1.000	.78	3	11700.0
10	57.6	56.0	52.8	55.7	56.5	1.000	1.21	3	11700.0
11	56.1	56.1	52.6	54.2	55.0	.987	1.29	3	11700.0
12	56.1	56.1	52.4	54.2	54.4	.968	1.48	3	11700.0
13	56.1	56.1	52.3	52.3	54.2	.947	1.53	2	800.0
14	56.1	56.1	52.1	52.1	54.0	.925	1.55	2	800.0
15	56.1	56.1	52.0	52.0	53.9	.902	1.55	2	800.0
16	56.1	56.1	51.9	51.9	53.8	.880	1.55	2	800.0
17	56.1	56.1	51.8	51.8	53.7	.857	1.57	2	800.0
18	56.1	56.1	51.7	51.7	53.6	.835	1.60	2	800.0
19	56.1	56.1	51.5	51.5	53.5	.812	1.64	2	800.0
20	56.1	56.1	51.3	51.3	53.3	.788	1.69	2	800.0
21	56.1	56.1	51.0	51.0	53.1	.764	1.76	2	800.0
22	56.1	56.1	50.5	50.5	52.9	.739	1.85	2	800.0
23	56.1	56.1	50.1	50.1	52.6	.712	1.94	2	800.0
24	56.0	56.0	49.8	49.8	52.4	.684	1.99	2	800.0
25	56.0	56.0	49.3	49.3	52.2	.655	2.05	2	800.0
26	56.0	56.0	48.7	48.7	51.9	.626	2.14	2	800.0
27	56.0	56.0	48.0	48.0	51.5	.595	2.24	2	800.0
28	55.9	55.9	47.2	47.2	51.2	.563	2.32	2	800.0
29	55.9	55.9	46.4	46.4	50.8	.529	2.41	2	800.0
30	55.9	55.9	45.1	45.1	50.3	.495	2.53	2	800.0
31	55.9	55.9	43.4	43.4	49.6	.458	2.69	2	800.0
32	55.8	55.8	40.6	40.6	48.8	.420	2.90	2	800.0
33	55.8	55.8	39.2	39.2	48.1	.378	3.00	2	800.0
34	55.7	55.7	37.5	37.5	47.0	.335	3.12	2	800.0
35	55.7	55.7	35.9	35.9	45.6	.290	3.27	2	800.0
36	55.7	55.7	34.4	34.4	43.6	.243	3.51	2	800.0
37	55.6	55.6	33.2	33.2	40.9	.192	3.74	2	800.0
38	55.6	55.6	32.8	32.8	39.2	.139	3.49	2	800.0
39	55.6	55.6	32.6	32.6	37.3	.088	3.07	2	800.0
40	55.5	55.5	32.4	32.4	35.5	.044	2.38	2	800.0
41	55.5	55.5	.0	.0	.0	.010	.00	0	.0

I	MFRLT	MLIQ	DTLM	P	V	H	HR
1	.0000	.0211	999.000	67.700	.7255	95.75	54.40
2	.0000	.0228	999.000	67.699	.7029	93.40	52.74
3	.0000	.0235	999.000	67.721	.6834	91.45	51.30
4	.0000	.0241	999.000	67.715	.6667	89.77	50.06
5	.0000	.0242	999.000	67.750	.6512	88.27	48.97
6	.0000	.0244	999.000	67.744	.6385	87.04	48.11
7	.0000	.0244	999.000	67.792	.6228	85.57	47.17
8	.0000	.0245	999.000	67.786	.6156	84.88	46.76
9	.0000	.0245	999.000	67.847	.6054	83.99	46.27
10	.0000	.0247	999.000	67.843	.5979	83.29	659.18
11	.0000	.0249	999.000	67.914	.5866	82.20	666.90
12	.0000	.0250	999.000	67.910	.5758	81.04	666.92
13	.0026	.0000	999.000	67.985	.5628	79.72	658.11
14	.0049	.0000	999.000	67.955	.5502	78.34	616.37
15	.0049	.0000	999.000	68.003	.5367	76.95	586.80
16	.0056	.0000	999.000	67.964	.5240	75.56	564.47
17	.0067	.0000	999.000	68.007	.5106	74.17	549.60
18	.0086	.0000	999.000	67.961	.4978	72.76	536.32
19	.0107	.0000	999.000	67.999	.4841	71.33	523.46
20	.0135	.0000	999.000	67.948	.4708	69.86	511.36
21	.0169	.0000	999.000	67.981	.4564	68.35	499.09
22	.0208	.0000	999.000	67.925	.4420	66.78	487.01
23	.0243	.0000	999.000	67.950	.4263	65.12	474.29
24	.0264	.0000	999.000	67.889	.4105	63.38	461.43
25	.0287	.0000	999.000	67.906	.3937	61.60	448.07
26	.0314	.0000	999.000	67.842	.3768	59.76	434.55
27	.0344	.0000	999.000	67.852	.3588	57.85	420.20
28	.0367	.0000	999.000	67.786	.3403	55.84	405.27
29	.0390	.0000	999.000	67.787	.3208	53.76	389.44
30	.0418	.0000	999.000	67.720	.3009	51.59	372.93
31	.0450	.0000	999.000	67.712	.2796	49.32	355.09
32	.0485	.0000	999.000	67.646	.2572	46.91	335.81
33	.0508	.0000	999.000	67.630	.2328	44.30	314.27
34	.0538	.0000	999.000	67.567	.2078	41.62	291.35
35	.0574	.0000	999.000	67.543	.1816	38.82	266.43
36	.0615	.0000	999.000	67.486	.1542	35.89	243.92
37	.0656	.0000	999.000	67.458	.1246	32.74	216.88
38	.0689	.0000	999.000	67.411	.0932	29.39	183.79
39	.0734	.0000	999.000	67.384	.0637	26.26	146.54
40	.0793	.0000	999.000	67.351	.0379	23.51	104.00
41	.0000	.0000	.000	67.334	.0178	21.38	.00

PPHR	PO	TO	XO	TAMB	RHA	PNXT
173.60	73.90	137.68	1.00	22.50	.90	78.00

TOTT	QHP	TEPF	TEF	EZ	ET	TMELT	TMVAP
216.	12425.	.00	490.29	82.83	577.92	3.42	.02

DFEF	EFFC	P(NPL)	DP	DHTF	SCLVG	XLVG	NTDROP
.8484	.8484	73.468	.432	424.89	.0	.041	0

I	T	TS	TWO	TWI	TWF	X	ESUM	IHTM	PATH
									4332211
1	137.7	61.2	93.5	93.5	96.2	1.000	2.71	3	51400.0
2	123.4	61.2	85.2	85.2	88.0	1.000	2.26	3	41500.0
3	111.4	61.3	78.1	78.1	81.0	1.000	1.90	3	31600.0
4	101.4	61.3	71.4	71.4	75.0	1.000	1.64	3	31600.0
5	92.8	61.3	65.8	65.8	69.6	1.000	1.42	3	31600.0
6	85.3	61.3	61.7	61.7	64.9	1.000	1.23	3	21700.0
7	78.8	61.3	56.4	56.4	64.6	1.000	1.43	3	31600.0
8	71.3	61.3	55.2	55.2	64.6	1.000	1.49	3	21700.0
9	63.6	61.4	52.2	52.2	62.5	1.000	1.46	3	21700.0
10	61.4	61.4	56.5	56.5	60.2	.986	1.10	3	21700.0
11	61.4	61.4	55.0	55.0	60.3	.970	1.17	3	21700.0
12	61.4	61.4	54.4	54.4	60.3	.954	1.20	3	21700.0
13	61.5	61.5	54.2	59.2	60.2	.936	1.35	3	11800.0
14	61.5	61.5	54.0	59.0	60.1	.918	1.50	3	11800.0
15	61.5	61.5	53.9	59.0	60.1	.896	1.50	3	11800.0
16	61.5	61.5	53.8	58.9	60.0	.875	1.55	3	11800.0
17	61.5	61.5	53.7	58.8	60.0	.853	1.62	3	11800.0
18	61.5	61.5	53.6	58.7	59.8	.831	1.75	3	11800.0
19	61.5	61.5	53.5	58.6	59.3	.806	1.88	3	11800.0
20	61.4	61.4	53.3	53.3	58.4	.780	1.94	2	900.0
21	61.5	61.5	53.1	53.1	58.2	.752	1.99	2	900.0
22	61.4	61.4	52.9	52.9	58.0	.724	2.06	2	900.0
23	61.4	61.4	52.6	52.6	57.7	.695	2.12	2	900.0
24	61.4	61.4	52.4	52.4	57.5	.666	2.16	2	900.0
25	61.4	61.4	52.2	52.2	57.3	.635	2.20	2	900.0
26	61.3	61.3	51.9	51.9	57.0	.604	2.25	2	900.0
27	61.3	61.3	51.5	51.5	56.7	.573	2.31	2	900.0
28	61.3	61.3	51.2	51.2	56.4	.540	2.35	2	900.0
29	61.3	61.3	50.8	50.8	56.1	.507	2.40	2	900.0
30	61.2	61.2	50.3	50.3	55.7	.474	2.46	2	900.0
31	61.2	61.2	49.6	49.6	55.2	.439	2.54	2	900.0
32	61.2	61.2	48.8	48.8	54.6	.404	2.62	2	900.0
33	61.1	61 1	48.1	48.1	54.0	.367	2.67	2	900.0
34	61.1	61.1	47.0	47.0	53.3	.330	2.73	2	900.0
35	61.1	61.1	45.6	45.6	52.4	.291	2.82	2	900.0
36	61.0	61.0	43.6	43.6	51.4	.252	2.94	2	900.0
37	61.0	61.0	40.9	40.9	50.1	.211	3.05	2	900.0
38	61.0	61.0	39.2	39.2	48.7	.168	3.06	2	900.0
39	60.9	60.9	37.3	37.3	46.6	.125	3.04	2	900.0
40	60.9	60.9	35.5	35.5	43.6	.082	2.93	2	900.0
41	60.9	60.9	.0	.0	.0	.041	.00	0	.0

I	MFRST	MLIQ	DTLM	P	V	H	HR
1	.0000	.0193	999.000	73.900	.6647	96.08	56.39
2	.0000	.0213	999.000	73.893	.6440	93.74	54.75
3	.0000	.0224	999.000	73.916	.6262	91.79	53.29
4	.0000	.0232	999.000	73.910	.6111	90.14	52.06
5	.0000	.0235	999.000	73.946	.5976	88.73	51.00
6	.0000	.0238	999.000	73.940	.5860	87.50	50.10
7	.0000	.0239	1.201	73.988	.5754	86.44	578.89
8	.0000	.0240	2.309	73.984	.5634	85.20	612.08
9	.0000	.0241	999.000	74.043	.5503	83.91	648.25
10	.0000	.0242	999.000	74.038	.5389	82.65	659.24
11	.0000	.0244	999.000	74.110	.5301	81.70	658.94
12	.0000	.0245	999.000	74.107	.5213	80.69	658.95
13	.0000	.0246	999.000	74.182	.5117	79.65	629.53
14	.0000	.0247	999.000	74.151	.5018	78.48	600.11
15	.0000	.0247	999.000	74.197	.4902	77.18	575.34
16	.0000	.0247	999.000	74.157	.4792	75.88	558.29
17	.0000	.0248	999.000	74.197	.4673	74.55	544.42
18	.0000	.0249	999.000	74.151	.4554	73.14	531.56
19	.0000	.0250	999.000	74.187	.4420	71.63	518.33
20	.0015	.0000	999.000	74.134	.4282	70.01	505.25
21	.0045	.0000	999.000	74.164	.4135	68.33	491.97
22	.0080	.0000	999.000	74.105	.3989	66.61	478.98
23	.0110	.0000	999.000	74.126	.3833	64.83	465.53
24	.0128	.0000	999.000	74.063	.3677	62.99	452.05
25	.0148	.0000	999.000	74.075	.3514	61.13	438.17
26	.0172	.0000	999.000	74.009	.3353	59.23	424.21
27	.0198	.0000	999.000	74.014	.3183	57.28	409.62
28	.0218	.0000	999.000	73.947	.3013	55.28	394.66
29	.0238	.0000	999.000	73.942	.2836	53.25	379.03
30	.0262	.0000	999.000	73.875	.2658	51.17	362.97
31	.0289	.0000	999.000	73.862	.2473	49.05	346.01
32	.0319	.0000	999.000	73.797	.2285	46.86	328.25
33	.0340	.0000	999.000	73.778	.2088	44.59	309.20
34	.0366	.0000	999.000	73.715	.1889	42.29	289.27
35	.0397	.0000	999.000	73.690	.1684	39.93	269.04
36	.0433	.0000	999.000	73.633	.1473	37.49	250.35
37	.0470	.0000	999.000	73.605	.1252	34.95	228.98
38	.0504	.0000	999.000	73.555	.1023	32.31	204.34
39	.0549	.0000	999.000	73.528	.0792	29.67	176.14
40	.0613	.0000	999.000	73.490	.0563	27.04	142.97
41	.0000	.0000	.000	73.468	.0342	24.51	.00

PPHR	PO	TO	XO	TAMB	RHA	PNXT
175.40	78.00	140.05	1.00	22.80	.93	88.30

TOTT	QHP	TEPF	TEF	EZ	ET	TMELT	TMVAP
240.	11359.	.00	531.88	75.73	653.64	3.71	.04

DFEF	EFFC	P(NPL)	DP	DHTF	SCLVG	XLVG	NTDROP
.8137	.8137	77.615	.385	348.26	.0	.144	0

I	T	TS	TWO	TWI	TWF	X	ESUM	IHTM	PATH
									4332211
1	140.1	64.6	96.2	96.2	98.1	1.000	2.75	3	61400.0
2	125.7	64.6	88.0	88.0	89.8	1.000	2.30	3	51500.0
3	113.8	64.6	81.0	81.0	82.8	1.000	1.93	3	41600.0
4	103.8	64.6	75.0	75.0	76.8	1.000	1.65	3	41600.0
5	95.2	64.7	69.6	69.6	71.6	1.000	1.43	3	41600.0
6	87.8	64.6	64.9	64.9	66.9	1.000	1.25	3	31700.0
7	81.4	64.7	64.6	64.6	72.5	1.000	1.68	3	41600.0
8	72.8	64.7	64.6	64.6	71.1	1.000	1.57	3	31700.0
9	64.8	64.7	62.5	62.5	63.4	1.000	1.08	3	31700.0
10	64.7	64.7	60.2	60.2	63.4	.985	1.17	3	31700.0
11	64.8	64.8	60.3	60.3	63.5	.968	1.17	3	31700.0
12	64.8	64.8	60.3	60.3	63.5	.952	1.18	3	31700.0
13	64.8	64.8	60.2	60.2	63.5	.935	1.18	3	21800.0
14	64.8	64.8	60.1	60.1	63.4	.919	1.18	3	21800.0
15	64.8	64.8	60.1	60.1	63.4	.902	1.18	3	21800.0
16	64.8	64.8	60.0	60.0	63.3	.886	1.18	3	21800.0
17	64.9	64.9	60.0	60.0	63.3	.869	1.18	3	21800.0
18	64.8	64.8	59.8	59.8	63.2	.853	1.18	3	21800.0
19	64.8	64.8	59.3	59.3	63.3	.836	1.21	3	21800.0
20	64.8	64.8	58.4	61.3	63.1	.819	1.32	3	11900.0
21	64.8	64.8	58.2	61.7	63.1	.801	1.52	3	11900.0
22	64.8	64.8	58.0	61.5	62.9	.779	1.76	3	11900.0
23	64.8	64.8	57.7	61.4	62.6	.755	1.97	3	11900.0
24	64.8	64.8	57.5	61.2	61.6	.727	2.05	3	11900.0
25	64.8	64.8	57.3	57.3	61.0	.698	2.09	2	1000.0
26	64.7	64.7	57.0	57.0	60.8	.669	2.13	2	1000.0
27	64.7	64.7	56.7	56.7	60.6	.639	2.18	2	1000.0
28	64.7	64.7	56.4	56.4	60.3	.609	2.21	2	1000.0
29	64.7	64.7	56.1	56.1	60.1	.578	2.25	2	1000.0
30	64.6	64.6	55.7	55.7	59.8	.547	2.29	2	1000.0
31	64.6	64.6	55.2	55.2	59.5	.514	2.35	2	1000.0
32	64.6	64.6	54.6	54.6	59.1	.482	2.41	2	1000.0
33	64.6	64.6	54.0	54.0	58.7	.448	2.45	2	1000.0
34	64.5	64.5	53.3	53.3	58.3	.414	2.50	2	1000.0
35	64.5	64.5	52.4	52.4	57.7	.379	2.57	2	1000.0
36	64.5	64.5	51.4	51.4	57.0	.343	2.65	2	1000.0
37	64.4	64.4	50.1	50.1	56.2	.306	2.73	2	1000.0
38	64.4	64.4	48.7	48.7	55.4	.268	2.81	2	1000.0
39	64.4	64.4	46.6	46.6	54.3	.229	2.93	2	1000.0
40	64.3	64.3	43.6	43.6	52.5	.188	3.10	2	1000.0
41	64.3	64.3	.0	.0	.0	.144	.00	0	.0

I	MFRST	MLIQ	DTLM	P	V	H	HR
1	.0000	.0174	999.000	78.000	.6301	96.32	57.09
2	.0000	.0198	999.000	77.992	.6103	93.97	55.50
3	.0000	.0212	999.000	78.015	.5932	92.00	54.02
4	.0000	.0222	999.000	78.009	.5788	90.35	52.78
5	.0000	.0227	999.000	78.044	.5660	88.94	51.72
6	.0000	.0231	999.000	78.039	.5551	87.72	50.82
7	.0000	.0232	1.838	78.086	.5450	86.65	572.31
8	.0000	.0233	999.000	78.082	.5317	85.21	610.33
9	.0000	.0235	999.000	78.141	.5186	83.87	647.79
10	.0000	.0236	999.000	78.136	.5110	82.95	647.97
11	.0000	.0238	999.000	78.206	.5022	81.94	647.70
12	.0000	.0240	999.000	78.202	.4939	80.94	647.71
13	.0000	.0240	999.000	78.275	.4851	79.93	617.30
14	.0000	.0241	999.000	78.244	.4769	78.92	592.38
15	.0000	.0241	999.000	78.289	.4682	77.91	572.59
16	.0000	.0242	999.000	78.252	.4601	76.91	557.53
17	.0000	.0242	999.000	78.292	.4515	75.90	546.49
18	.0000	.0243	999.000	78.249	.4434	74.89	536.70
19	.0000	.0244	999.000	78.286	.4348	73.87	527.25
20	.0000	.0245	999.000	78.239	.4265	72.84	518.44
21	.0000	.0246	999.000	78.273	.4169	71.71	508.90
22	.0000	.0248	999.000	78.221	.4064	70.41	498.69
23	.0000	.0249	999.000	78.250	.3938	68.91	486.93
24	.0000	.0250	999.000	78.192	.3802	67.22	474.42
25	.0013	.0000	999.000	78.212	.3655	65.47	461.32
26	.0035	.0000	999.000	78.150	.3510	63.68	448.35
27	.0057	.0000	999.000	78.161	.3358	61.86	434.95
28	.0075	.0000	999.000	78.096	.3206	59.99	421.43
29	.0093	.0000	999.000	78.100	.3049	58.10	407.42
30	.0114	.0000	999.000	78.034	.2893	56.18	393.21
31	.0138	.0000	999.000	78.029	.2730	54.22	378.35
32	.0164	.0000	999.000	77.963	.2566	52.21	363.02
33	.0183	.0000	999.000	77.950	.2395	50.15	346.82
34	.0206	.0000	999.000	77.885	.2223	48.06	330.08
35	.0233	.0000	999.000	77.866	.2046	45.92	312.39
36	.0264	.0000	999.000	77.803	.1865	43.72	293.74
37	.0297	.0000	999.000	77.779	.1677	41.46	273.83
38	.0327	.0000	999.000	77.721	.1484	39.12	256.54
39	.0367	.0000	999.000	77.693	.1284	36.72	237.14
40	.0422	.0000	999.000	77.643	.1077	34.21	214.93
41	.0000	.0000	.000	77.615	.0856	31.56	.00

PPHR	PO	TO	XO	TAMB	RHA	PNXT
189.10	88.30	142.26	1.00	23.30	.94	100.40

TOTT	QHP	TEPF	TEF	EZ	ET	TMELT	TMVAP
264.	12275.	.00	561.43	81.83	735.48	3.92	.06

DFEF	EFFC	P(NPL)	DP	DHTF	SCLVG	XLVG	NTDROP
.7634	.7634	87.686	.614	302.73	.0	.115	1

I	T	TS	TWO	TWI	TWF	X	ESUM	IHTM	PATH
									4332211
1	142.3	72.5	98.1	98.1	101.7	1.000	2.88	3	71400.0
2	128.5	72.5	89.8	89.8	93.3	1.000	2.45	3	61500.0
3	116.9	72.6	82.8	82.8	86.2	1.000	2.09	3	51600.0
4	107.0	72.6	76.8	76.8	80.1	1.000	1.80	3	51600.0
5	98.5	72.6	71.6	71.6	81.0	1.000	2.04	3	51600.0
6	88.9	72.6	66.9	66.9	81.0	1.000	2.19	3	41700.0
7	78.7	72.6	72.5	72.5	76.6	1.000	1.70	3	51600.0
8	72.6	72.6	71.1	71.1	70.8	.995	1.31	3	41700.0
9	72.7	72.7	63.4	63.4	71.2	.977	1.60	3	41700.0
10	72.7	72.7	63.4	63.4	71.2	.956	1.60	3	41700.0
11	72.7	72.7	63.5	63.5	71.1	.935	1.60	3	41700.0
12	72.7	72.7	63.5	63.5	71.0	.914	1.60	3	41700.0
13	72.7	72.7	63.5	63.5	71.0	.893	1.60	3	31800.0
14	72.7	72.7	63.4	63.4	70.9	.872	1.59	3	31800.0
15	72.7	72.7	63.4	63.4	70.9	.850	1.59	3	31800.0
16	72.7	72.7	63.3	63.3	70.8	.829	1.59	3	31800.0
17	72.7	72.7	63.3	63.3	70.8	.808	1.59	3	31800.0
18	72.7	72.7	63.2	63.2	70.8	.787	1.59	3	31800.0
19	72.7	72.7	63.3	63.3	70.7	.766	1.59	3	31800.0
20	72.6	72.6	63.1	63.1	70.7	.745	1.59	3	21900.0
21	72.7	72.7	63.1	63.1	70.6	.724	1.59	3	21900.0
22	72.6	72.6	62.9	62.9	70.6	.703	1.60	3	21900.0
23	72.6	72.6	62.6	62.6	70.5	.682	1.61	3	21900.0
24	72.6	72.6	61.6	61.6	70.5	.661	1.65	3	21900.0
25	72.6	72.6	61.0	66.4	70.2	.639	1.74	3	12000.0
26	72.5	72.5	60.8	67.8	70.0	.616	1.87	3	12000.0
27	72.5	72.5	60.6	67.9	69.9	.591	2.02	3	12000.0
28	72.5	72.5	60.3	67.7	69.7	.565	2.14	3	12000.0
29	72.5	72.5	60.1	67.4	69.6	.536	2.26	3	12000.0
30	72.4	72.4	59.8	67.1	69.2	.507	2.40	3	12000.0
31	72.4	72.4	59.5	66.8	68.3	.475	2.54	3	12000.0
32	72.4	72.4	59.1	59.1	66.4	.442	2.62	2	1100.0
33	72.4	72.4	58.7	58.7	66.0	.407	2.64	2	1100.0
34	72.3	72.3	58.3	58.3	65.5	.372	2.67	2	1100.0
35	72.3	72.3	57.7	57.7	65.0	.337	2.70	2	1100.0
36	72.2	72.2	57.0	57.0	64.3	.301	2.74	2	1100.0
37	72.2	72.2	56.2	56.2	63.6	.265	2.80	2	1100.0
38	72.2	72.2	55.4	55.4	62.8	.228	2.83	2	1100.0
39	72.2	72.2	54.3	54.3	61.7	.191	2.87	2	1100.0
40	72.1	72.1	52.5	52.5	60.1	.153	2.94	2	1100.0
41	72.1	72.1	.0	.0	.0	.115	.00	0	.0

I	MFRST	MLIQ	DTLM	P	V	H	HR
1	.0000	.0156	999.000	88.300	.5527	96.32	60.84
2	.0000	.0183	999.000	88.292	.5356	94.03	59.30
3	.0000	.0199	999.000	88.318	.5205	92.09	57.78
4	.0000	.0211	999.000	88.311	.5075	90.43	56.48
5	.0000	.0218	1.248	88.351	.4959	89.00	534.55
6	.0000	.0224	2.931	88.345	.4829	87.39	573.31
7	.0000	.0223	999.000	88.398	.4682	85.64	618.71
8	.0000	.0225	999.000	88.392	.4572	84.30	647.32
9	.0000	.0229	999.000	88.462	.4491	83.26	647.07
10	.0000	.0230	999.000	88.458	.4396	81.99	647.08
11	.0000	.0232	999.000	88.532	.4298	80.72	616.98
12	.0000	.0233	999.000	88.498	.4205	79.45	587.43
13	.0000	.0234	999.000	88.542	.4108	78.18	567.24
14	.0000	.0235	999.000	88.499	.4016	76.92	553.42
15	.0000	.0235	999.000	88.538	.3920	75.65	540.86
16	.0000	.0235	999.000	88.488	.3828	74.39	529.61
17	.0000	.0236	999.000	88.522	.3732	73.12	518.78
18	.0000	.0237	999.000	88.467	.3641	71.86	508.69
19	.0000	.0238	999.000	88.496	.3545	70.60	498.69
20	.0000	.0238	999.000	88.437	.3454	69.34	489.17
21	.0000	.0240	999.000	88.459	.3359	68.07	479.56
22	.0000	.0241	999.000	88.396	.3267	66.81	470.28
23	.0000	.0243	999.000	88.411	.3172	65.55	460.81
24	.0000	.0244	999.000	88.345	.3080	64.27	451.50
25	.0000	.0243	999.000	88.354	.2982	62.96	441.78
26	.0000	.0244	999.000	88.286	.2881	61.58	431.64
27	.0000	.0245	999.000	88.290	.2770	60.09	420.47
28	.0000	.0246	999.000	88.220	.2653	58.49	408.51
29	.0000	.0247	999.000	88.216	.2526	56.79	395.52
30	.0000	.0248	999.000	88.145	.2395	55.00	381.74
31	.0000	.0249	999.000	88.132	.2253	53.10	366.66
32	.0003	.0000	999.000	88.062	.2104	51.08	350.52
33	.0020	.0000	999.000	88.042	.1949	49.01	333.27
34	.0042	.0000	999.000	87.973	.1795	46.91	315.50
35	.0066	.0000	999.000	87.948	.1637	44.80	296.84
36	.0094	.0000	999.000	87.883	.1478	42.65	279.64
37	.0124	.0000	999.000	87.854	.1315	40.48	262.75
38	.0152	.0000	999.000	87.795	.1150	38.26	244.17
39	.0189	.0000	999.000	87.764	.0983	36.02	223.55
40	.0239	.0000	999.000	87.714	.0813	33.74	200.33
41	.0000	.0000	.000	87.686	.0638	31.41	.00

PPHR	PO	TO	XO	TAMB	RHA	PNXT
205.30	100.40	143.79	1.00	23.80	.96	109.30

TOTT	QHP	TEPF	TEF	EZ	ET	TMELT	TMVAP
288.	12714.	.00	573.95	84.76	820.24	4.00	.09

DFEF	EFFC	P(NPL)	DP	DHTF	SCLVG	XLVG	NTDROP
.6997	.6997	99.574	.826	259.31	.0	.131	0

I	T	TS	TWO	TWI	TWF	X	ESUM	IHTM	PATH
									4332211
1	143.8	81.0	101.7	101.7	104.6	1.000	2.96	3	81400.0
2	131.0	81.0	93.3	93.3	96.5	1.000	2.57	3	71500.0
3	120.0	81.0	86.2	86.2	89.6	1.000	2.22	3	61600.0
4	110.5	81.0	80.1	80.1	86.8	1.000	2.18	3	61600.0
5	101.2	81.1	81.0	81.0	86.8	1.000	2.19	3	61600.0
6	91.9	81.1	81.0	81.0	86.8	1.000	2.21	3	51700.0
7	82.7	81.1	76.6	76.6	80.5	1.000	1.84	3	61600.0
8	81.1	81.1	70.8	70.8	79.2	.982	1.91	3	51700.0
9	81.2	81.2	71.2	71.2	79.2	.958	1.91	3	51700.0
10	81.1	81.1	71.2	71.2	79.2	.934	1.90	3	51700.0
11	81.2	81.2	71.1	71.1	79.1	.911	1.90	3	51700.0
12	81.2	81.2	71.0	71.0	79.0	.887	1.90	3	51700.0
13	81.2	81.2	71.0	71.0	79.0	.863	1.90	3	41800.0
14	81.1	81.1	70.9	70.9	78.9	.840	1.90	3	41800.0
15	81.2	81.2	70.9	70.9	78.8	.816	1.90	3	41800.0
16	81.1	81.1	70.8	70.8	78.8	.792	1.90	3	41800.0
17	81.1	81.1	70.8	70.8	78.7	.769	1.90	3	41800.0
18	81.1	81.1	70.8	70.8	78.6	.745	1.89	3	41800.0
19	81.1	81.1	70.7	70.7	78.6	.722	1.89	3	41800.0
20	81.1	81.1	70.7	70.7	78.5	.698	1.89	3	31900.0
21	81.1	81.1	70.6	70.6	78.4	.675	1.89	3	31900.0
22	81.0	81.0	70.6	70.6	78.3	.651	1.89	3	31900.0
23	81.0	81.0	70.5	70.5	78.3	.628	1.89	3	31900.0
24	81.0	81.0	70.5	70.5	78.2	.605	1.88	3	31900.0
25	81.0	81.0	70.2	70.2	78.1	.581	1.89	3	22000.0
26	80.9	80.9	70.0	70.0	78.0	.558	1.89	3	22000.0
27	80.9	80.9	69.9	69.9	77.9	.534	1.89	3	22000.0
28	80.9	80.9	69.7	69.7	77.8	.511	1.89	3	22000.0
29	80.9	80.9	69.6	69.6	77.7	.487	1.89	3	22000.0
30	80.8	80.8	69.2	69.2	77.6	.464	1.89	3	22000.0
31	80.8	80.8	68.3	68.3	77.5	.441	1.92	3	22000.0
32	80.8	80.8	66.4	68.0	77.4	.417	2.00	3	12100.0
33	80.7	80.7	66.0	72.0	76.9	.392	2.11	3	12100.0
34	80.7	80.7	65.5	73.1	76.5	.366	2.24	3	12100.0
35	80.7	80.7	65.0	73.1	76.2	.338	2.39	3	12100.0
36	80.6	80.6	64.3	72.7	75.8	.309	2.58	3	12100.0
37	80.6	80.6	63.6	72.2	75.1	.277	2.76	3	12100.0
38	80.6	80.6	62.8	71.5	73.6	.243	2.91	3	12100.0
39	80.5	80.5	61.7	61.7	70.5	.207	3.01	2	1200.0
40	80.5	80.5	60.1	60.1	69.2	.169	3.08	2	1200.0
41	80.5	80.5	.0	.0	.0	.131	.00	0	.0

I	MFRST	MLIQ	DTLM	P	V	H	HR
1	.0000	.0136	999.000	100.400	.4810	96.13	65.13
2	.0000	.0167	999.000	100.392	.4664	93.97	63.66
3	.0000	.0186	999.000	100.423	.4534	92.09	62.14
4	.0000	.0200	.720	100.416	.4421	90.47	524.18
5	.0000	.0206	.986	100.461	.4305	88.88	558.86
6	.0000	.0212	2.785	100.454	.4190	87.28	597.41
7	.0000	.0213	999.000	100.514	.4068	85.67	639.70
8	.0000	.0216	999.000	100.508	.3976	84.32	647.44
9	.0000	.0220	999.000	100.582	.3880	82.93	647.20
10	.0000	.0222	999.000	100.576	.3787	81.54	617.65
11	.0000	.0223	999.000	100.623	.3692	80.14	586.26
12	.0000	.0225	999.000	100.581	.3601	78.75	569.63
13	.0000	.0225	999.000	100.621	.3507	77.36	554.86
14	.0000	.0226	999.000	100.570	.3416	75.97	541.95
15	.0000	.0226	999.000	100.604	.3322	74.58	529.77
16	.0000	.0227	999.000	100.546	.3231	73.19	518.50
17	.0000	.0227	999.000	100.574	.3138	71.81	507.42
18	.0000	.0228	999.000	100.510	.3048	70.42	496.86
19	.0000	.0229	999.000	100.530	.2955	69.04	486.25
20	.0000	.0230	999.000	100.461	.2864	67.65	475.97
21	.0000	.0231	999.000	100.473	.2772	66.27	465.52
22	.0000	.0233	999.000	100.401	.2682	64.89	455.28
23	.0000	.0234	999.000	100.407	.2589	63.51	444.81
24	.0000	.0235	999.000	100.332	.2499	62.13	434.48
25	.0000	.0235	999.000	100.332	.2407	60.75	423.89
26	.0000	.0236	999.000	100.256	.2317	59.37	413.35
27	.0000	.0237	999.000	100.248	.2225	57.99	402.51
28	.0000	.0238	999.000	100.172	.2135	56.61	391.69
29	.0000	.0239	999.000	100.158	.2043	55.23	380.57
30	.0000	.0240	999.000	100.082	.1952	53.85	369.40
31	.0000	.0241	999.000	100.062	.1860	52.47	357.87
32	.0000	.0242	999.000	99.988	.1768	51.07	346.08
33	.0000	.0242	999.000	99.964	.1670	49.60	333.38
34	.0000	.0243	999.000	99.891	.1569	48.06	319.77
35	.0000	.0244	999.000	99.863	.1459	46.42	304.83
36	.0000	.0246	999.000	99.794	.1343	44.67	291.82
37	.0000	.0247	999.000	99.761	.1218	42.79	276.93
38	.0000	.0249	999.000	99.697	.1083	40.77	259.83
39	.0005	.0000	999.000	99.663	.0941	38.65	240.18
40	.0051	.0000	999.000	99.606	.0794	36.45	217.80
41	.0000	.0000	.000	99.574	.0643	34.20	.00

PPHR	PO	TO	XO	TAMB	RHA	PNXT
167.10	109.30	144.38	1.00	24.60	.97	109.60

TOTT	QHP	TEPT	TEF	EZ	ET	TMELT	TMVAP
312.	11361.	.00	574.75	75.74	895.97	4.01	.14

DFEF	EFFC	P(NPL)	DP	DHTF	SCLVG	XLVG	NTDROP
.6415	.6415	108.622	.678	207.32	.0	.001	4

I	T	TS	TWO	TWI	TWF	X	ESUM	IHTM	PATH
									4332211
1	144.4	86.8	104.6	104.6	101.1	1.000	2.61	3	91400.0
2	130.7	86.8	96.5	96.5	92.7	1.000	2.22	3	81500.0
3	119.1	86.8	89.6	89.6	85.9	1.000	1.88	3	71600.0
4	109.4	86.8	86.8	86.8	87.0	1.000	2.03	3	71600.0
5	99.0	86.8	86.8	86.8	87.0	1.000	2.05	3	71600.0
6	88.6	86.8	86.8	86.8	85.1	1.000	1.94	3	61700.0
7	86.8	86.8	80.5	80.5	83.9	.975	1.95	3	71600.0
8	86.8	86.8	79.2	79.2	84.0	.945	1.99	3	61700.0
9	86.9	86.9	79.2	79.2	83.7	.914	1.99	3	61700.0
10	86.8	86.8	79.2	79.2	83.6	.883	1.98	3	61700.0
11	86.9	86.9	79.1	79.1	83.5	.853	1.98	3	61700.0
12	86.8	86.8	79.0	79.0	83.3	.822	1.98	3	61700.0
13	86.8	86.8	79.0	79.0	83.3	.791	1.97	3	51800.0
14	86.8	86.8	78.9	78.9	83.1	.761	1.97	3	51800.0
15	86.8	86.8	78.8	78.8	83.0	.730	1.96	3	51800.0
16	86.8	86.8	78.8	78.8	82.9	.700	1.96	3	51800.0
17	86.8	86.8	78.7	78.7	82.8	.670	1.95	3	51800.0
18	86.8	86.8	78.6	78.6	82.7	.639	1.95	3	51800.0
19	86.8	86.8	78.6	78.6	82.5	.609	1.94	3	51800.0
20	86.7	86.7	78.5	78.5	82.4	.579	1.93	3	41900.0
21	86.7	86.7	78.4	78.4	82.2	.549	1.93	3	41900.0
22	86.7	86.7	78.3	78.3	82.1	.520	1.92	3	41900.0
23	86.7	86.7	78.3	78.3	81.9	.490	1.91	3	41900.0
24	86.7	86.7	78.2	78.2	81.7	.460	1.90	3	41900.0
25	86.6	86.6	78.1	78.1	81.5	.431	1.89	3	32000.0
26	86.6	86.6	78.0	78.0	81.2	.402	1.88	3	32000.0
27	86.6	86.6	77.9	77.9	81.0	.373	1.86	3	32000.0
28	86.6	86.6	77.8	77.8	80.7	.344	1.85	3	32000.0
29	86.6	86.6	77.7	77.7	80.4	.315	1.83	3	32000.0
30	86.5	86.5	77.6	77.6	80.1	.287	1.82	3	32000.0
31	86.5	86.5	77.5	77.5	79.8	.259	1.80	3	32000.0
32	86.5	86.5	77.4	77.4	79.4	.231	1.78	3	22100.0
33	86.5	86.5	76.9	76.9	79.1	.204	1.76	3	22100.0
34	86.5	86.5	76.5	76.5	78.6	.177	1.73	3	22100.0
35	86.4	86.4	76.2	76.2	78.0	.150	1.70	3	22100.0
36	86.4	86.4	75.8	75.8	77.2	.124	1.66	3	22100.0
37	86.4	86.4	75.1	75.1	76.3	.098	1.61	3	22100.0
38	86.4	86.4	73.6	73.6	75.2	.073	1.57	3	22100.0
39	86.4	86.4	70.5	70.2	73.5	.049	1.55	3	12200.0
40	86.4	86.4	69.2	64.8	69.0	.025	1.54	3	12200.0
41	86.4	86.4	.0	.0	.0	.001	.00	0	.0

I	MFRST	MLIQ	DTLM	P	V	H	HR
1	.0000	.0116	999.000	109.300	.4377	95.90	55.29
2	.0000	.0150	999.000	109.292	.4230	93.56	53.96
3	.0000	.0171	999.000	109.313	.4102	91.56	52.60
4	.0000	.0186	.030	109.308	.3991	89.87	450.31
5	.0000	.0193	.062	109.338	.3869	88.05	484.28
6	.0000	.0198	999.000	109.334	.3743	86.21	522.67
7	.0000	.0202	999.000	109.376	.3631	84.47	529.55
8	.0000	.0205	999.000	109.371	.3522	82.71	520.78
9	.0000	.0209	999.000	109.399	.3410	80.93	482.29
10	.0000	.0210	999.000	109.372	.3301	79.14	459.92
11	.0000	.0212	999.000	109.393	.3189	77.36	445.28
12	.0000	.0214	999.000	109.358	.3080	75.59	432.49
13	.0000	.0214	999.000	109.374	.2969	73.81	420.54
14	.0000	.0215	999.000	109.333	.2861	72.04	409.27
15	.0000	.0215	999.000	109.343	.2751	70.27	398.22
16	.0000	.0216	999.000	109.298	.2642	68.51	387.45
17	.0000	.0216	999.000	109.301	.2533	66.75	376.65
18	.0000	.0217	999.000	109.253	.2426	65.00	365.96
19	.0000	.0218	999.000	109.251	.2317	63.25	355.13
20	.0000	.0219	999.000	109.201	.2210	61.51	344.29
21	.0000	.0220	999.000	109.194	.2102	59.77	333.25
22	.0000	.0222	999.000	109.143	.1996	58.04	322.13
23	.0000	.0223	999.000	109.130	.1889	56.31	310.77
24	.0000	.0224	999.000	109.080	.1783	54.60	299.27
25	.0000	.0224	999.000	109.063	.1677	52.89	287.50
26	.0000	.0225	999.000	109.014	.1573	51.19	275.58
27	.0000	.0226	999.000	108.994	.1469	49.51	263.37
28	.0000	.0227	999.000	108.947	.1365	47.84	251.42
29	.0000	.0228	999.000	108.925	.1263	46.18	241.39
30	.0000	.0229	999.000	108.880	.1161	44.53	230.85
31	.0000	.0230	999.000	108.857	.1060	42.90	219.72
32	.0000	.0231	999.000	108.816	.0960	41.29	207.99
33	.0000	.0231	999.000	108.793	.0861	39.70	195.57
34	.0000	.0232	999.000	108.757	.0763	38.12	182.33
35	.0000	.0234	999.000	108.736	.0666	36.56	168.16
36	.0000	.0235	999.000	108.705	.0571	35.03	152.96
37	.0000	.0237	999.000	108.686	.0479	33.55	136.44
38	.0000	.0239	999.000	108.662	.0389	32.10	118.17
39	.0000	.0242	999.000	108.647	.0301	30.69	97.17
40	.0000	.0246	999.000	108.631	.0214	29.30	70.32
41	.0000	.0000	.000	108.622	.0128	27.92	.00

APPENDIX IV

TABLE OF CONVERSION FACTORS

Acceleration

$1\ ft/s^2 = 3.0480*10^{-1}\ m/s^2$

$1\ in/s^2 = 2.5400*10^{-2}\ m/s^2$

Area

$1\ ft^2 = 9.2903*10^{-2}\ m^2$

$1\ in^2 = 6.4516*10^{-4}\ m^2$

Energy

$1\ Btu = 1.0551*10^{3}\ J$

$1\ ft \cdot lbf = 1.3558\ J$

$1\ Btu = 2.9307*10^{-4}\ kW \cdot h$

Force

$1\ lbf = 4.4482\ N$

Heat Transfer Coefficient

$1\ Btu/(h \cdot ft^2 \cdot {}^{\circ}F) = 5.6783\ W/(m^2 \cdot K)$

Length

$1\ ft = 3.0480*10^{-1}\ m$

$1\ in = 2.5400*10^{-2}\ m$

Mass

$1\ lbm = 4.5359*10^{-1}\ kg$

Mass Density

$1\ lbm/ft^3 = 1.6018*10\ kg/m^3$

$1\ lbm/in^3 = 2.7680*10^{4}\ kg/m^3$

Mass Flow Rate

$1\ lbm/h = 1.2600*10^{-4}\ kg/s$

Power

1 Btu/h = $2.9307*10^{-1}$ W

1 ft·lbf/h = $3.7662*10^{-4}$ W

1 ton (refrigeration) = $3.5169*10^{3}$ W

Pressure

1 lbf/ft^2 = $4.7880*10$ Pa

1 lbf/in^2 (psi) = $6.8948*10^{3}$ Pa

Specific Heat

1 Btu/(lbm·°F) = $4.1868*10^{3}$ J/(kg·K)

Temperature

T(°C) = T(K) - 273.15

T(°F) = 1.8 * T(°C) + 32

T(°F) = 1.8 * T(K) - 459.67

T(°R) = 1.8 * T(K)

1°F difference = 1°R difference

= 5/9°C difference = 5/9K difference

Thermal Conductivity

1 Btu/(h·ft·°F) = 1.7307 W/(m·K)

Velocity

1 ft/h = $8.4667*10^{-5}$ m/s

Viscosity (dynamic)

1 lbm/(ft·h) = $4.1338*10^{-4}$ Pa·s

Volume

1 ft^3 = $2.8317*10^{-2}$ m^3

1 in^3 = $1.6387*10^{-5}$ m^3

Volume Flow Rate

$$1\ ft^3/min = 4.7195*10^{-4}\ m^3/s$$